



Norwegian University of
Science and Technology

RSW Systems with CO₂ as Refrigerant

Testing of new system solutions for sea water coolers

Sondre Sætrang

Master of Science in Engineering and ICT

Submission date: June 2009

Supervisor: Trygve Magne Eikevik, EPT

Norwegian University of Science and Technology
Department of Energy and Process Engineering

Problem Description

R-22 is the most common refrigerant in RSW (Refrigerated Sea Water) systems on fishing vessels today. The Montreal Protocol, which Norway has signed, calls for the phase-out of refrigerants with high GWP (Greenhouse Warming Potential). From 2010 all import of R-22 will be forbidden. Current replacements are artificially developed chemicals like HFCs (Hydrofluorocarbons) or natural refrigerants (found in nature). HFCs have high GWP, between 1300 and 3300 times greater than CO₂. For this reason, the HFCs are charged an environmental tax; HFC-404A, for instance, is taxed about NOK 590/kg. Previous research show refrigerant losses from the Norwegian fishing vessels of about 30% annually on average, and this imposes an environmental problem as well as large costs for the vessel owners.

In close cooperation within GEMINI-center Applied Refrigeration at NTNU and SINTEF the focus is directed towards using natural refrigerants such as ammonia (NH₃), carbon dioxide (CO₂) and hydrocarbons (methane, ethane, propane etc). This community has a world leading position on revitalization of CO₂ (used on transport vessels 60 to 80 years ago). The former professor Gustav Lorentzen with coworkers took out patents in the late 1980s which takes advantage of the carbon dioxides positive properties.

In the laboratories of NTNU and SINTEF, a prototype RSW system using CO₂ as refrigerant has shown very promising results. The system is rigged with measurement instrumentation and experimental results are available, but there is still room for improvement with regards to system design and component optimization. The system has been rebuilt to include a suction gas heat exchanger and this has improved the performance of the evaporator system. In this work it will be focused on optimizing the transcritical system with an adjustable bypass valve in front of the suction gas heat exchanger.

Assignment given: 21. January 2009
Supervisor: Trygve Magne Eikevik, EPT

i Project description

Norwegian University
of Science and Technology
NTNU

Department of Energy
and Process Engineering

EPT-M-2009-69



MASTER THESIS

For

Stud.techn. Sondre Sætrang
Spring 2009

RSW systems with CO₂ as refrigerant - testing of new system solutions for sea water coolers

RSW system med CO₂ som kuldemedium – utprøving av nye systemløsninger for sjøvannskjølere

Background and objective

R-22 is the most common refrigerant in RWS (Refrigerated Sea Water) systems on fishing vessels today. The Montreal Protocol, which Norway has signed, calls for the phase-out of refrigerants with high GWP (Greenhouse Warming Potential). From 2010 all import of R-22 will be forbidden. Current replacements are artificially developed chemicals like HFCs (Hydrofluorocarbons) or natural refrigerants (found in nature). HFCs have high GWP (Global Warming Potential), between 1300 and 3300 times greater than CO₂. For this reason, the HFCs are charged an environmental tax; HFC-404A, for instance, is taxed about NOK 590/kg. Previous research show refrigerant losses from the Norwegian fishing vessels of about 30% annually on average, and this imposes an environmental problem as well as large costs for the vessel owners.

In close cooperation within GEMINI-center Applied Refrigeration at NTNU and SINTEF the focus is directed toward using natural refrigerants such as ammonia (NH₃), carbon dioxide (CO₂) and hydrocarbons (methane, ethane, propane etc). This community has a world leading position on revitalization of CO₂ (used on transport vessels 60 to 80 years ago). The former professor Gustav Lorentzen with coworkers took out patents in the late 1980s which takes advantage of the carbon dioxides positive properties.

In the laboratories of NTNU and SINTEF, a prototype RSW system using CO₂ as refrigerant has shown very promising results. The system is rigged with measurement instrumentation and experimental results are available, but there is still room for improvements with regards to system design and component optimization. The system has been rebuilt to include a suction gas heat exchanger and this has improved the performance of the evaporator system. In this work it would be focused on optimizing the transcritical system with an adjustable bypass valve in front of the suction gas heat exchanger.

The following questions should be considered in the project work:

1. Literature review of RSW systems
2. Dimensioning and installation of a bypass valve in front of the suction heat exchanger
3. Design and performance of the experimental test of the operation of the installed valve

Page 1 of 2

4. Development of a calculation tool to optimize the combinations of the high pressure and the temperature in front of the expansion valve.
5. Make a draft of a publication of the results from the work
6. Make proposal for further improvements

-- ” --

Within 14 days of receiving the written text on the diploma thesis, the candidate shall submit a research plan for his project to the department.

When the thesis is evaluated, emphasis is put on processing of the results, and that they are presented in tabular and/or graphic form in a clear manner, and that they are analyzed carefully.

The thesis should be formulated as a research report with summary both in English and Norwegian, conclusion, literature references, table of contents etc. During the preparation of the text, the candidate should make an effort to complete a well presented report. In order to ease the evaluation of the thesis, it is important that the cross references is correct. In the making of the report, strong emphasis should be placed on both a thorough discussion of the results and an orderly presentation.

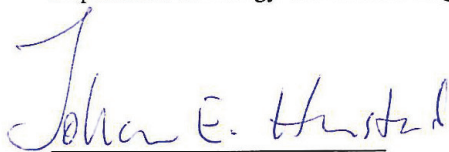
The candidate is requested to initiate and keep close contact with his/her specialist teacher and academic supervisor(s) throughout the working period. The candidate must follow the rules and regulations of NTNU as well as passive directions given by the Department of Energy and Process Engineering.

Pursuant to “Regulations concerning the supplementary provisions to the technology study program/Master of Science” at NTNU §20, the Department reserves the permission to utilize all the results for teaching and research purposes as well as in future publications.

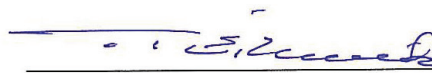
One – 1 complete original of the thesis shall be submitted to the authority that handed out the set subject. (A short summary including the author’s name and the title of the thesis should also be submitted, for use as reference in journals (max. 1 page with double spacing)).

Two – 2 – copies of the thesis shall be submitted to the Department. Upon request, additional copies shall be submitted directly to research advisors/companies. A CD-ROM (Word format or corresponding) containing the thesis, and including the short summary and all relevant information used must also be submitted to the Department of Energy and Process Engineering

Department of Energy and Process Engineering, January 12th 2009



Professor Johan E. Hustad
Department Manager



Prof. Trygve M. Eikevik
Academic Supervisor

Research Advisors:
Håvard Rekstad, NTNU, e-mail: havard.rekstad@ntnu.no

Page 2 of 2

ii Preface

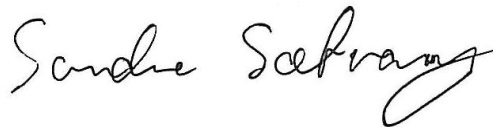
This master thesis is a result of my study in Engineering Science and ICT - Industrial Process Engineering at the Norwegian University of Science and Technology (NTNU), Faculty of Engineering Science and Technology, Department of Energy and Process Engineering.

Engineering Science and ICT is a Master of Science degree at NTNU which combines thorough insight in the design and development of computational software with a deep understanding of technical subjects. In my case the technical part of the study included fluid dynamics, thermodynamics, and specialization in oil and gas processing and heating and refrigeration systems.

In this thesis a bypass valve was placed in front of a suction gas heat exchanger in a transcritical RSW system using CO₂ as refrigerant. The goal of the project was to create a simulation tool and use this to optimize the system efficiency by controlling both the high side pressure and suction gas heat exchanger bypass.

I would like to thank my supervisors Trygve M. Eikevik and Håvard I. Rekstad for their time, patience and support over the course of this project, as well as the always helpful guys down in the lab.

Trondheim, 08.06.2009



Sondre Sætrang

iii Abstract

In a refrigerated seawater (RSW) system using carbon dioxide (CO₂) as the refrigerant, a variable bypass valve was installed in front of a suction gas heat exchanger (SGHX). A simulation tool was developed and utilized to optimize the systems transcritical performance (COP) with respect to the gas cooler pressure and choke valve inlet temperature for cooling and combined cooling and water heating. The simulations indicate that the RSW system performance can be increased compared to running a system with a traditional non-variable suction gas heat exchanger, but only when the cooling water temperatures are high (above ~25°C).

Experimental testing of the cooling performance with transcritical gas cooler pressure show little or no improvement at cooling water temperature levels below 25°C compared to previous experiments. The optimum setting turned out to be maximum suction gas heat exchange (no bypass). Previous experiments also show that for low cooling water temperatures (20°C and below), the optimum gas cooler pressure is subcritical.

The introduction of a variable suction gas heat exchanger made it possible to also use the system for water heating. The optimum and only possible SGHX setting was to bypass the SGHX altogether, as heat exchange would cause overheating at the compressor outlet. In other words, if the current system is to be used for water heating, the possibility to fully bypass the SGHX was essential.

The concept of a variable SGHX appears not to be beneficial in a water cooled RSW system with low cooling water temperature, but the simulations indicate that it has potential in systems where air is used as the cooling medium, for instance commercial or mobile refrigeration. For cooling purposes, experiments and simulations show that a non-variable suction gas heat exchanger can reach near-optimum conditions in the RSW system when low cooling water temperatures are available. It is strongly recommended that a system to be used for simultaneous cooling and heating should have an improved design compared to the current setup, as this mode of operation shows low cooling capacity and poor energy efficiency.

iv Sammendrag (abstract in Norwegian)

I et RSW-anlegg med karbondioksid (CO_2) som kjølemedium ble det installert en variabel bypassventil foran sugegassvarmeveksleren. Et simuleringsverktøy ble utviklet og brukt til å optimere driften av systemet (COP, effektivitet) med hensyn til gasskjølertrykk og temperaturen foran strupeventilen for både kjøling og kombinert kjøling og oppvarming av vann. Simuleringene peker i retning av et potensial for økt systemeffektivitet ved bruk av en variabel sugegassvarmeveksler for kjølevannstemperaturer høyere enn 25 °C.

Forsøk utført viser ingen forbedring i systemets kjølekapasitet og effektivitet ved transkritisk gasskjølertrykk og kjølevannstemperaturer under 25 °C sammenlignet med tidligere eksperimenter. Den optimale driften viser seg å være null bypass av sugegassvarmeveksleren. Tidligere forsøk viste at optimalt gasskjølertrykk var underkritisk for kjølevannstemperaturer på 20 °C eller lavere, og dette ble bekreftet da høyere effektivitet ikke kunne oppnås ved overkritisk trykk.

Innføringen av muligheten for å variere effektiviteten av sugegassvarmeveksleren gjorde det mulig å bruke systemet til varmtvannsoppvarming. Den optimale og eneste måten å kjøre anlegget på var å ikke bruke sugegassvarmeveksleren (full bypass), da varmeveksling førte til overheting ved kompressorutløpet. Med andre ord var muligheten for å kjøre uten sugegassvarmeveksler helt essensiell ved varmtvannsoppvarming.

Konseptet med en variabel sugegassvarmeveksler synes å ikke være nødvendig i et vannkjølt RWS-anlegg, men simuleringer antyder at det har potensial for anlegg der luft benyttes som kjølemedium, for eksempel kommersiell eller mobil kjøling. Til kjøleformål antyder forsøk og simuleringer at en ikke-variabel sugegassvarmeveksler kan ligge nært opptil det optimale driftspunkt når kaldt kjølevann er tilgjengelig. Det anbefales på det sterkeste å endre systemdesign dersom anlegget skal benyttes til samtidig kjøling og vannoppvarming, ettersom anlegget i nåværende form viser lav kjølekapasitet og lav energieffektivitet.

v Table of contents

I	PROJECT DESCRIPTION	I
II	PREFACE	III
III	ABSTRACT	V
IV	SAMMENDRAG (ABSTRACT IN NORWEGIAN)	VI
V	TABLE OF CONTENTS	VII
VI	LIST OF FIGURES	IX
VII	LIST OF TABLES	XII
VIII	NOMENCLATURE, NOTATION AND ABBREVIATIONS	XIII
1	INTRODUCTION AND BACKGROUND	1
1.1	THESIS BACKGROUND.....	1
1.2	REFRIGERANTS AT SEA.....	1
1.3	MAINTAINING FISH HAUL QUALITY.....	2
1.4	REFRIGERATED SEA WATER (RSW).....	3
1.5	CARBON DIOXIDE AS A REFRIGERANT.....	8
2	THE RSW SYSTEM	15
2.1	THE SYSTEM HISTORY.....	15
2.2	PROPOSED AND IMPLEMENTED SYSTEM MODIFICATION: SGHX BYPASS.....	19
3	SYSTEM MODELING	21
3.1	MODEL TOOLS.....	21
3.2	COMPRESSOR MODEL.....	21
3.3	GAS COOLER MODEL.....	23
3.4	SUCTION GAS HEAT EXCHANGER MODEL.....	25
3.5	CHOKE VALVE MODEL.....	27
3.6	EVAPORATOR MODEL.....	27
3.7	SUCTION PIPE MODEL.....	28
3.8	ASSEMBLED MODEL, SOLUTION APPROACH.....	28
4	SYSTEM OPTIMIZATION	31
4.1	GOAL FUNCTION.....	31
4.2	PROOF OF CONCEPT.....	31
4.3	OPTIMIZATION, SYSTEM COOL DOWN.....	33
4.4	OPTIMIZATION, COOLING MODE.....	35
4.5	OPTIMIZATION, WATER HEATING MODE.....	36
4.6	OTHER MEANS OF OPTIMIZATION.....	38
5	EXPERIMENTAL RESULTS	39
5.1	EXPERIMENTAL SETUP.....	39
5.2	COOLING MODE.....	40
5.3	WATER HEATING MODE.....	41
5.4	MODEL VERIFICATION.....	43
6	DISCUSSIONS	47
6.1	SYSTEM PERFORMANCE.....	47
6.2	SYSTEM CONTROL.....	48
6.3	MODEL ACCURACY.....	49
6.4	THE CONCEPT OF VARIABLE SGHX BYPASS.....	49
7	SUGGESTED MODEL IMPROVEMENTS	51
7.1	CALCULATION TOOLS.....	51
7.2	GAS COOLER PRESSURE DROP.....	51

7.3	EVAPORATOR PRESSURE DROP.....	52
7.4	OTHER POSSIBLE IMPROVEMENTS.....	52
8	SUGGESTED SYSTEM IMPROVEMENTS AND FUTURE WORK.....	53
8.1	SYSTEM CONTROL.....	53
8.2	SYSTEM DESIGN.....	53
9	CONCLUSIONS.....	57
10	BIBLIOGRAPHY.....	59
11	APPENDICES.....	63
	APPENDIX 1 EQUATIONS USED IN CALCULATION OF EXPERIMENTAL RESULTS.....	63
	APPENDIX 2 MEASURING POINTS.....	65
	APPENDIX 3 SGHX CONTROL, PSEUDO-CODE.....	67
	APPENDIX 4 EXPERIMENTAL RESULTS, COOLING.....	68
	APPENDIX 5 EXPERIMENTAL RESULTS, WATER HEATING.....	69
	APPENDIX 6 INITIAL GAS COOLER MODEL.....	70
	APPENDIX 7 GAS COOLER PRESSURE DROP.....	70
	APPENDIX 8 SUCTION PIPE PRESSURE DROP.....	71
	APPENDIX 9 EVAPORATOR PRESSURE DROP, DATA FROM 2007.....	71
	APPENDIX 10 THE ORIGINAL SYSTEM.....	72
	APPENDIX 11 GAS COOLER SOLVER.....	73
	APPENDIX 12 COMPRESSOR MODEL DATA.....	74
	APPENDIX 13 GAS COOLER MODEL TESTING.....	75
	APPENDIX 14 SGHX MODEL DATA.....	76
	APPENDIX 15 MEDIUM COOLING WATER FLOW RATE INTERPOLATION TABLE.....	76
	APPENDIX 16 MODEL VERIFICATION DATA.....	77
	APPENDIX 17 NEW GAS COOLER MODEL DATA.....	78
	APPENDIX 18 SGHX PRESSURE DROP CALCULATION.....	79
	APPENDIX 19 COOLING, 2008 RESULTS.....	80
	APPENDIX 20 COOLING, 2007 RESULTS.....	81
	APPENDIX 21 SUCTION GAS HEAT EXCHANGER.....	86
	APPENDIX 22 EXCEL SOLVER SET UP.....	88
	APPENDIX 23 ARTICLE DRAFT.....	89

vi List of figures

Figure 1-1: Refrigerant charge in the global fleet of merchant marine, fishing and naval vessels. Data from UNEP(2006).	2
Figure 1-2: Simplified overview of an RSW system. The fish is suspended by an upward water flow. A fraction of the water flow can be bled out and replaced by clean sea water in order to maintain clean conditions. Figure made on basis of system description by Teknotherm Marine Refrigeration (2008a).	3
Figure 1-3: Initial refrigeration (time τ_1), temperature increasing caused by the fish haul (time τ_2) and decline as haul and water is refrigerated (time τ_3) (Thorsteinsson et al, 2003).	4
Figure 1-4: The use of directional water flows and air bubbles to unload the fish. Based on figure and system description by Dagbjartsson et al (1982).	5
Figure 1-5: A simple description of a vacuum fish pump. On suction the inlet valve is open, and the vacuum relief and exit valves are closed, bringing water and fish into the vacuum tank. Closing the inlet valve and opening the other two valves discharge the water and fish. ..	5
Figure 1-6: A traditional RSW system. The refrigerant absorbs and emits heat at a close-to-constant temperature, because of phase change. The cooling water and RSW absorbs/emits heat at gliding temperature.	6
Figure 1-7: A typical live chilling system using a well boat (Skjervold et al, 2002).	8
Figure 1-8: Refrigerant use over the years (Pearson, 2005). Carbon dioxide (CO ₂) was rediscovered as a refrigerant by G. Lorentzen (Lorentzen , 1990; Lorentzen, 1994).	9
Figure 1-9: Volumetric capacity of refrigerants based on 20 °C condensation temperature and no subcooling or superheating. Graph created using Excel and the rnlb extension.	10
Figure 1-10: Saturation pressure versus evaporation temperatures for a selection of refrigerants. Graph created using Excel and the rnlb extension.	11
Figure 1-11: A subcritical cycle for carbon dioxide. The condensation temperature was set to 25 °C, evaporation at -5 °C. No subcooling or superheating. The critical point is at 31.1 °C (73.8 bara), where the saturation curve is at its maximum.	11
Figure 1-12: Transcritical cycle. Temperature out of the gas cooler is set to 21 °C, evaporation at -5°C. There is no phase change on the high pressure side. On the low pressure side evaporation takes place as normal.	12
Figure 1-13: Effect of increased high side pressure. The thin lines show the path from Figure 1-12. The gas cooler outlet temperature is set to the same value for both.	12
Figure 1-14: System using a suction gas heat exchanger. Figure from Lorentzen (1994).	13
Figure 1-15: The effect of installing a suction gas heat exchanger is a reduction in the throttle valve inlet temperature and an increase in both the compressor suction temperature and outlet temperature.	13
Figure 1-16: COP variations with gas cooler pressure and IHX (SGHX) efficiency. Note that the optimum pressure varies with the IHX efficiency. Figure from Chen at al (2005).	14
Figure 2-1: A properly sized evaporator outlet tube has a low gas velocity. Any droplets following the gas flow will drain back down into the evaporator (left). If the evaporator outlet tube velocity is too high, the droplets are carried with the flow by the shear force from the high velocity gas.	16
Figure 2-2: The evaporator. The upper horizontal tube is the suction drum, and the four vertical tubes are the exit tubes which are assumed to have a too small diameter.	16
Figure 2-3: The system with the suction gas heat exchanger installed.	17
Figure 2-4: The original setup of the suction gas heat exchanger.	18
Figure 2-5: Attempted hot water production from the previous round of experiments. The compressor outlet temperature (circle, upper right corner) hindered a sufficiently high pressure, leading to a very high gas cooler outlet temperature.	19

Figure 2-6: The modified system with a bypass valve in front of the suction gas heat exchanger. The bypass valve allows for variations in the SGHX efficiency by bypassing high pressure gas.	20
Figure 2-7: The modified suction gas heat exchanger. By opening the vertical ball valve and closing the horizontal ball valve one can bypass the suction gas heat exchanger.....	20
Figure 3-1: Compressor isentropic efficiency as a function of the pressure ratio (pout/pin) based on experimental data.	22
Figure 3-2: Compressor volumetric efficiency as a function of the pressure ratio based on experimental data.	22
Figure 3-3: The finite elements, directions, symbols and indexing used in the gas cooler simulation.	23
Figure 3-4: The gas cooler sections. The upper part is the hot gas stream from the gas cooler; the lower part is the cold gas stream from the evaporator. The flow is counter-current.....	23
Figure 3-5: Tube cross sectional area decrease factor declines linearly from 600 to 300 kg/h.	24
Figure 3-6: Altering the effective water tube cross sectional area for calculation of the convection coefficient reduces the low cooling water flow error.	25
Figure 3-7: Gas cooler pressure drop model.	25
Figure 3-8: Suction gas heat exchanger pressure drop model.....	26
Figure 3-9: Evaporator pressure drop model based on experimental results.	27
Figure 3-10: Suction pipe pressure drop as a function of the Reynolds number, calculated from 2007 the experimental data.....	28
Figure 3-11: The simplified system and array numbering used in the system. Points 5 and 6 were not used (they were set equal to point 7), as the SGHX was not modeled in detail.....	29
Figure 3-12: Some of the system interdependencies.....	29
Figure 3-13: The iterative approach for solving the system.....	30
Figure 4-1: Ideal pressure varies with both cooling water temperature and SGHX efficiency for -6 °C (left) and -2 °C (right).	32
Figure 4-2: Relative COP using different SGHX efficiencies for evaporation temperature -6°C (left) and -2°C (right). The relative COP using the ideal SGHX efficiency is unity (1). A relative COP of 0.8 means the setting gives a COP of only 80% compared to the optimum setting.	32
Figure 4-3: Ideal SGHX efficiency (left) and the corresponding choke inlet temperature (right) varies with both the cooling water temperature and evaporation temperature.	32
Figure 4-4: Ideal pressure as a function of evaporation temperature and cooling water temperature. The 10 and 15 °C cooling water temperature curves overlap. The step shape is a result of the resolution used for optimization, in this case 2 bar.....	33
Figure 4-5: Ideal choke valve inlet temperatures as a function of evaporation temperature and cooling water temperature.	34
Figure 4-6: The ideal IHX (SGHX) efficiency as a function of evaporation temperature and cooling water temperature.....	34
Figure 4-7: The maximum achievable SGHX efficiency at different evaporation temperatures.	34
Figure 4-8: The solution space for 10 °C and 5000 kg/h cooling water at an evaporation temperature of	35
Figure 4-9: Ideal pressure as a function of cooling water flow rate for an evaporation temperature of -6°C.....	36
Figure 4-10: Ideal choke valve inlet temperature as a function of cooling water flow for an evaporation temperature of -6°C.....	36
Figure 4-11: COP as a function of cooling water flow.	37

Figure 4-12: Cooling water flow for desired gas cooler outlet temperature. The different colors represent cooling water inlet temperature, in °C.....	37
Figure 4-13: The flow rate trend for varying water inlet temperature for each of the goal temperatures.....	38
Figure 5-1: The 2008(lines) and 2009 (square markings) cooling results. The dotted vertical line indicates critical pressure. COP values are for compressor work only.....	40
Figure 5-2: Cooling mode COP for both high and medium cooling water flow. Results are within 5%, but are systematically underestimated.....	40
Figure 5-3: Simulated and experimental cooling capacity.....	41
Figure 5-4: Cooling COP for the water heating mode. Deviations are larger, but for the most part within 10%.....	41
Figure 5-5: Experimental and simulated cooling capacity for water heating.....	42
Figure 5-6: Combined COP as a function of cooling water temperature. Each color represents an outlet temperature.....	42
Figure 5-7: Volumetric efficiency calculations compared to the experimental values.....	43
Figure 5-8: The isentropic efficiency was overestimated for hot water production (on the left) and underestimated for the cooling (on the right hand side), but the accuracy is within 8% for all experiments.....	43
Figure 5-9: Simulated and experimental compressor suction pressures.....	44
Figure 5-10: Simulated and experimental pressure drop. The percentage error is quite large, but relative to the high pressure it is insignificant.....	44
Figure 5-11: Temperature approach cooling on the left, hot water mode on the right. Simulation values are within one exception for the 25/80 hot water mode experiment, within 1.5 K.....	45
Figure 5-12: The evaporator pressure drop when in cooling mode.....	45
Figure 5-13: Hot water production.....	45
Figure 6-1: Cycle (upper) and gas cooler temperature profile (lower) at full water flow using 25 °C cooling water temperature. The blue line is the cooling water temperature.....	47
Figure 6-2: Cycle (upper) and gas cooler temperature profile (lower) at heating mode with 70°C outlet temperature using 25 °C cooling water. The temperature difference between the CO ₂ and the water was much lower than for the full flow experiment, so less heat was transferred.....	48
Figure 7-1: Suggested gas cooler pressure drop model based on the circulated mass flow in cooling mode.....	51
Figure 7-2: Model error is within 15%.....	51
Figure 7-3: Evaporator pressure drop in both cooling and hot water mode.....	52
Figure 8-1: Simplified overview of a system with a dedicated gas cooler for water heating.....	54
Figure 8-2: Ejector principle. Converting pressure to velocity creates a suction effect at the secondary fluid inlet (from the evaporator). Figure from Chunnanond et al (2004).	54
Figure 8-3: Simplified overview of a system with a dedicated gas cooler for water heating and an ejector replacing the choke valve.....	55
Figure 11-1: The measuring points.....	66
Figure 11-2: Initial gas cooler model error as a function of cooling water flow.....	70
Figure 11-3: The system as it was before any modification.....	72
Figure 11-4: CAD drawing of part used to mount the SGHX to the existing piping.....	86
Figure 11-5: Details of the suction gas heat exchanger.....	87
Figure 11-6: Excel Solver setup.....	88

vii List of tables

Table 1-1: Refrigerant charge in the global fleet of merchant marine, fishing and naval vessels. Data from UNEP(2006)	1
Table 1-2: Positive and negative aspects of RSW systems from different sources.	8
Table 2-1: Short description of the most important system components	15
Table 2-2: SGHX design conditions	17
Table 2-3: Suction gas heat exchanger design parameters.....	17
Table 2-4: Simple description of the suction gas heat exchanger design.....	18
Table 2-5: The result of installing the suction gas heat exchanger.	19
Table 4-1: Pressure and SGHX combinations used for proof of concept	31
Table 4-2: Variable combinations for each operating condition (cooling water temp, cooling water flow, evaporation temperature) used for batch simulations.	33
Table 4-3: Ideal choke valve inlet temperatures at 5000 kg/h cooling water flow.	33
Table 4-4: Ideal pressure and choke inlet temperatures for medium cooling water flow rate.	35
Table 4-5: Ideal pressure and choke inlet temperatures for high cooling water flow rate.	35
Table 4-6: The simulated optimum values for water heating mode. COP is based on cooling capacity and compressor work only.	37
Table 5-1: Experiment matrix.	39
Table 11-1: Measuring points, channels and naming.....	65
Table 11-2: Experimental cooling results	68
Table 11-3: Experimental water heating results.....	69
Table 11-4: Gas cooler pressure drops from the 2007 experiments.....	70
Table 11-5: Pressure drops based on 2007 experiments without suction gas heat exchanger, and mass flow calculated from the compressor model used at that time.	71
Table 11-6: Evaporator pressure drops, 2007 data.....	71
Table 11-7: Data used for creating models for isentropic and volumetric efficiency for the compressor	74
Table 11-8. Gas cooler model testing. The length was adjusted to minimize the sum of squared error.....	75
Table 11-9: Data used for estimationg the SGHX performance	76
Table 11-10: Medium water flow rate used for linear interpolation.	76
Table 11-11: Model verification data.....	77
Table 11-12: Data used for the new gas cooler model, sorted by mass flow.....	78
Table 11-13. SGHX pressure drop calculations.....	79
Table 11-14: Cooling results, 2008.....	80
Table 11-15: Cooling results, 2007 at 90 bara gas cooler pressure.....	81
Table 11-16: Cooling results, 2007 at 80 bara gas cooler pressure.....	82
Table 11-17: Cooling results, 2007 at 70 bara gas cooler pressure.....	83
Table 11-18: Cooling results, 2007 at 60 bar gas cooler pressure	84
Table 11-19: Cooling results, 2007 at 50 bara gas cooler pressure.....	85

viii Nomenclature, notation and abbreviations

Symbol	Description	Unit
D	Diameter	m
D_h	Hydraulic diameter	m
h	Enthalpy, specific	$\frac{kJ}{kg}$
P	Pressure	Pa (absolute)
R	Thermal resistance	$\frac{K}{W}$
s	Entropy, specific	$\frac{kJ}{kgK}$
T	Temperature	$^{\circ}C$
U	Velocity	$\frac{m}{s}$
v	Specific volume	$\frac{m^3}{kg}$
ϵ_{SGHX}	Suction gas heat exchanger efficiency (defined in equation (11.10))	-
η_{is}	Isentropic efficiency (defined in equation (11.6))	-
λ	Volumetric efficiency (defined in equation (11.7))	-
μ	Dynamic viscosity	$Pa \cdot s$
ν	Kinematic viscosity	$\frac{m^2}{s}$
ρ	Density	$\frac{kg}{m^3}$

Note: All pressures are absolute values [bara]

Abbreviation	Description
SGHX	Suction gas heat exchanger
IHX	Internal heat exchanger. Same as SGHX
GWP	Greenhouse warming potential
RSW	Refrigerated Sea Water

Notation	Description
\dot{Q}	A dot over a symbol means time derivative. This particular example is heat transfer per time unit.
$\bar{\rho}$	A line over a symbol means that it is an average value. This particular example is average density.

1 Introduction and background

1.1 Thesis background

Leakage of refrigerants with high greenhouse warming potential (GWP) poses a threat to our environment, and one of the possible replacements is carbon dioxide (CO₂), which does not have any negative impact when leaked. There are challenges however, and these challenges will be addressed further in this master thesis.

In a refrigeration system using CO₂ the gas cooler pressure has to be controlled for transcritical operation. In traditional systems of this kind, a non-variable suction gas heat exchanger is specifically tailored to a specific operating condition. The optimum gas cooler pressure varies with the evaporation temperature and the cooling medium flow and temperature (Sarkar et al, 2004).

For systems undergoing large variations in operating conditions, it is impossible to design a suction gas heat exchanger (SGHX) that ensures optimum system efficiency for all conditions. In order to compensate for this, one can introduce a suction gas heat exchanger bypass, so that the SGHX efficiency (countercurrent heat exchanger efficiency, defined in eq.(11.10)) can be varied according to the current operating condition. The optimum gas cooler pressure then also has to consider the SGHX efficiency in addition to the evaporation temperature, cooling medium flow and temperature (more on this in section 1.5.3).

The main objective of this project was to investigate if there is any benefit of controlling both gas cooler pressure and suction gas heat exchanger efficiency in a RSW system, and create a tool for optimizing system efficiency using gas cooler pressure and choke inlet temperature as the controlled parameters.

1.2 Refrigerants at sea

According to the United Nations Environmental Program (UNEP, 2006), about 70% of merchant marine, fishing and naval vessels use R-22 as refrigerant for refrigeration and air conditioning (only vessels above 300 gross tons are included in this survey) on a global basis. Table 1-1 shows the charge of R-22 compared to other refrigerants. Note that the vessels using R-22 in number contribute to 70% of the fleet, but is responsible for 83% of the fill charge (Figure 1-1). This indicates that the R-22 systems on average are larger than systems using other refrigerants.

	HCFC-22 (R-22)	Other refrigerants	All refrigerants
Number of vessels (>300 gross tons)	45000	19000	64000
Percentage of vessels	70%	30%	100%
Total charge (tons)	10000	2070	12070
Percentage of total charge	83%	17%	100%
Annual leakage (tons)	2500 (25%)	419 (20%)	2919 (24%)

Table 1-1: Refrigerant charge in the global fleet of merchant marine, fishing and naval vessels. Data from UNEP(2006)

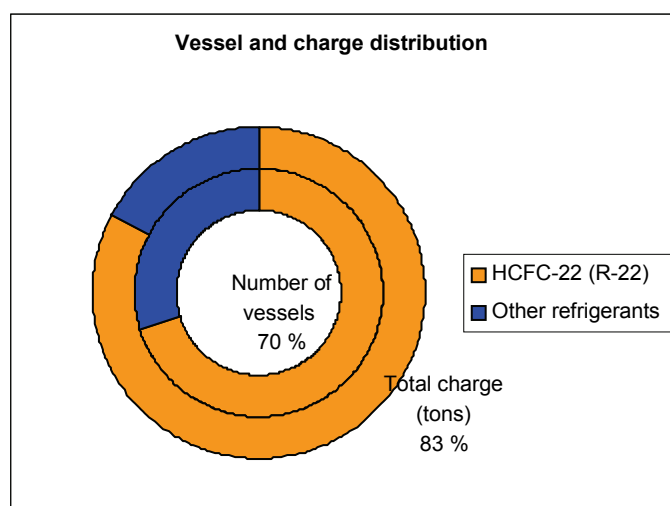


Figure 1-1: Refrigerant charge in the global fleet of merchant marine, fishing and naval vessels. Data from UNEP(2006).

Table 1-1 shows how marine applications contribute to large amounts of green house gas emissions. The annual leakage rates are on average approximately 24% of the total charge. The R-22 leakage is five percent higher than the other refrigerants; a possible explanation can be that the R-22 systems are older.

1.3 Maintaining fish haul quality

Fish haul has traditionally been preserved on board fishing vessels using flake ice made from fresh water, where fish and ice are placed in boxes in alternating layers. This is still the most common method of preservation. The advantage of ice is that as long as it is ice in the box, the temperature will be constant at 0 °C, the melting point of fresh water ice (Heen, 1982). The layering of fish and ice is unfortunately labor intensive, and the flake ice does allow some oxygen to come in contact with the fish. The flake ice also tends to have sharp edges, causing visual damage to the fish (Piñeiro et al, 2004). Flake ice has to be brought from shore, which is unpractical; a large amount of ice is needed on long journeys (Wang et al, 2005).

Super-chilling is a method of increasing the allowable storage time for fish haul. The fish is cooled down to slightly below its freezing point, which reduces the biological activity and gives the fish a refrigeration buffer, as the phase change prevents a temperature increase. The fish is then stored on ice, but the amount of ice can be reduced compared to traditional flake ice, as the fish itself is partially frozen. Storage time can be increased, but the super-chilling process has to be carefully monitored in order to prevent too much freezing of the fish, which can drastically reduce the quality. Super-chilling is further described in the article by Bahuaud et al (2008).

Refrigerated seawater (RSW) involves using a refrigeration system to cool seawater. This seawater is circulated through tanks in which fish is stored. This topic will be further discussed later in this thesis.

Another method utilizes a mixture of ice and water. Barros-Velázquez et al (2008) investigated the use of a mixture of water and ice (40% ice, 60% water), which has proven to be a good alternative to RSW and flake ice. The aforementioned problem with bringing ice from shore is not relevant here, because the ice for this purpose can be created on board using sea water, and it requires no manual labor to mix the ice with the water. Such a mixture,

known as slurry ice (SI), holds a temperature of $-1.8\text{ }^{\circ}\text{C}$, the freezing point of seawater (with a salinity of 35). The heat capacity of slurry ice is much better than RSW, and helps to reduce the fish core temperature faster.

1.4 Refrigerated Sea Water (RSW)

Refrigerated sea water (RSW) systems are widely used to chill fish haul in a simple and effective way. The concept is based on using a refrigeration system to cool down sea water, which is then circulated in large tanks containing sea water and fish. The refrigeration system can be installed on board fishing vessels, and removes the necessity of carrying ice from shore (Wang et al, 2005; Jul, 1986), reducing weight during transport to the fishing location. A simple overview is shown in Figure 1-2.

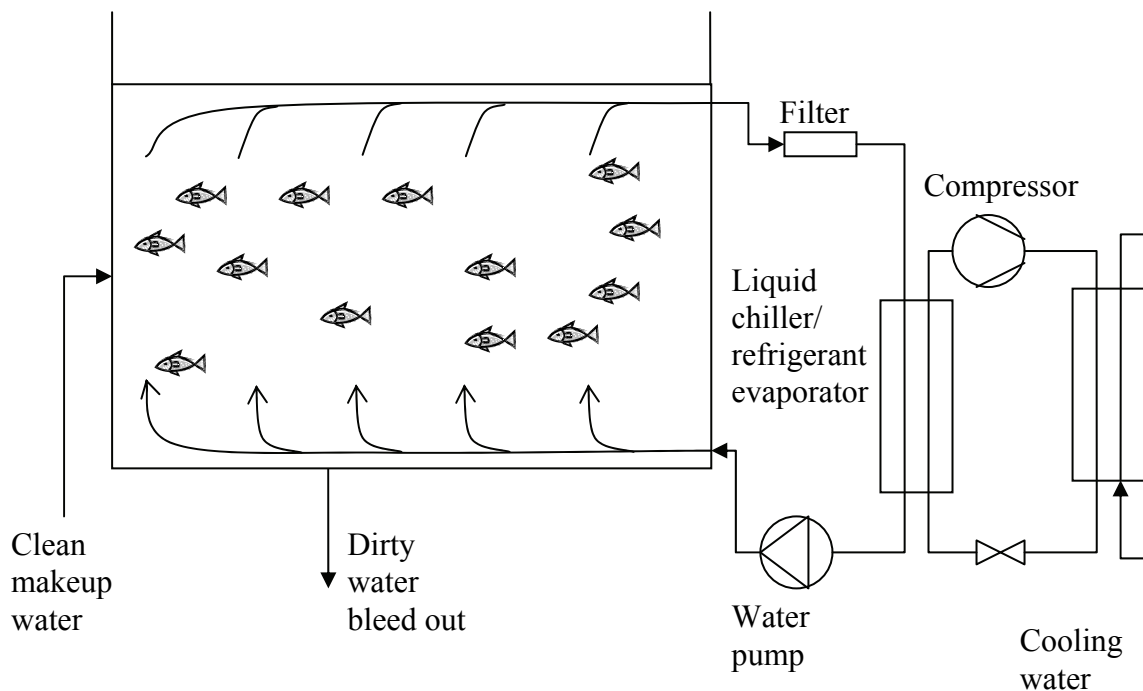


Figure 1-2: Simplified overview of an RSW system. The fish is suspended by an upward water flow. A fraction of the water flow can be bled out and replaced by clean sea water in order to maintain clean conditions. Figure made on basis of system description by Teknotherm Marine Refrigeration (2008a).

In preparation for hauling fish, large onboard tanks are filled with seawater and pre-cooled using the refrigeration system. Caught fish is dumped into the tanks, which increases the temperature of the water. The refrigeration unit is used to circulate and cool the water (Figure 1-3), which cools the fish haul. The salt content of sea water allows for low water temperature, usually set around $-1\text{ }^{\circ}\text{C}$. As shown in Figure 1-2, the water flows into the tank through a distribution plate on the bottom of the tank, and out of the tank in the upper part. This creates an upward water flow, keeping the fish suspended (Teknotherm Marine Refrigeration, 2008a). This method prevents pressure damage (bruising), which is common when storing large quantities of fish, caused by the weight load on fish in the bottom layers of storage (Heen, 1982).

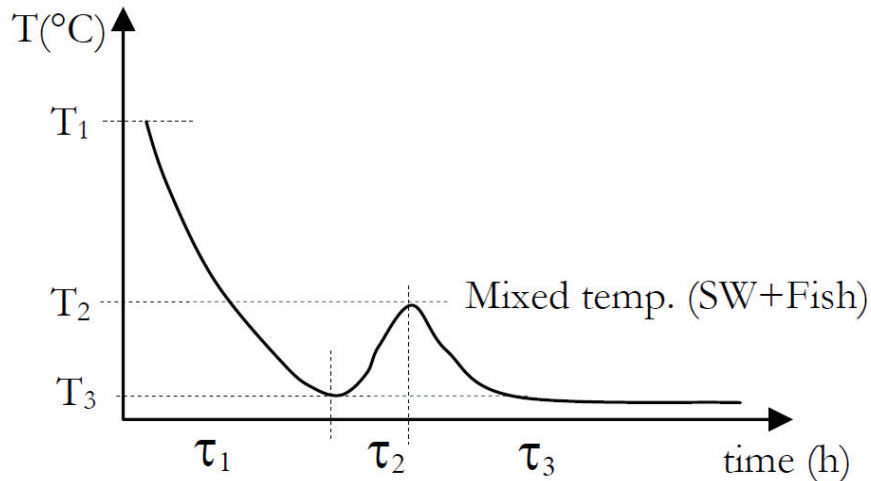


Figure 1-3: Initial refrigeration (time τ_1), temperature increasing caused by the fish haul (time τ_2) and decline as haul and water is refrigerated (time τ_3) (Thorsteinsson et al, 2003).

Upon arrival at shore, the tanks on board consist of approximately 70% fish and 30% water. In order to maintain a low fish temperature, the tanks have to be emptied in an efficient manner. One method of unloading was described by Dagbjartsson et al (1982), as shown in Figure 1-4, using a conveyor belt to empty an onshore RSW tank, but this is unpractical on board a trawler. The most common solution is to use a vacuum fish pump.

A fish pump, shown in Figure 1-5, draws a vacuum in a vacuum tank, which is connected to the RSW tank via a suction pipe. The vacuum allows for fish and water to be sucked out of the RSW tank. When the vacuum tank is full, a valve on the suction pipe is closed. An exit valve is then opened, allowing the fish and water to exit the vacuum tank. In this way, the fish is never in direct contact with any moving parts, preventing damage and maintaining high quality. To maintain continuous pumping, there are usually two vacuum tanks, so that one fills up while the other is emptied. (AGK-Kronawitter, 2008)

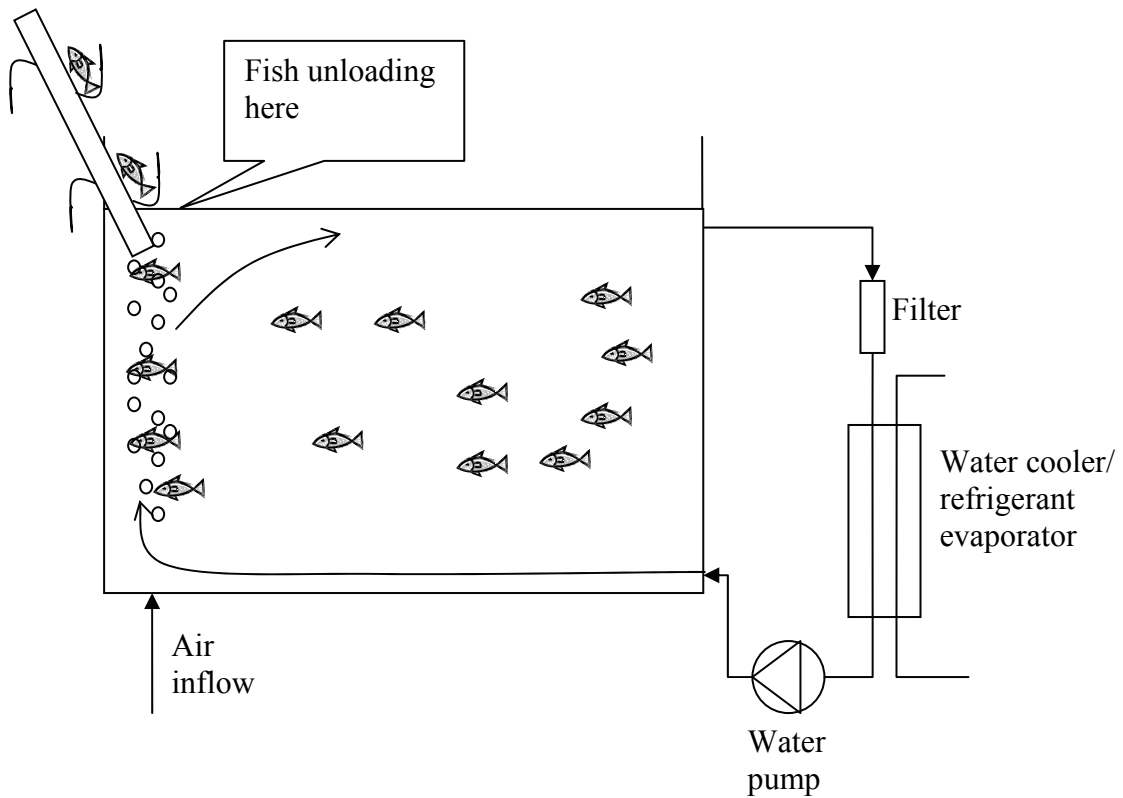


Figure 1-4: The use of directional water flows and air bubbles to unload the fish. Based on figure and system description by Dagbjartsson et al (1982).

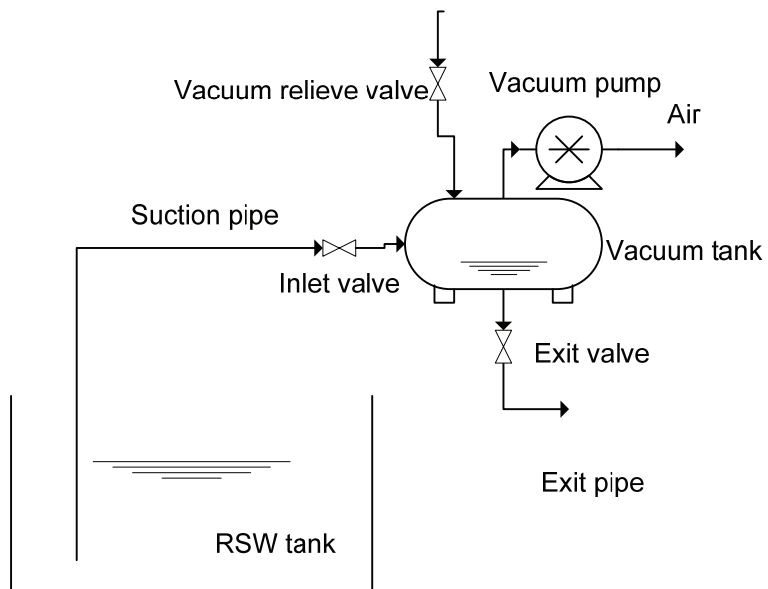


Figure 1-5: A simple description of a vacuum fish pump. On suction the inlet valve is open, and the vacuum relief and exit valves are closed, bringing water and fish into the vacuum tank. Closing the inlet valve and opening the other two valves discharge the water and fish.

1.4.1 Traditional RSW systems in detail

The most common method of constructing a RSW chiller is to use a flooded evaporator (Teknotherm Marine Refrigeration, 2008b). A flooded evaporator has that refrigerant on the shell side of the evaporator, surrounding the tubes. The water is flowing inside the tubes, and the refrigerant is boiling on the tube surfaces. Evaporation of this kind is known as pool boiling, and is capable of high heat transfer coefficients (Incropera et al, 2007). In order to prevent water from freezing on the tube walls, the evaporation temperature of the refrigerant cannot be too low. The condenser is usually a shell and tube heat exchanger, but plate heat exchangers can also be used. The condenser is usually cooled by seawater (Teknotherm Marine Refrigeration, 2008b).

Piñeiro et al (2004) discusses the importance of a well functioning filtration system to prevent fouling. Fouling is when pollution in the RSW (fish scale etc.) attaches to the water tube walls, which can reduce the cooling capacity significantly.

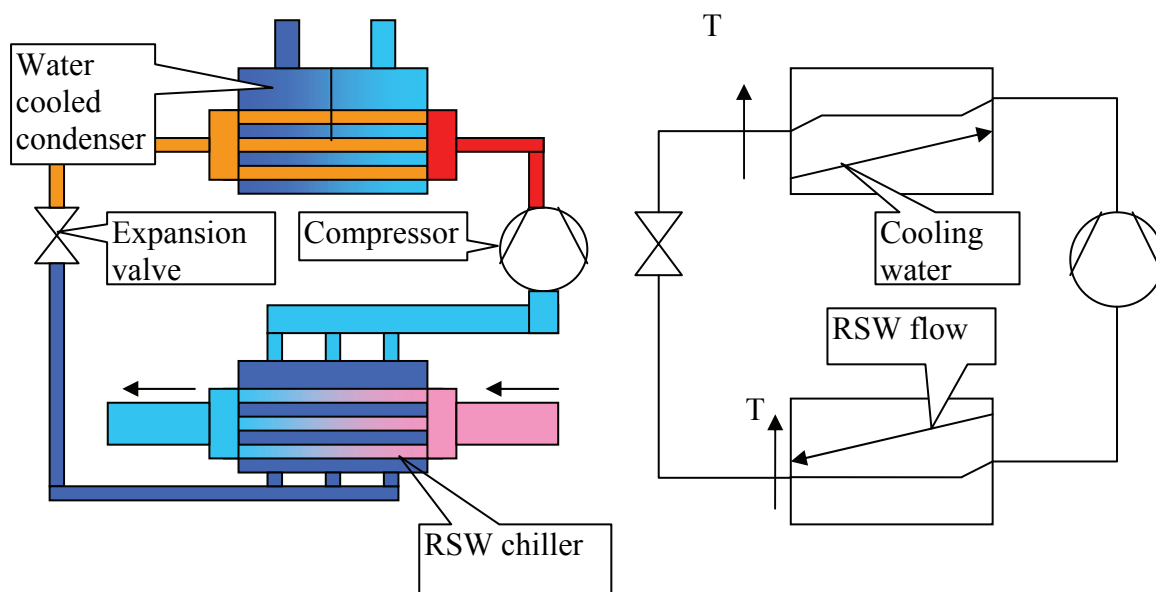


Figure 1-6: A traditional RSW system. The refrigerant absorbs and emits heat at a close-to-constant temperature, because of phase change. The cooling water and RSW absorbs/emits heat at gliding temperature.

An RSW system has large variations in cooling load (Figure 1-3). The initial cool-down has the highest cooling demand, followed by the fish haul cool-down. When the desired haul temperature has been reached (approximately -1°C), the only heat to be removed is the heat leakage into the tank. These variations necessitate a way of controlling the cooling capacity of compressor.

Both the evaporator and condenser are exposed to sea water. Since sea water is highly corrosive on steel, titanium or corrosion resistant alloys are used for parts that need such protection.

It should be mentioned that vapor-compression refrigeration as described above is not the only means of cooling. Wang et al (2005) described an ice generator utilizing waste heat from the engine using an absorption system. This is out of scope for this thesis, and will not be discussed further.

1.4.2 Advantages, disadvantages and alternative usage

The main advantage of RSW is the removal of flake ice as a cooling approach. Jul (1985) describes RSW system as they were in the 1980's:

“However, packing in ice, whether in boxes or pounds, is labour intensive and must be replaced by other methods. Refrigerated sea water (RSW) was labour saving and an acceptable, but not ideal, successor. It requires complicated pumping and filtering systems; it is highly costly and impractical to install on board a compressor of sufficient capacity to chill large hauls quickly. An inherent defect of the system is that one no longer has a guarantee that 0 °C will be maintained. In fact, we have a guarantee that it will not, because if it were, the condenser would most likely be choked by ice”.

There are a few errors in the above quote. First of all, the water cooling takes place in the evaporator, not in the condenser. Another important issue is that normal sea water, with a salinity of 35 (35 grams/liter), freezes at -1.8 °C, thus water can leave the evaporator at about -1°C without freezing. More important than water freezing is that the RSW temperature limits the speed of fish cool-down. An article by Magnussen et al (2008) discusses how the temperature difference, which is the driving force of heat transfer, is very low when using RSW. Even though the RSW temperature may be -1 °C, it takes a very long time before the fish core temperature actually reaches this level. Much research has been made in the later years to work around this problem, and super-chilling, which utilizes partial freezing of the fish, has been pointed out as a good or better alternative to RSW based on storage time and quality (Bahuaud et al, 2008; Magnussen et al, 2008). Another option is slurry ice, which was described earlier.

Musgrove et al (2006) performed a study in Australia for adding value to sardines which at the time were mostly sold as bait because of low quality. RSW was evaluated as an option for increasing the sardine quality. The study showed that the cool down time had a great influence on the fish quality, and the RSW system they used was not able to maintain the quality of the sardines. It is to be noted that the RSW system used in this study was not performing well, mostly due to bad circulation, which caused increased water temperature in the upper parts of the tank.

Piñeiro et al (2004) emphasizes some of the problems with RSW systems:

“(…) hydro-cooling systems, such as (RSW), have proved to be an easy and rapid method of chilling fish products, although they have certain limitations. Among these are the complicated pumping and filtering systems required to prepare RSW, which make this cooling method quite expensive”

A RSW system can be utilized for haul other than fish. The Department of Fisheries and Aquaculture Government of Newfoundland and Labrador (DFAGNL, 2002) performed tests on snow crab and for shrimps. By adding oxygen to the RSW, they managed to keep the crabs alive for several days until unloading. They concluded the use of the RSW system as a great success.

Live chilling was introduced in the Norwegian salmon farming industry in the 1990s. The chilling serves as a mild anaesthesia caused by hypothermia, which reduces the activity level of the fish, easing the further processing and reducing the handling stress on the fish (Erikson

et al, 2006). An article by Skjervold et al (2002) describes a way of predicting the chilling dynamics of live salmon using a full-size prototype RSW system (140kW). The prediction is based on initial water temperature, fish size and refrigeration temperature, and is proposed as a method to control the fish body temperature and cooling time. Both the body temperature and the cooling time have a great influence on product quality according to the article, supporting what Magnussen et al (2008) described.

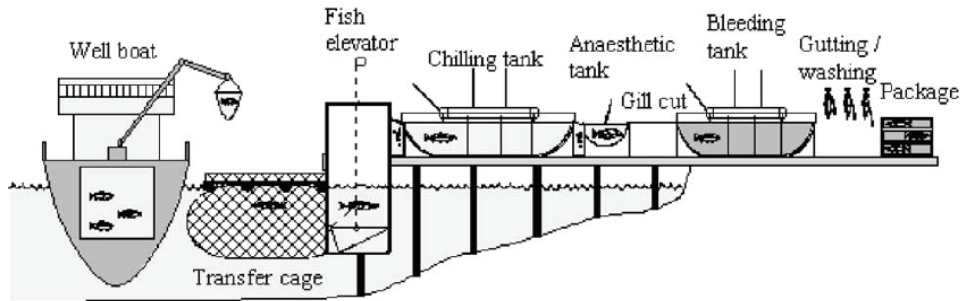


Figure 1-7: A typical live chilling system using a well boat (Skjervold et al, 2002).

Positive	Negative	Source
Easy handling and avoids bruising (compared to ice)	Does not improve shelf life compared to ice Increased salt uptake	Heen (1982)
	Slow compared to super chilling	Magnussen et al (2008)
Easy and rapid chilling	Pumping and filtering challenges	Pineiro et al (2004)
Can utilize waste engine heat to drive a refrigerating system (absorption system) Prevents bringing large amounts of ice		Wang et al (2005)
Increased storage time Less weight gain	Increased salt content Sanitary challenges	Muñoz-Delgado (1978)
Can go on longer voyages, and still maintaining quality		Persson (1982)
Reduced or eliminated cost of ice Fishing time increased		Department of Fisheries and Aquaculture Government of Newfoundland and Labrador (DFAGNL, 2002)

Table 1-2: Positive and negative aspects of RSW systems from different sources.

1.5 Carbon dioxide as a refrigerant

Kim et al (2004) gives an overview of carbon dioxide as a refrigerant throughout the history of refrigeration. In the early days (late 19th century), carbon dioxide was commonly used as refrigerant, as it was readily available, but the equipment for withstanding the high pressure of CO₂ was large and heavy. Ammonia based refrigeration, featuring low pressures and low energy consumption, became increasingly more popular, despite its smell and toxicity when leaked. In marine refrigeration, CO₂ was the most common refrigerant until the 1950's

particularly for safety reasons. After the introduction of CFC's in the 1940's, carbon dioxide experienced a rapid decline in popularity.

This quote by Kim et al (2004) describes the abandonment of carbon dioxide as a refrigerant:

“As the CFC fluids were introduced in the 1930s and 1940s, these ‘safety refrigerants’ eventually replaced the old working fluids in most applications. Although the major argument in their favour was improved safety compared to fluids like ammonia and sulphur dioxide, CO₂ was also displaced by this transition to CFC. There is no single reason why the use of CO₂ declined, but a number of factors probably contributed. These factors included high-pressure containment problems, capacity and efficiency loss at high temperature (aggravated by the need to use air cooling instead of water), aggressive marketing of CFC products, low-cost tube assembly in competing systems, and a failure of CO₂ system manufacturers to improve and modernize the design of systems and machinery.”

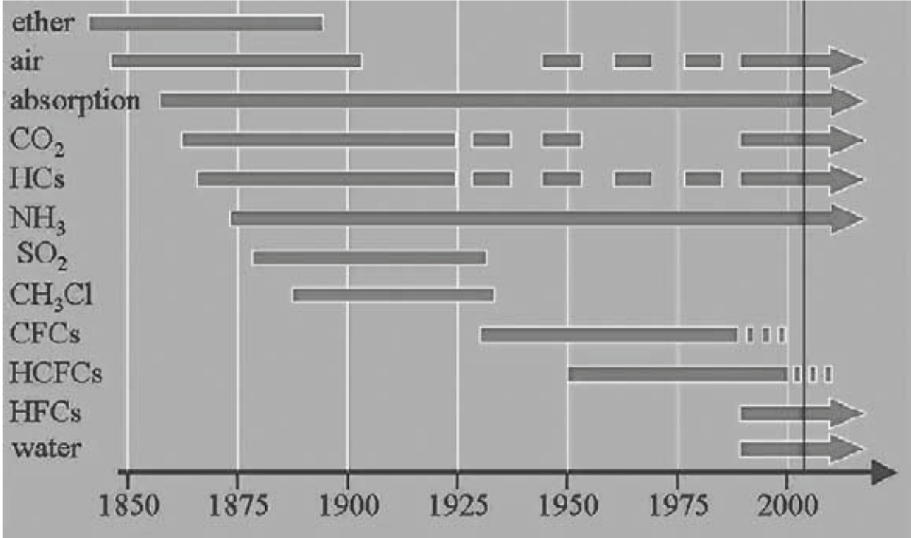


Figure 1-8: Refrigerant use over the years (Pearson, 2005). Carbon dioxide (CO₂) was rediscovered as a refrigerant by G. Lorentzen (Lorentzen , 1990; Lorentzen, 1994).

As the CFC's turned out to be harmful to the environment, the search was on for new alternatives (Pearson, 2005). Natural refrigerants once more gained attention, and in 1990 Gustav Lorentzen rediscovered carbon dioxide in the search for a natural, safe refrigerant for use in automotive air conditioning (Lorentzen, 1990). This rediscovery has led to tremendous effort in researching how to improve technology in order to overcome the challenges of using CO₂ for refrigeration purposes, and make it competitive compared to other refrigerants (Kim et al, 2004).

1.5.1 Carbon dioxide compared to other refrigerants

A brief overview of the carbon dioxide properties will be given here. A much more detailed description can be found in the article by Kim et al (2004). The most important positive properties of carbon dioxide in refrigeration can be summarized as:

- A high volumetric capacity means that the volume flow needed for a particular cooling capacity is small; the compressor can have a suction volume of only 20-25% of that required for other refrigerants.
- High pressures, but low pressure ratios. The low pressure ratio over the compressor ($p_{\text{discharge}}/p_{\text{suction}}$) leads to high volumetric *efficiency*.
- Low viscosity. A small volumetric flow combined with low viscosity means that tubing can be made smaller due to small pressure drops.
- Small dT/dP means a pressure reduction result in only minor temperature drop, which means we can accept higher pressure losses, or gain higher efficiency. A low dT/dP also means high dP/dT , so low superheating is needed for bubble formation.
- Non-toxic
- Non-flammable
- Low surface tension for liquid CO_2 . The surface tension is also very low for liquid CO_2 , which leads to very efficient boiling heat transfer (Loebl et al, 2005)

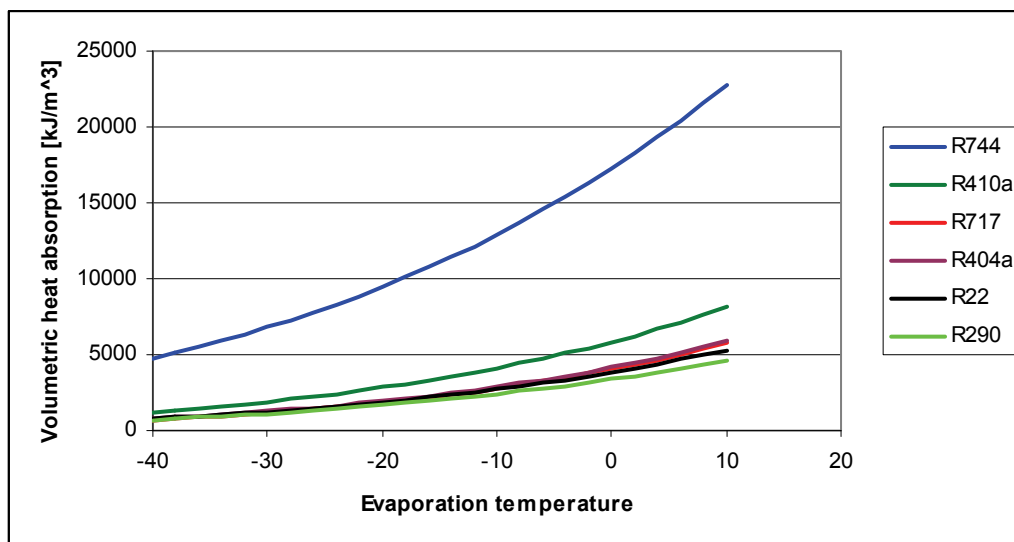


Figure 1-9: Volumetric capacity of refrigerants based on 20 °C condensation temperature and no subcooling or superheating. Graph created using Excel and the rnlb extension.

The drawbacks consist of:

- Large throttling losses
- Low critical temperature

The large expansion (throttling) losses can be countered by two-stage throttling combined with multi-stage compression, but at the cost of increased system complexity. The low critical temperature forces transcritical operation at high condenser/gas cooler temperature. The high pressure level of carbon dioxide (Figure 1-10) means that traditional system components rated at 25/40 bar cannot be used (can be used in low temperature applications such as freezing, but this will not be discussed further in this thesis). This is especially important at transcritical operation, where the high side pressure can exceed 120 bar.

Calm et al (2008) lists a range of possible natural refrigerants like ammonia (R717) and hydrocarbons, particularly propane (R290) and iso-butane (R600a). Ammonia is a very energy efficient refrigerant, but is toxic and flammable, and with the leakage rates seen in marine refrigeration it will require advanced systems for leakage detection and ventilation. The same applies for propane or other hydrocarbons, which are flammable.

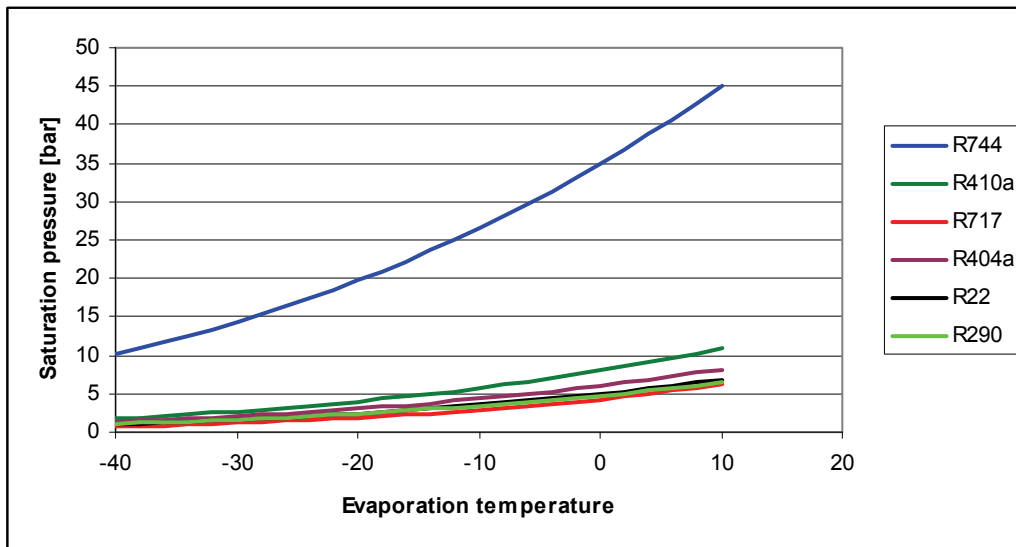


Figure 1-10: Saturation pressure versus evaporation temperatures for a selection of refrigerants. Graph created using Excel and the rnlb extension.

1.5.2 Subcritical and transcritical operation

Subcritical operation is the traditional refrigeration cycle featuring condensation and evaporation at a constant temperature.

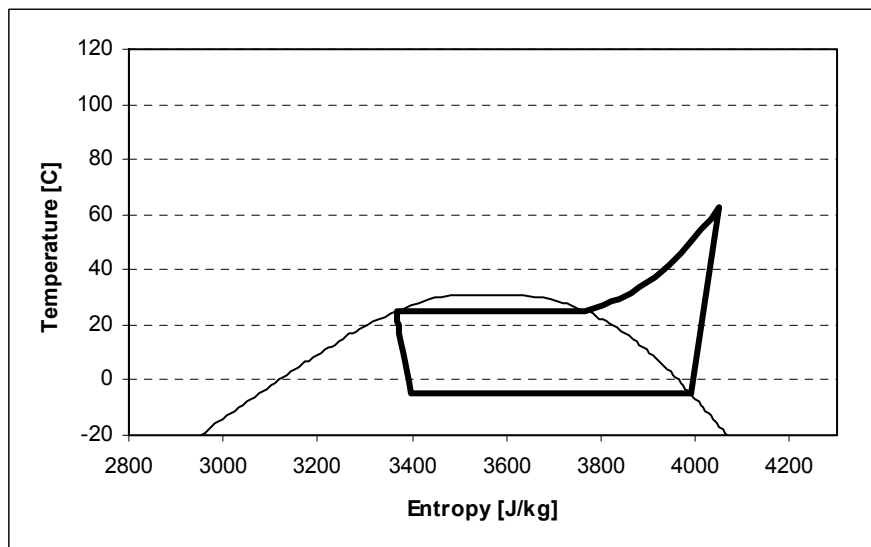


Figure 1-11: A subcritical cycle for carbon dioxide. The condensation temperature was set to 25 °C, evaporation at -5 °C. No subcooling or superheating. The critical point is at 31.1 °C (73.8 bara), where the saturation curve is at its maximum.

The low critical temperature of carbon dioxide sets an upper limit to the condensation temperature. If we need to remove heat at a higher temperature, the pressure will exceed the critical point. The pressure above critical is defined as supercritical. The heat dissipation will then no longer take place as condensation at constant temperature, but with a gliding temperature (Cabello et al, 2008). The gliding temperature (Figure 1-12) by itself is no advantage in refrigeration systems, but can be advantageous for producing hot water (Kim et al, 2004). A high temperature difference between the carbon dioxide and the cooling medium means one can often achieve a gas cooler outlet temperature close to the cooling medium inlet

temperature, usually 2-4K. This temperature difference is often referred to as the *temperature approach*.

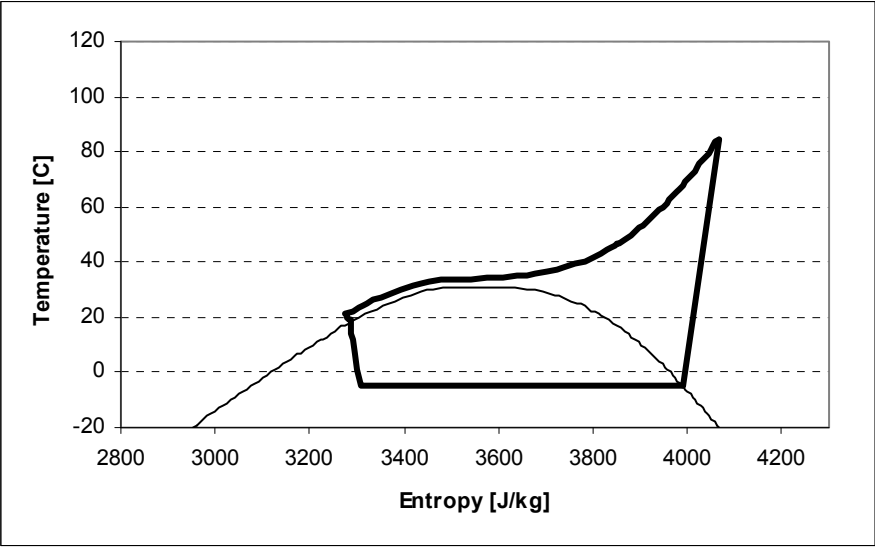


Figure 1-12: Transcritical cycle. Temperature out of the gas cooler is set to 21 °C, evaporation at -5°C. There is no phase change on the high pressure side. On the low pressure side evaporation takes place as normal.

After throttling, the pressure is below the critical (subcritical pressure). The term transcritical is used for a system that operates between subcritical (evaporation) and supercritical pressure.

1.5.3 Transcritical process optimization

The effect of an increase in the high side pressure is shown in Figure 1-13. The flash gas amount is reduced giving increased cooling (as the curve has moved further to the left), but the work has increased as well (work is represented by area enclosed by the curve). The optimum high side pressure balances the increased work with the increased cooling. Another effect is the increased temperature difference between the carbon dioxide and the cooling medium (blue line), which increases the gas cooler heat transfer (the carbon dioxide outlet temperature exit at a temperature closer to the cooling medium temperature).

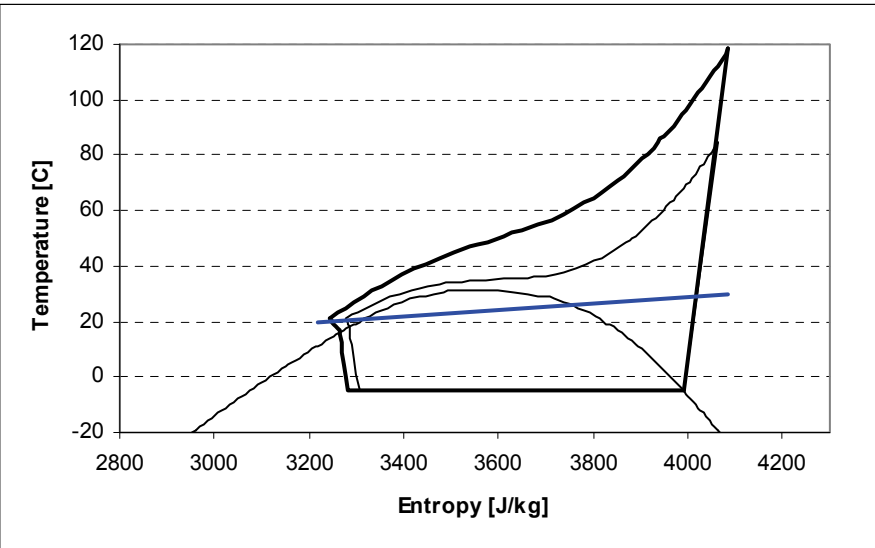


Figure 1-13: Effect of increased high side pressure. The thin lines show the path from Figure 1-12. The gas cooler outlet temperature is set to the same value for both.

Another way of increasing the temperature difference in the gas cooler is to include a suction gas heat exchanger (SGHX), also commonly known as internal heat exchanger (IHX). An example system using an SGHX is shown in Figure 1-14 (between point b and c). The suction gas heat exchanger uses the cold flow from the evaporator to cool down the stream from the gas cooler. This reduces the temperature in front of the throttling valve, but it also increases the compressor suction temperature (Figure 1-15). This leads to, as with increased pressure, an increased compressor outlet temperature. This increased temperature means more heat can be removed earlier in the gas cooler (as before, because of greater temperature difference), leading to a lower temperature approach. The reduced throttling temperature produces less flash gas, but the cost is a reduction in the circulated mass, as the specific volume at the compressor inlet increases with the temperature.

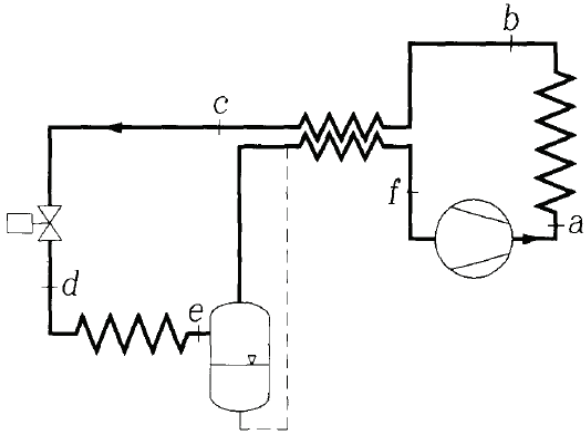


Figure 1-14: System using a suction gas heat exchanger. Figure from Lorentzen (1994).

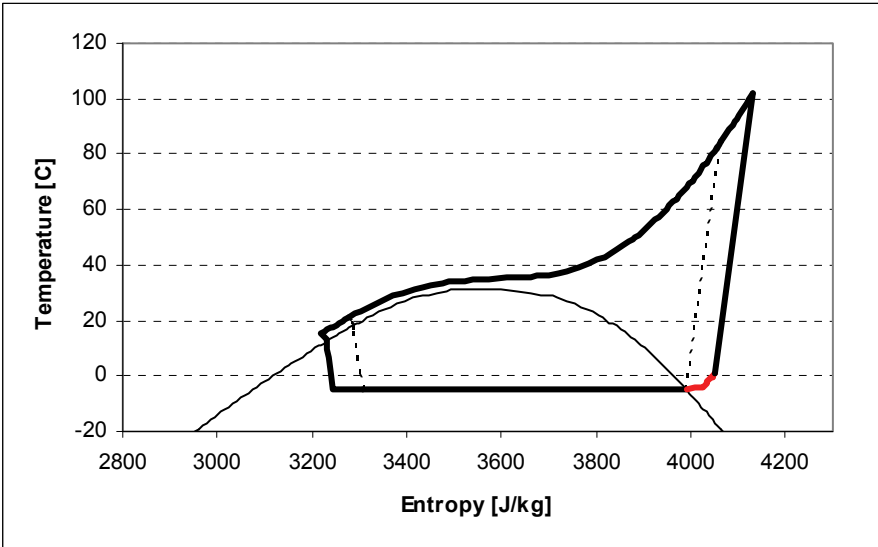


Figure 1-15: The effect of installing a suction gas heat exchanger is a reduction in the throttle valve inlet temperature and an increase in both the compressor suction temperature and outlet temperature.

To sum things up: Increased internal heat exchange leads to a lower temperature approach, but reduces the circulated mass for a given compressor. Increased gas cooler pressure also leads to a lower temperature approach and reduces the amount of flash gas from throttling, but increases the work input to the compressor. An optimization must balance these positive and negative aspects. Figure 1-16 shows an example of how the system performance (COP)

depends on both gas cooler pressure and the efficiency of the suction gas heat exchanger. Further information about high side pressure optimization can be found in the articles by Ge et al (2009) and Cabello et al (2008). A more mathematical approach is discussed by Chen et al (2005).

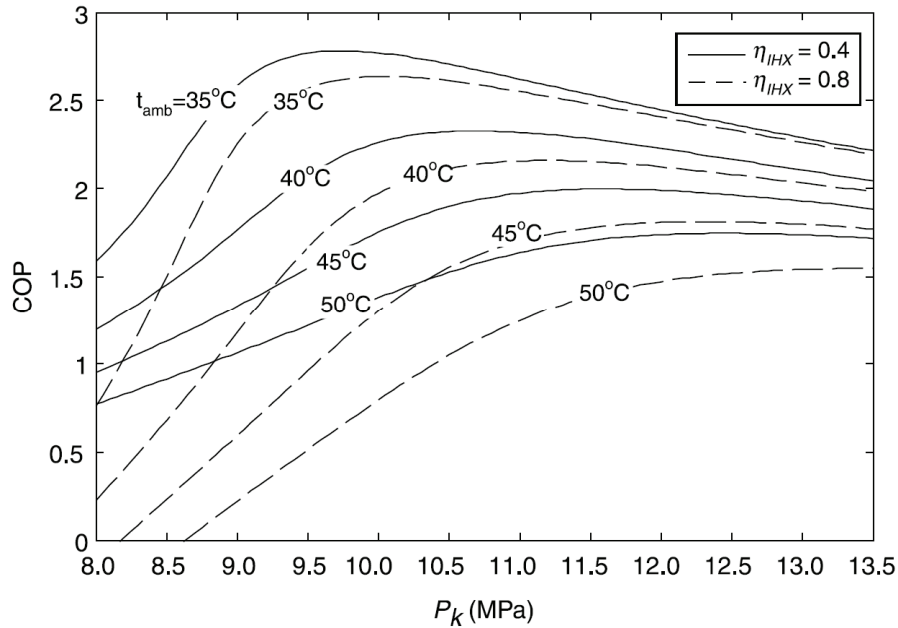


Figure 1-16: COP variations with gas cooler pressure and IHX (SGHX) efficiency. Note that the optimum pressure varies with the IHX efficiency. Figure from Chen et al (2005).

Sarkar et al (2004) gives a detailed description of the parameters that has influence the performance in a transcritical system, and concludes in equation 27 in their article that

$$COP = f(t_{evap}, t_{gc,out}, \eta_{is,compr}, p_{gc}, \epsilon_{SGHX}) \quad (1.1)$$

and the optimum pressure

$$p_{opt} = f(t_{evap}, t_{gc,out}, \eta_{is,compr}, \epsilon_{SGHX}) \quad (1.2)$$

Additionally, the gas cooler outlet temperature is a function of the cooling medium flow, cooling medium temperature and the gas cooler design.

From these equations it is easy to see that a variable suction gas heat exchanger may be beneficial, but that it also complicates the calculation of the optimum pressure. These challenges will be addressed in chapters 3 and 4.

2 The RSW system

The system in question was originally built without a suction gas heat exchanger. The system was designed for transcritical operation with a high cooling water flow. Under-dimensioned evaporator outlet tubes caused liquid carryover (droplets in the compressor suction gas), which required the system to be run with reduced capacity. A suction gas heat exchanger was then installed, but at some conditions the compressor outlet temperature overheated. The last modification was the installation of a bypass solution, so that the suction gas heat exchanger efficiency can be modified depending on the operating condition.

2.1 The system history

2.1.1 The initial design and associated problems

The initial system (Appendix 10) experienced problems with liquid carryover from the evaporator. The charge had to be kept low, and the compressor speed had to be adjusted in order to maintain a sufficiently high evaporation temperature (a limit was set at $-7\text{ }^{\circ}\text{C}$ in order to prevent the brine from freezing on the tube walls).

Table 2-1: Short description of the most important system components

Component	Description
Compressor	A Mycom, semi-hermetic, reciprocating compressor with two cylinders. Swept volume: 12.46 m ³ /h at 1451 RPM (143.14 ccm/rev) Driver: Frequency modulated by inverter. Outlet temperature limit: 130 °C
Liquid chiller/evaporator	Single pass shell-and-tube with a design capacity of 40kW cooling capacity at $-5\text{ }^{\circ}\text{C}$ evaporation temperature. Carbon dioxide on the shell side, water in tube bundle. Design brine flow 575 l/min at $+1/0\text{ }^{\circ}\text{C}$ in/out Length: 4 meters Shell inner diameter: 148.3 mm Inner tubes (water): 19 titanium, 17.2/19 mm, 3.0m each. Tube pitch 25.4 mm, 30 deg layout angle.
Gas cooler, water cooled	4 pass tube in tube (4x1m), 8 parallel tubes. 13.7/16mm ID/OD inner (water side) 20/23 mm ID/OD outer tube (CO ₂ side) Inner tube outer surface side has surface enhancement, increasing the area by a factor of 3.6.
Water heaters	Heater one (two steps): 5500 or 11100 W Heater two: 11665,6 W Heater three (two steps): 4000 or 8000 W

Liquid droplets leaving the evaporator are known as liquid carryover. The incompressible nature of liquids can cause major damage to a compressor (Forsthoffer, 2005), and liquid carryover should therefore not be tolerated. According to Rekstad et al (2008), too small evaporator outlet tubes caused the liquid droplet carryover, and this restricted the allowable evaporator fill rate. As a replacement or modification of the evaporator was no alternative, it was decided to modify the system by installing a suction gas heat exchanger to evaporate liquid droplets.

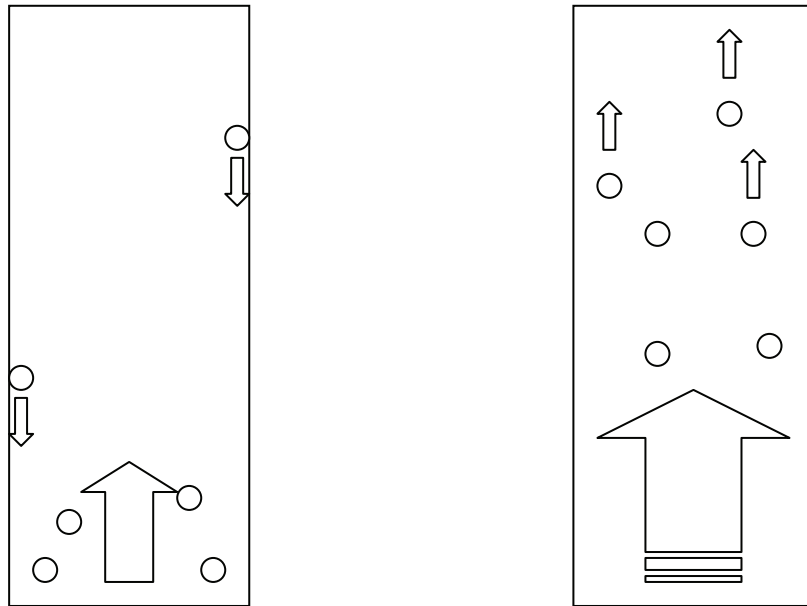


Figure 2-1: A properly sized evaporator outlet tube has a low gas velocity. Any droplets following the gas flow will drain back down into the evaporator (left). If the evaporator outlet tube velocity is too high, the droplets are carried with the flow by the shear force from the high velocity gas.

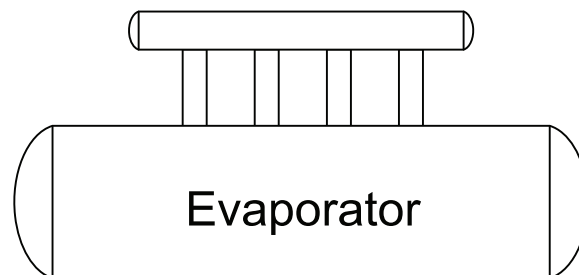


Figure 2-2: The evaporator. The upper horizontal tube is the suction drum, and the four vertical tubes are the exit tubes which are assumed to have a too small diameter.

The instrumentation consisted of

- 19 temperature measurements (thermocouples on tube walls, wrapped with alu-tape and insulation)
- 2 pressure transducers for absolute pressure measurements at the compressor inlet and outlet.
- 2 pressure difference measurements, across gas cooler and evaporator.
- 2 flow meters for measuring cooling water and brine (RSW) flow.
- The electric heaters had known power consumption, and the total heat input was logged manually.

A more detailed instrumentation description can be found in Jakobsen et al (2007). All measurements were logged using a computer logging software. The instrumentation layout is described in Appendix 2.

2.1.2 Introducing a suction gas heat exchanger

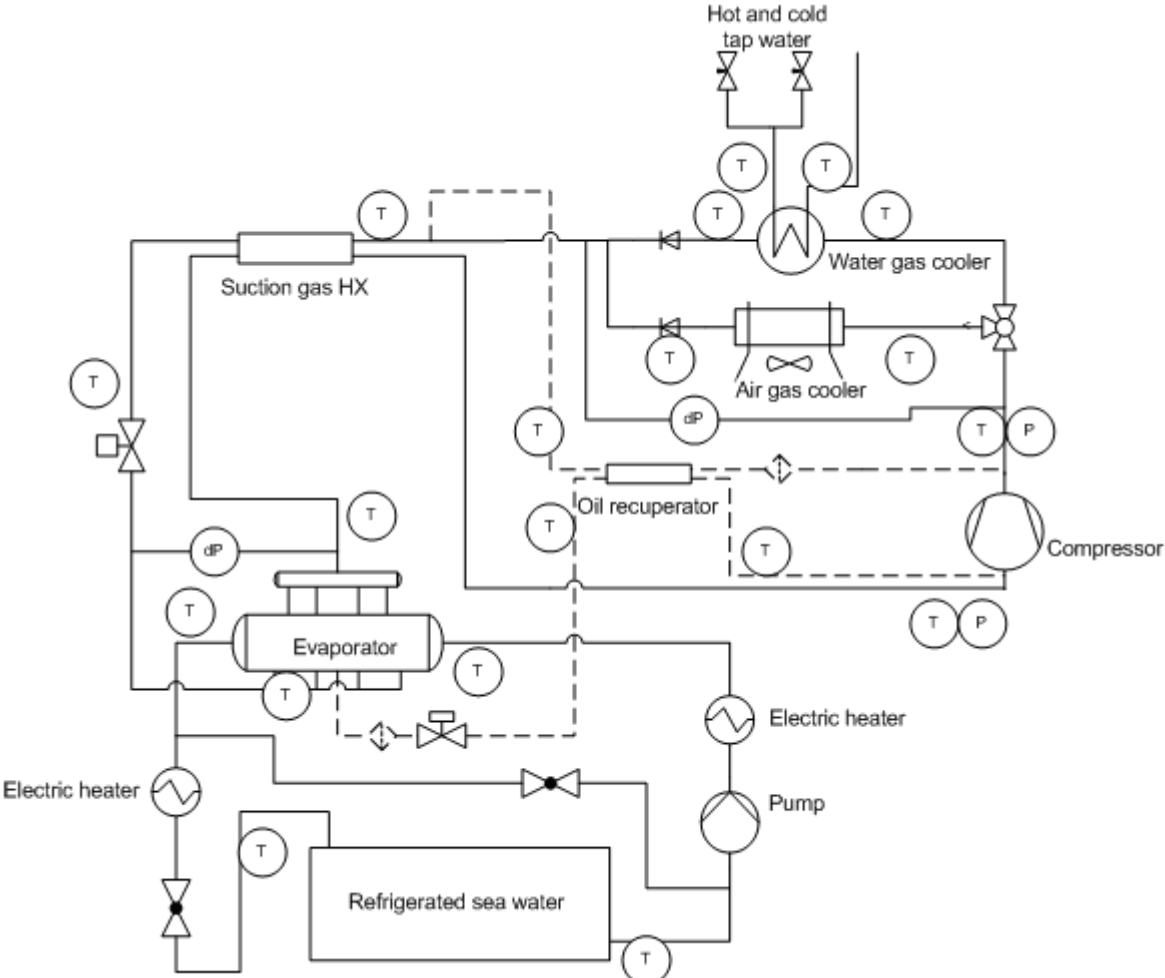


Figure 2-3: The system with the suction gas heat exchanger installed.

In order to deal with the liquid carryover, a suction gas heat exchanger was installed (Figure 2-3) to ensure superheating at the compressor inlet. This solved the problem with liquid carryover, but made it impossible for combined refrigeration and hot water production, as excessive superheating hindered a sufficiently high pressure in the gas cooler.

Table 2-2: SGHX design conditions

Property	Value
Compressor outlet pressure	80 bar
Gas cooler outlet temperature	12 °C
Evaporation temperature	-5 °C
Gas quality compressor outlet	0.9 [kg gas/kg total]

Table 2-3: Suction gas heat exchanger design parameters

Length	2 meters total, bent
Outer tube	21/25 mm ID/OD
Inner tubes	3x6/8mm ID/OD
Material	SS 316

The suction gas heat exchanger reduced the temperature in front of the throttling valve by transferring heat to the compressor suction flow. As a result, the pre-throttling temperature

decreased, thus producing less flash gas, whilst the compressor outlet temperature increased. This was explained in more detail in section 1.5.3. A more detailed description of the suction gas heat exchanger can be found in Appendix 21.

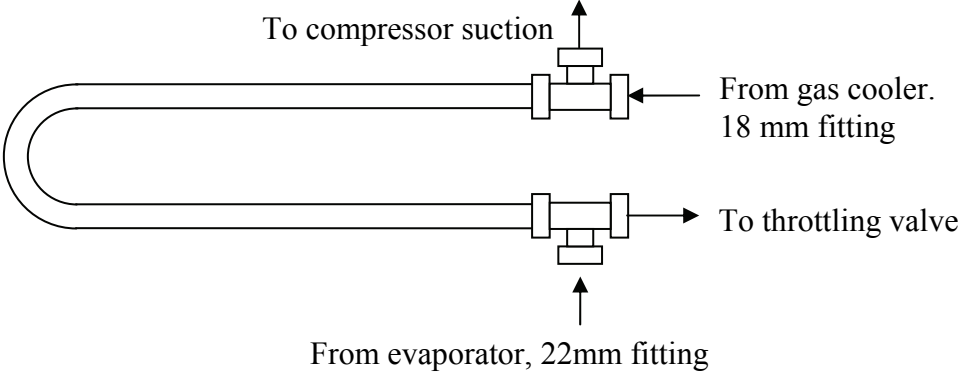


Figure 2-4: The original setup of the suction gas heat exchanger

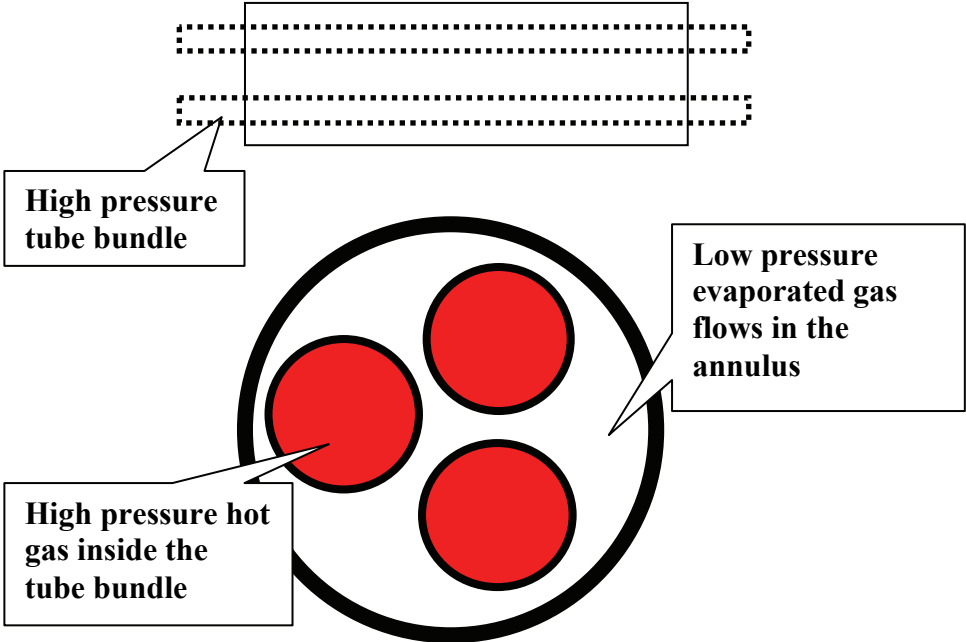


Table 2-4: Simple description of the suction gas heat exchanger design.

As found in the 2008 experiments, the suction gas heat exchanger allowed for a large increase in both COP and cooling capacity (Table 2-5) but unfortunately it also hindered a sufficiently high pressure due to overheating at the compressor outlet when attempting to produce hot water - at such conditions, the suction gas heat exchanger should have been far less efficient (Figure 2-5). The low pressure caused the pinch point to exist inside the gas cooler, which led to a high outlet temperature.

The results showed that the liquid carryover was much less than expected, and the SGHX transferred far more heat than necessary to evaporate liquid. This was particularly evident when attempting to produce hot water, experiments that proved impossible due to overheating at the compressor outlet. At the 60/15 experiment (Table 2-5) the cooling capacity and COP dropped compared to previous experiments without an SGHX, and it is assumed that this was

caused by a severe drop in the circulated mass, due to the increased specific volume at the compressor inlet caused by SGHX superheating.

Table 2-5: The result of installing the suction gas heat exchanger.

Conditions	Cooling capacity (kW)			COP (-)		
	Old	New	Change (%)	Old	New	Change (%)
50 bar, 10°C	16,4	17,2	4,8	1,8	2,0	8,8
60 bar, 10°C	34,4	34,7	0,8	3,1	3,3	6,6
70 bar, 10°C	24,7	37,7	52,7	3,0	3,2	7,9
80 bar, 10°C	26,2	36,7	40,0	2,3	2,9	25,4
	2007	2008		2007	2008	
60 bar, 15°C	26,1	23,9	-8,4	2,3	2,2	-2,8
70 bar, 15°C	30,6	34,0	11,4	2,5	2,9	15,8
80 bar, 15°C	27,8	34,8	25,4	2,3	2,7	17,9
90 bar, 15°C	26,9	33,4	23,9	2,0	2,4	22,6
70 bar, 20°C	21,9	32,5	48,3	1,8	2,7	52,7
80 bar, 20°C	29,8	33,3	11,7	2,1	2,6	20,8
90 bar, 20°C	27,7	31,6	14,3	1,9	2,3	22,0
80 bar, 25°C	28,0	31,5	12,4	2,0	2,4	21,5
90 bar, 25°C	26,6	30,5	14,8	1,7	2,2	27,3

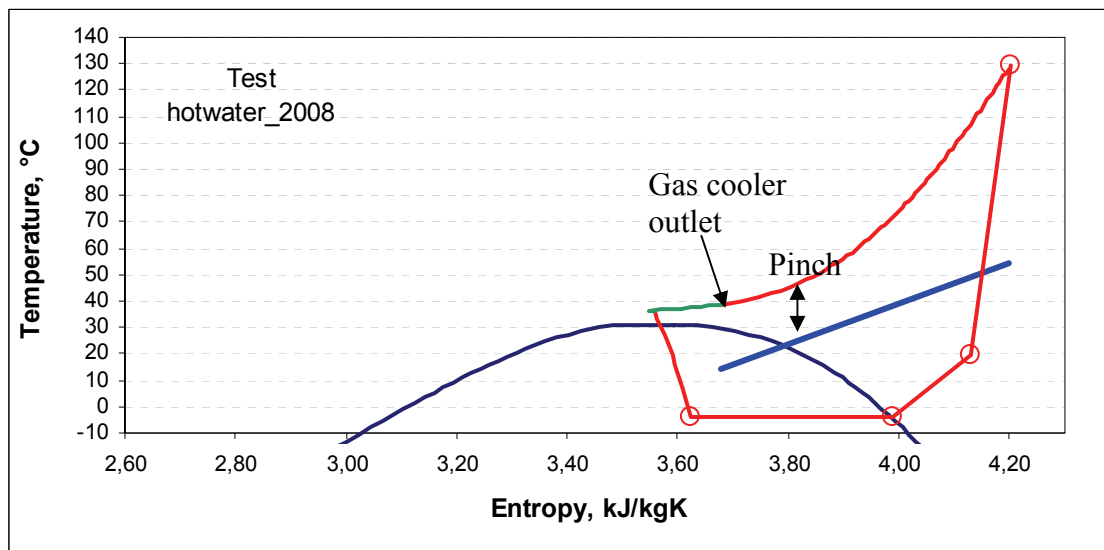


Figure 2-5: Attempted hot water production from the previous round of experiments. The compressor outlet temperature (circle, upper right corner) hindered a sufficiently high pressure, leading to a very high gas cooler outlet temperature.

2.2 Proposed and implemented system modification: SGHX bypass

As the system showed improvement with the SGHX installed, but failed to produce hot water, the idea of using a heat exchanger with variable efficiency was born. A system experiencing strongly varying operating conditions may need a very high efficiency suction gas heat exchanger at certain conditions, and none or very little SGHX capacity for others. The suggested improvement with a bypass valve in front of the SGHX (Figure 2-6) will ensure optimum efficiency at varying conditions. This modification will be explored further in this paper, both by simulations and through implementation in an actual system.

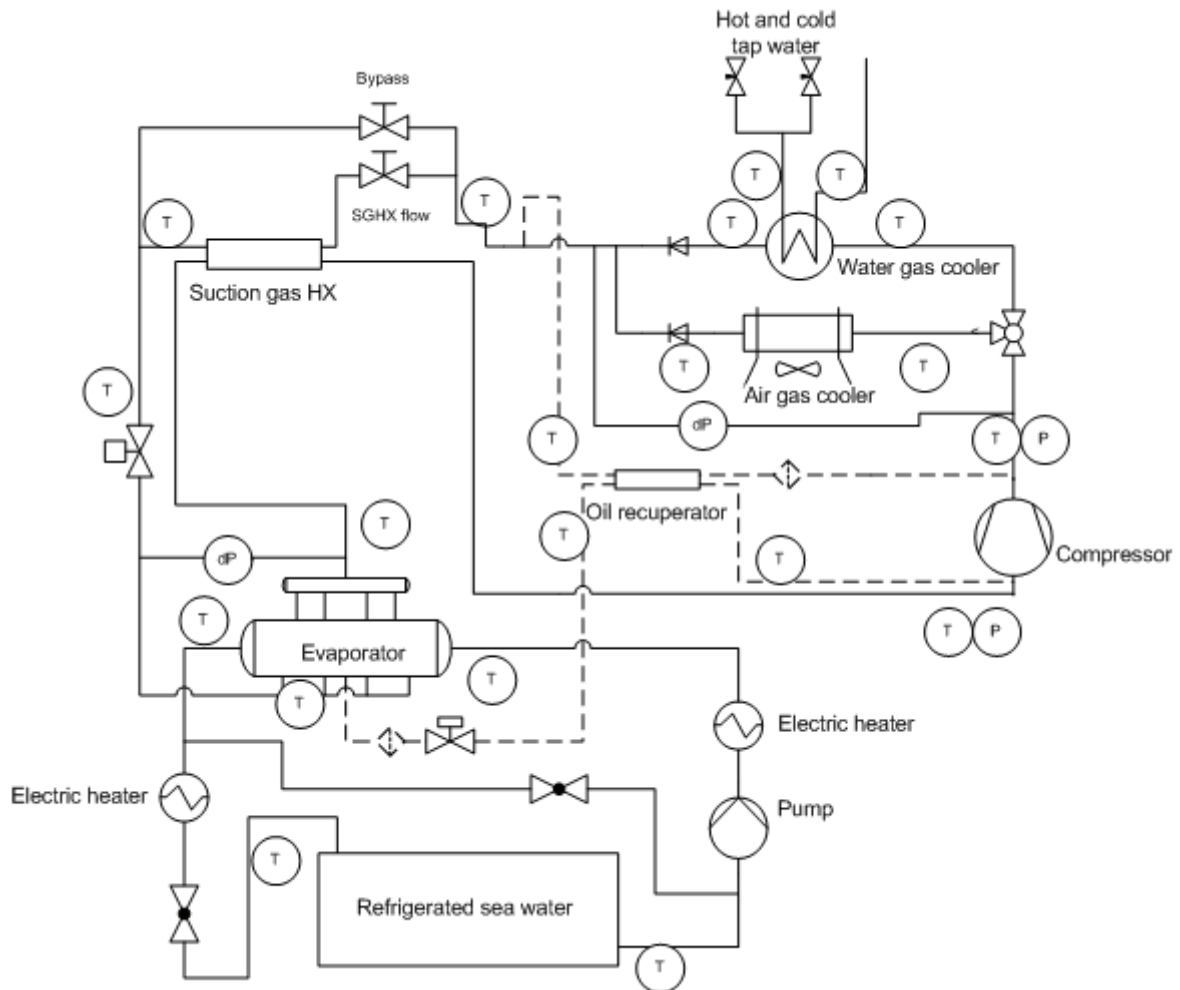


Figure 2-6: The modified system with a bypass valve in front of the suction gas heat exchanger. The bypass valve allows for variations in the SGHX efficiency by bypassing high pressure gas.

As an appropriate mixing valve was unobtainable, two ball valves were installed as shown in Figure 2-7. These valves made it possible to adjust the flow of high-pressure gas through the suction gas heat exchanger.

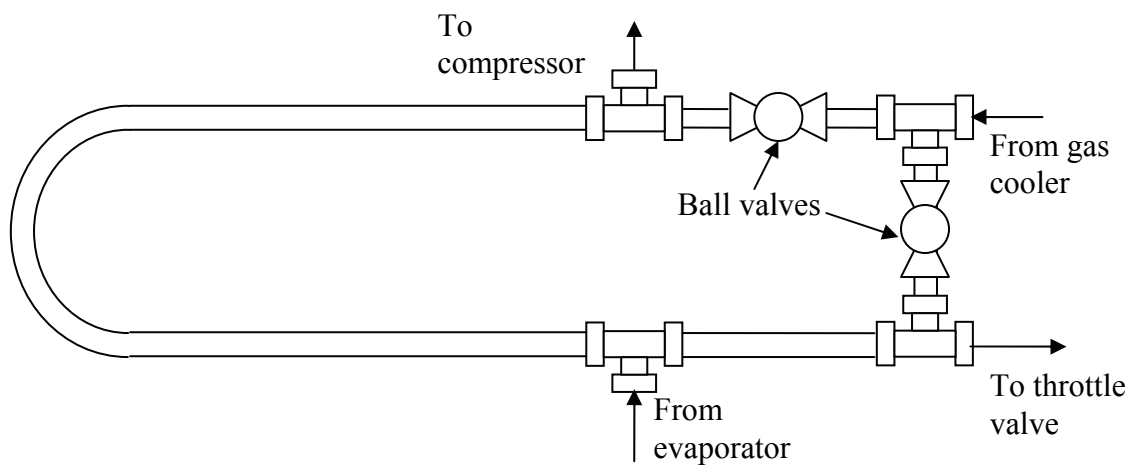


Figure 2-7: The modified suction gas heat exchanger. By opening the vertical ball valve and closing the horizontal ball valve one can bypass the suction gas heat exchanger.

3 System modeling

The system model was based on experimental data which was already available, both with (experiments from 2008) and without the suction gas heat exchanger installed (experiments from 2007). The model was kept fairly simple, but as will be shown, the results are adequate.

Einstein once made a statement on simplicity: “*It can scarcely be denied that the supreme goal of all theory is to make the irreducible basic elements as simple and as few as possible without having to surrender the adequate representation of a single datum of experience*” (Einstein, 1934), or as it became known in less academic circles, “*Make things as simple as possible, but not simpler*”.

3.1 Model tools

The component models are based on a library collection (*kktdlls*) made by SINTEF for calculating thermodynamic properties. The libraries had an Excel front-end, which made it logical to use Excel and macros to create a simple system model. For most cases, traditional model parameters were used, with the exception of pressure drops in the gas cooler and evaporator. All thermodynamic data are calculated using these libraries.

The *kktdlls* package contains several libraries. *rnlb* (a refrigerant library) was used for calculating water properties and finding dynamic viscosity for carbon dioxide. *co2lib* (a library for calculation of thermodynamic properties based on Span-Wagners equation of state for carbon dioxide) was used to find all carbon dioxide related properties except dynamic viscosity, and finally *htclib*, a library for calculation of convection coefficients, was used for heat transfer calculations for both carbon dioxide and water in the gas cooler model.

3.2 Compressor model

The compressor has a swept volume of 143.14ccm per revolution, giving a swept volume (V_{swept}) of 12.46 m³/hour at full speed (1451 RPM). Some initial tests after installation indicated that the assumed isentropic and volumetric efficiencies previously used for calculation were not suitable, and it was decided to make new models based on previous measurements. The model uses the pressure ratio (p_r) as a variable to calculate volumetric (λ) and isentropic (η_{is}) efficiency. Both models are based on the work performed on the gas, calculated using the inlet and outlet properties, as well as the circulated mass of CO₂ based on the gas cooler heat balance.

The isentropic efficiency was calculated as

$$\eta_{\text{is}} = \frac{h_{\text{compr out, isentropic}} - h_{\text{compr, in}}}{h_{\text{compr out, measured}} - h_{\text{compr, in}}} \quad (3.1)$$

and the volumetric efficiency as

$$\lambda = \frac{\dot{m}_{\text{co2, gc}} V_{\text{compr, in}}}{\dot{V}_{\text{swept}}} \quad (3.2)$$

The resulting models are shown in Figure 3-1 and Figure 3-2. The data table used for calculation can be found in Appendix 12.

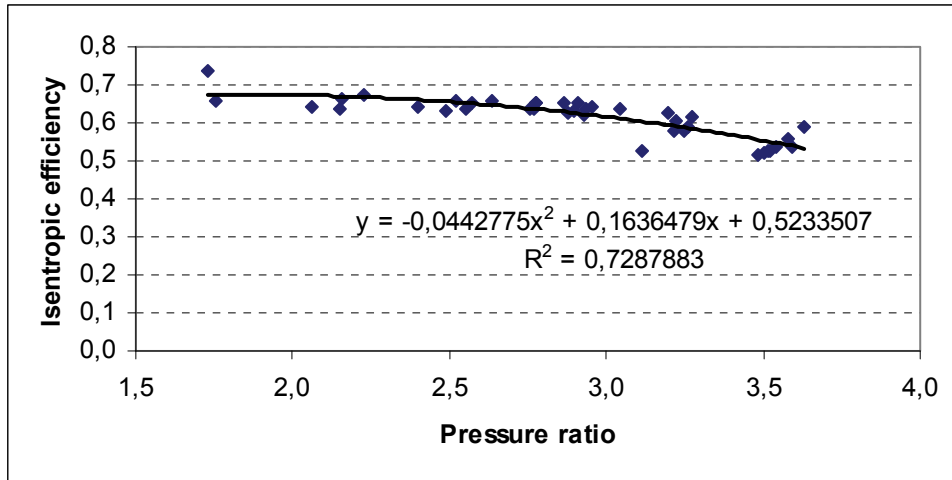


Figure 3-1: Compressor isentropic efficiency as a function of the pressure ratio (p_{out}/p_{in}) based on experimental data.

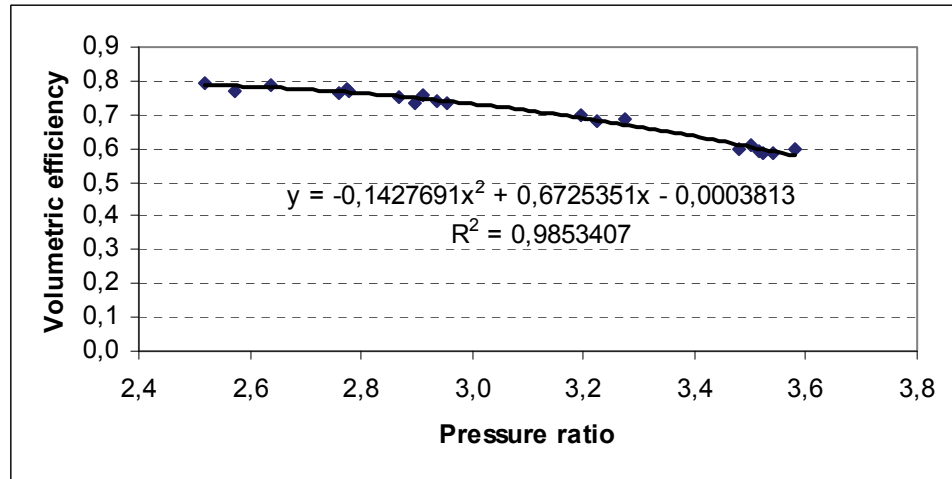


Figure 3-2: Compressor volumetric efficiency as a function of the pressure ratio based on experimental data.

The compressor model uses the following equations:

$$\dot{V}_{swept} = 0.000143139 \cdot \frac{\text{RPM}}{60} \left[\frac{\text{m}^3}{\text{s}} \right] \quad (3.3)$$

$$\dot{V}_{suction} = \dot{V}_{swept} \cdot \lambda \quad (3.4)$$

$$h_{discharge} = h_{suction} + \frac{(h_{isentropic} - h_{suction})}{\eta_{is}} \quad (3.5)$$

$$\eta_{is} = -0.0442775 p_r^2 + 0.1636479 p_r + 0.5233507 \quad (3.6)$$

$$\lambda = -0.1427691 p_r^2 + 0.6725351 p_r + 0.0003813 \quad (3.7)$$

$$p_r = \frac{p_{discharge}}{p_{suction}} \quad (3.8)$$

$$\dot{m}_{circulated} = \dot{V}_{suction} \cdot \rho_{suction} \quad (3.9)$$

$$\dot{W}_{compressor} = \dot{m}_{circulated} (h_{discharge} - h_{suction}) \quad (3.10)$$

3.3 Gas cooler model

To calculate the temperature approach, a finite element approach with ten sections was used. For simplicity, the heat exchanger was calculated as a single concentric straight tube with a length of 4.85 meters, and the dimensions described in Table 2-1. The length was tuned using previous experiments and showed good accuracy. The solution approach used can be seen in Appendix 11.

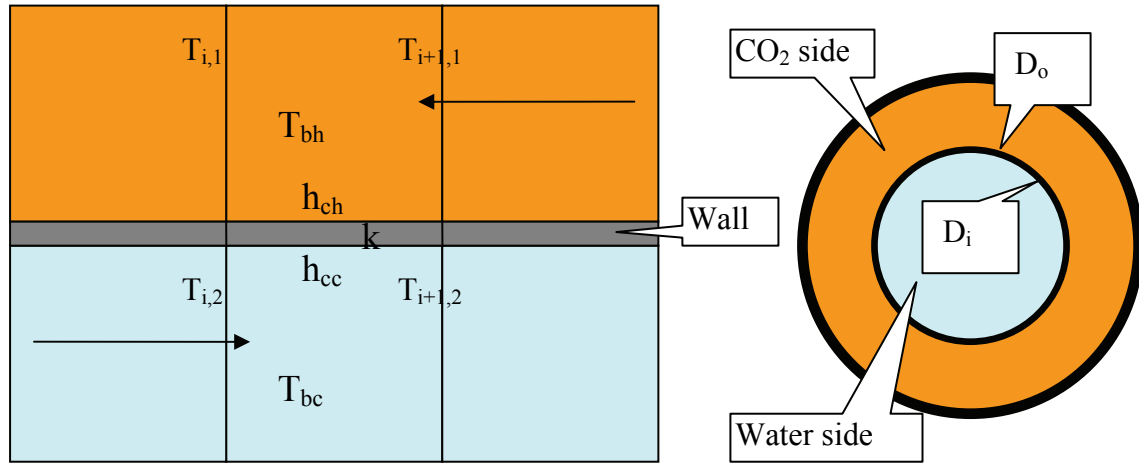


Figure 3-3: The finite elements, directions, symbols and indexing used in the gas cooler simulation.

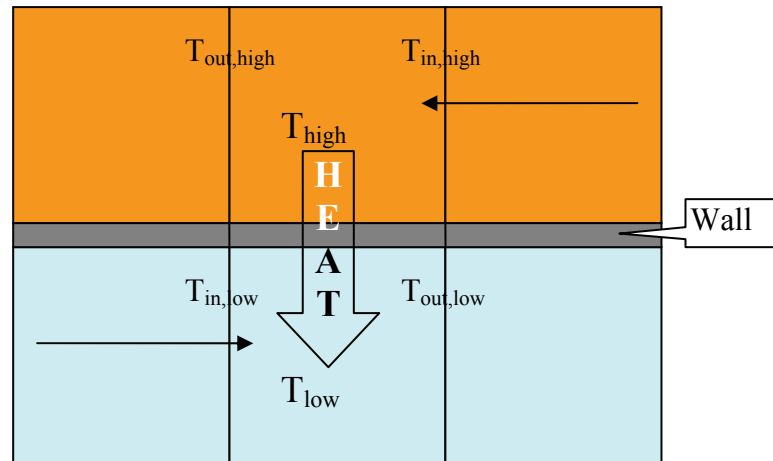


Figure 3-4: The gas cooler sections. The upper part is the hot gas stream from the gas cooler; the lower part is the cold gas stream from the evaporator. The flow is counter-current.

$$\dot{Q}_{convective} = \frac{T_{high} - T_{low}}{R_{tot}} \quad (3.11)$$

$$R_{tot} = \frac{1}{A_{inner} \cdot h_{inner}} + \frac{L/n_{sections}}{2\pi k} \ln(D_o/D_i) + \frac{1}{A_{outer} \cdot h_{outer}} \quad (3.12)$$

$$\dot{Q}_{flow} = \dot{m}_{co2} (h_{co2,gc in} - h_{co2,gc out}) \quad (3.13)$$

$$Error = Q_{convective} - Q_{flow} \quad (3.14)$$

T_{high} and T_{low} are the bulk temperatures in the section on the high and low-pressure side of the gas cooler, calculated as the section average of the inlet and outlet temperature. h is the convective heat transfer coefficient, k is the thermal conductivity of the wall. D_i is the inner diameter of the small inside tubes (CO₂ tubes), D_o is the outer diameter. A_{inner} is the section area based on the inner circumference and section length, and A_{outer} is the section area based on the inner tube's outer circumference. The wall heat resistance equation (3.12) was based on equations from Incropera et al (2007c).

The first attempts to create a gas cooler model showed poor accuracy for low cooling water flow rates. The heat transfer for low water flow rates were underestimated. An explanation can be that in real life, the tube bends in the gas cooler induces more turbulence than a straight tube, and consequently the model underestimated the heat transfer for low cooling water flows, giving too high gas cooler outlet temperatures (Appendix 6). In order to compensate for this, it was decided to introduce a factor that narrows the effective tube cross sectional area, thereby increasing the convection coefficient. The factor decreases linearly until 600 l/h:

$$F_{reduction} = \max(1 + 0.001 \cdot (600 - massflow); 1.0), \quad (3.15)$$

where *massflow* is the cooling water flow in kg/hour

600 l/h was chosen based on the error calculations shown in Figure 11-2 (Appendix 6).

At 10°C cooling water, 600 l/h corresponds to a Reynolds number (Re) of approximately 3000 in the gas cooler. The transition from laminar to turbulent flow is usually set to 2300, but fully turbulent conditions are not reached until Re is around 10000 (Incropera et al, 2007d), so a shift below Re of 3000 is understandable, and can be the cause of the need for such a modification. The Reynolds number was calculated using the equation

$$Re = \frac{UD_h}{\nu}, \quad (3.16)$$

where U is the bulk water velocity, D_h is the hydraulic diameter for an annulus (eq. (11.18)) and ν is the kinetic viscosity.

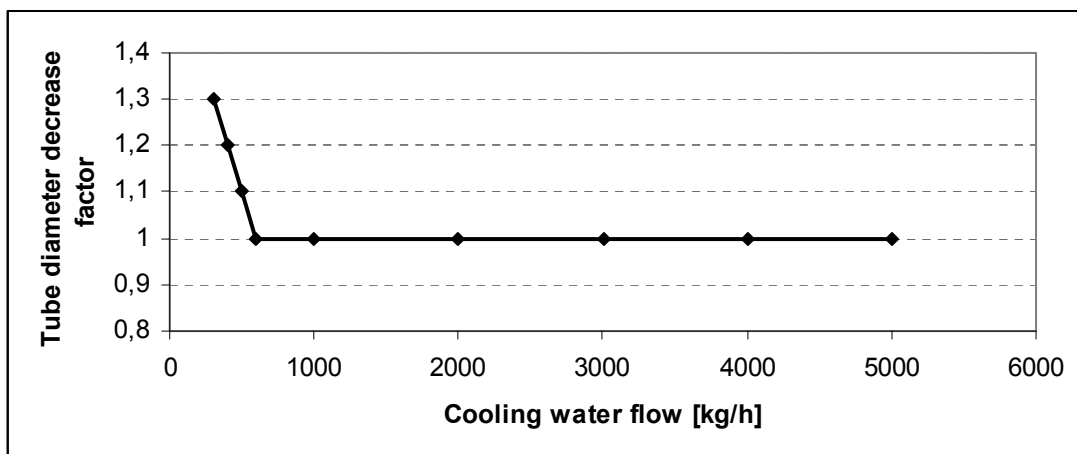


Figure 3-5: Tube cross sectional area decrease factor declines linearly from 600 to 300 kg/h.

By using the reduction factor, the model could predict the gas cooler outlet temperature to within 1K for all the previous experimental data (Figure 3-6).

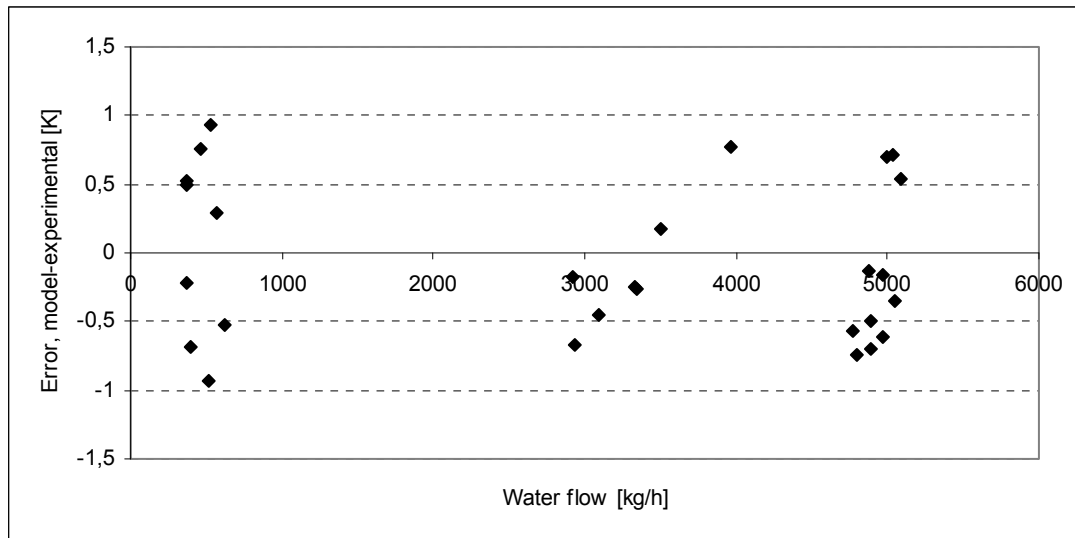


Figure 3-6: Altering the effective water tube cross sectional area for calculation of the convection coefficient reduces the low cooling water flow error.

The overall gas cooler pressure drop was modeled with just the mass flow as input, based on the 2007 measurements without a suction gas heat exchanger (Appendix 7). The mass flow used was the flow calculated using the compressor volumetric efficiency and revolution speed.

$$dP_{GC} = (1.8469 \text{ m}^2 - 9.1012 \text{ m}) \cdot 10^3 \text{ [Pa]} \quad (3.17)$$

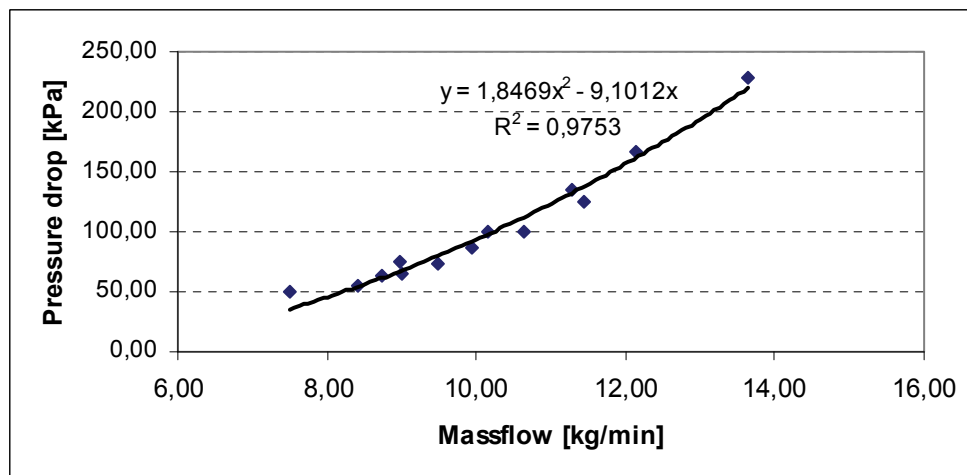


Figure 3-7: Gas cooler pressure drop model.

3.4 Suction gas heat exchanger model

In the 2008 experiments, the suction gas heat exchanger (SHGX) showed a quite stable U-value in the transcritical area, with values ranging from 1425.8-1572.0 W/m²K, with an average of 1479.63 W/m²K, based on the inner area (Appendix 14). The average value was used to estimate the maximum performance of the SGHX. If the heat transfer exceeded this value, the result was discarded (see Figure 3-13 and equation (3.21)).

The SGHX was calculated as if there was full flow through the SGHX, but with the efficiency changed. In the experiments, the SGHX flow was adjusted with the choke inlet temperature as the variable.

The SGHX low side pressure drop was calculated from the total pressure drop between the evaporator outlet and the compressor suction. A suction pipe pressure drop model from previous experiments (section 3.7) was subtracted, and the remaining drop was assumed to be a result of the SGHX. This is by far an ideal model, but it's good enough for this use. The high side pressure drop was assumed to be low (pressure loss relative to the high pressure), and the pressure drop was therefore ignored on the SGHX high side. This model can, not be verified, as no measurements of the SGHX are made in the current system setup.

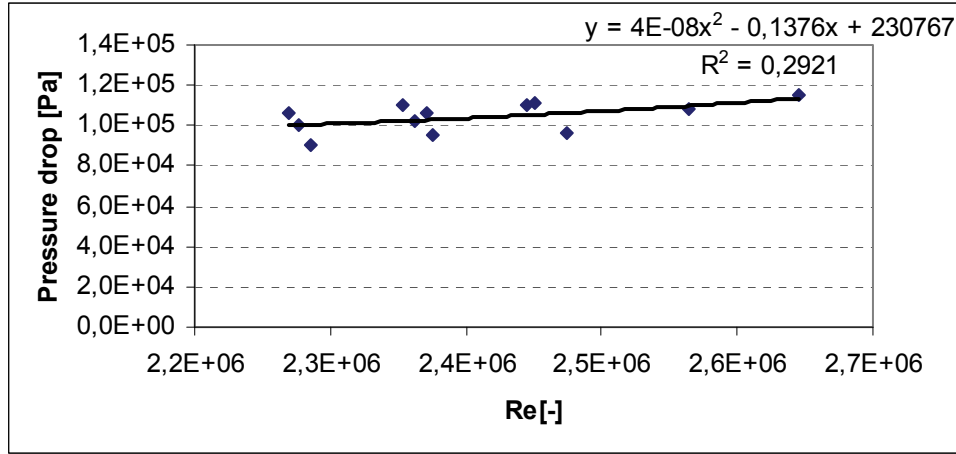


Figure 3-8: Suction gas heat exchanger pressure drop model.

Heat transfer from the high pressure side in the SGHX was calculated as follows:

$$\dot{Q}_{\max} = \dot{m} \cdot \min((h_{in} - h_{out})_{hot}, (h_{out} - h_{in})_{cold}) \quad (3.18)$$

$$\dot{Q}_{transferred} = \dot{Q}_{\max} \cdot \epsilon_{SGHX} \quad (3.19)$$

$$h_{out} = h_{in} - \dot{Q}_{transfer} / \dot{m} \quad (3.20)$$

Within the same system iteration (more on the iterative approach in section 3.8), the high-pressure side heat transfer was added to the cold side (low pressure) stream, so for each iteration, there is heat balance over the SGHX. In order to check for a viable solution (obtainable in the actual system), a validity check for suction gas heat exchanger was introduced:

$$\dot{Q}_{transfer} \leq \Delta T_{LMTD} \cdot A_{HX} h_{\text{experimental}} \quad (3.21)$$

where $h_{\text{experimental}}$ is the average heat transfer coefficient and the logarithmic mean temperature difference (Incropera et al, 2007b):

$$\Delta T_{LMTD} = \frac{(T_{SGHX,HPin} - T_{SGHX,LPout}) - (T_{SGHX,HPout} - T_{SGHX,LPin})}{\ln \frac{(T_{SGHX,HPin} - T_{SGHX,LPout})}{(T_{SGHX,HPout} - T_{SGHX,LPin})}} \quad (3.22)$$

3.5 Choke valve model

The throttling was assumed isenthalpic based on the temperature measurement in front of the throttle valve and the gas cooler outlet pressure.

$$h_{choke,out} = h_{choke,in}(T_{choke,in}, P_{choke,in}) \quad (3.23)$$

$$P_{out} = P_{sat}(t_{evap}) \quad (3.24)$$

$$t_{out} = t_{evap} \quad (3.25)$$

3.6 Evaporator model

The evaporator pressure drop was modeled using the saturated gas flow rate (by the assumption that the liquid has very low influence on the pressure drop), calculated using the evaporator inlet temperature. The model was based on the 2007 experiments (Appendix 9).

$$dP_{evap} = (2 \cdot 10^7 \cdot V_{satflow}^2 - 26466 \cdot V_{satflow}) \cdot 10^3 \text{ [Pa]} \quad (3.26)$$

$$V_{satflow} = \dot{m} \cdot v_{satgas}(t_{evap}) \quad (3.27)$$

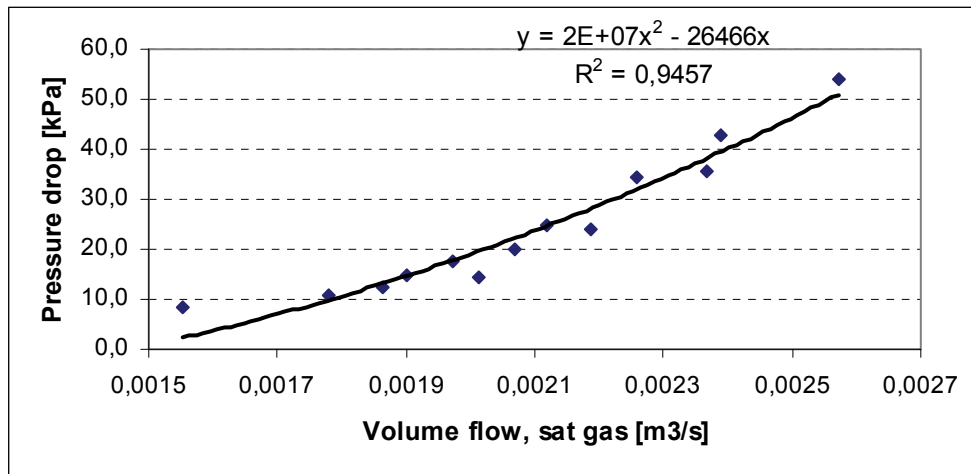


Figure 3-9: Evaporator pressure drop model based on experimental results.

The evaporator heat transfer was not modeled, but the evaporation temperature itself was used as an input parameter in the simulation, rather than simulating the evaporator using water temperature and charge level. An outlet superheat of 1K was chosen, even though liquid carryover may occur. This choice was made because the previous experiments show a rather low liquid carryover, and it simplified the calculations. This superheating assumption is also more interesting for properly designed systems without liquid carryover. The outlet temperature was calculated as

$$T_{evap,out} = T_{sat}(P_{evap,out}) + 1^{\circ}C \quad (3.28)$$

3.7 Suction pipe model

The suction pipe pressure drop was modeled using the Reynolds number, based on *average properties* in the suction pipe. The enthalpy was assumed constant (negligible heat transfer).

$$dP_{suction} = -0.00000007 \text{Re}^2 + 0.2578\text{Re} \text{ [Pa]} \quad (3.29)$$

$$\text{Re} = \frac{\bar{\rho}\bar{U}\bar{D}}{\bar{\mu}} \quad (3.30)$$

Dynamic viscosity calculated using rnlb, other properties calculated using co2_lib.

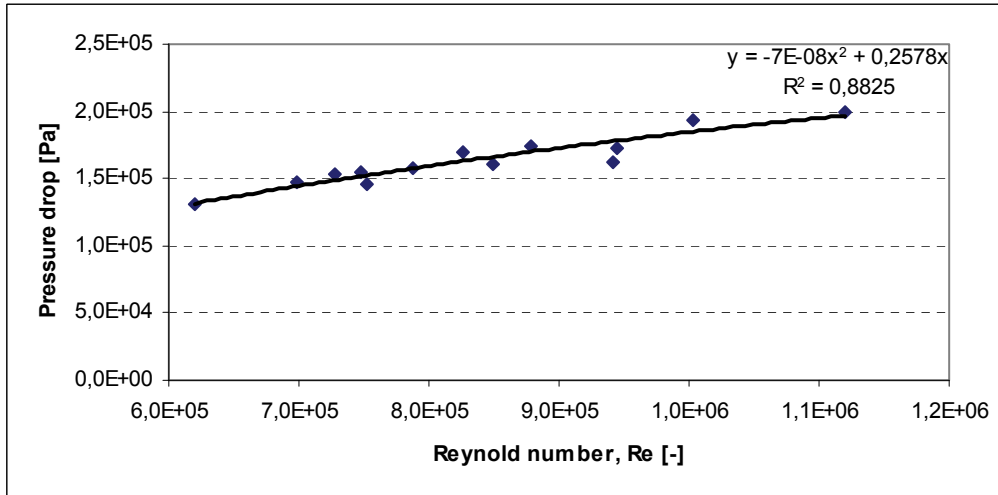


Figure 3-10: Suction pipe pressure drop as a function of the Reynolds number, calculated from 2007 the experimental data.

3.8 Assembled model, solution approach

The calculation model was simplified as mentioned earlier. The pipes connecting the system components were not modeled, except for the suction pipe pressure drop, but as can be seen from the numbering the model is prepared for such calculations (Figure 3-11). Points 5 and 6 were not used in the current model, but they were included in order to facilitate future model improvements.

An upper limit of 130°C was set on the compressor outlet temperature, as higher temperatures were feared to cause decomposition of the lubrication oil.

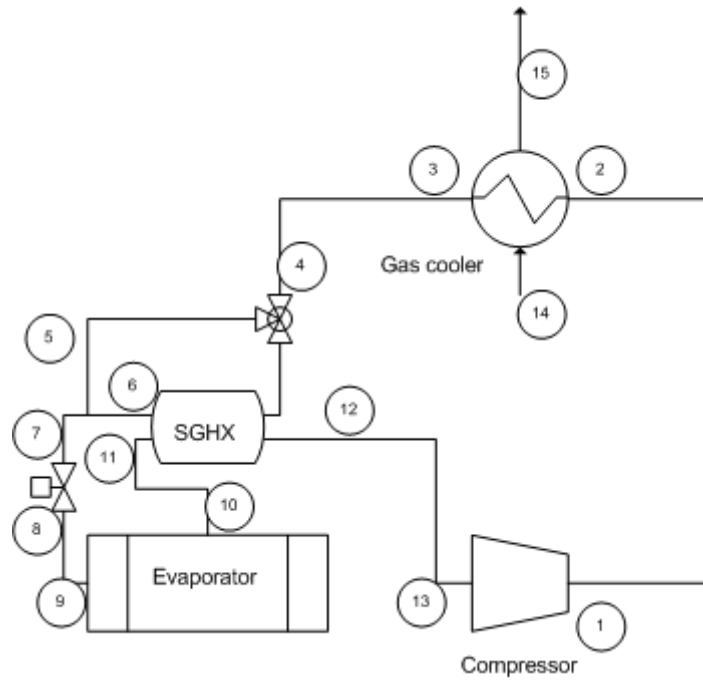


Figure 3-11: The simplified system and array numbering used in the system. Points 5 and 6 were not used (they were set equal to point 7), as the SGHX was not modeled in detail.

In order to reach a system solution a number of iterations had to be made because of interdependency (Figure 3-12). The iterative approach is shown schematically in Figure 3-13.

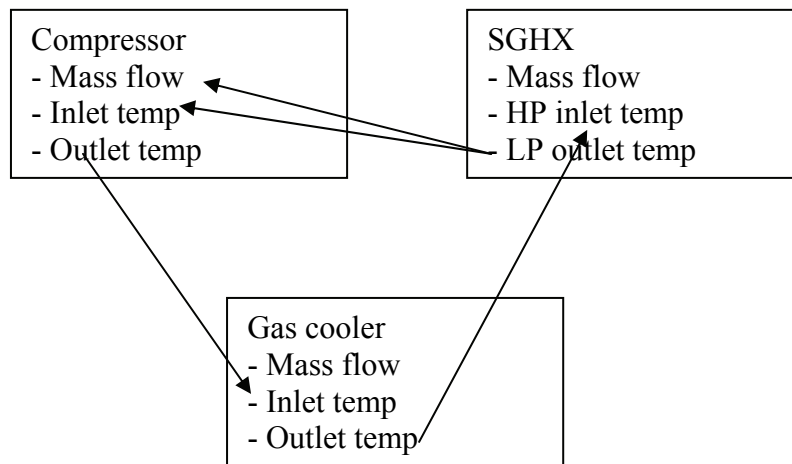


Figure 3-12: Some of the system interdependencies.

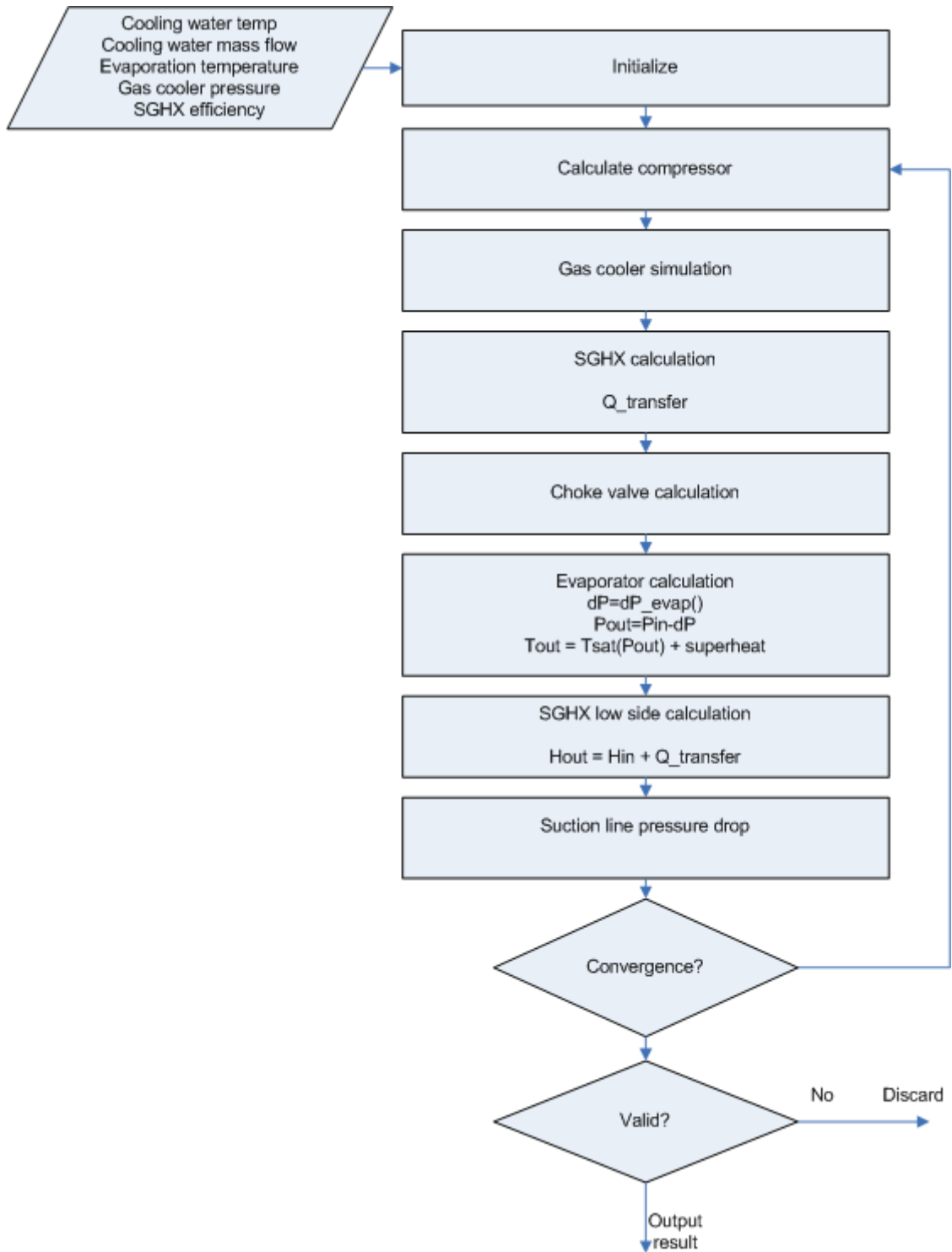


Figure 3-13: The iterative approach for solving the system.

4 System optimization

The optimization process is focused on transcritical operation, as this has particular use for high pressure control. The goal of this master thesis is not to find the perfect optimization algorithm; the purpose here is to see if the concept of a variable SGHX can be beneficial. The simulations were run with a number of combinations of pressure and SGHX efficiency, and then automatically choosing the setting combination which provided the highest COP. As the SGHX efficiency is not directly measurable in a real system, the throttling valve inlet temperature was selected as the controlled parameter in addition to the gas cooler pressure.

4.1 Goal function

The system simulations calculate all properties of the system. The goal function outputs the COP (neglecting brine pump work), and by running combinations of gas cooler pressure and SGHX efficiency the highest COP for each cooling water flow, cooling water temp and evaporation temperature (later referred to as operating conditions) was selected.

The system COP was calculated using the cooling capacity and compressor work,

$$COP = \frac{h(T_{evap,out}, P_{evap,out}) - h(T_{choke}, P_{gc,out})}{h(T_{compr,out}, P_{compr,out}) - h(T_{compr,in}, P_{compr,in})} \quad (4.1)$$

If the system did not converge or the converged result violated any of the restrictions set (exceeding the maximum compressor outlet temperature (130°C) or the heat transfer was higher than obtainable in the SGHX), the COP was set to zero.

For water heating (combined cooling and heating) it was necessary to use a trial and error approach on the cooling water flow in order to reach the desired outlet temperature, since the highest COP for a given cooling water flow not necessarily meant that the correct water temperature had been reached.

4.2 Proof of concept

In order to show the use of the variable SGHX concept, a series of simulations was run with a theoretical suction gas heat exchanger with a maximum efficiency of 0.9; in other words, the SGHX heat transfer restriction was temporarily removed from the system simulation model. The simulations were run at full cooling water flow (5000 kg/h) with inlet temperatures ranging from 10 to 50 °C. Simulations were also run with constant SGHX efficiencies of 0.3 and 0.6 in order to plot the differences. The compressor outlet temperature was limited to 130 °C.

Table 4-1: Pressure and SGHX combinations used for proof of concept

Variable	Low	High	Step size	# Steps
Pressure [bar]	74	110	2	19
SGHX efficiency [-]	0	0.9	0.1	10
Total combinations				190

As seen in Figure 4-2, the COP can deviate far from the optimum with different cooling water temperatures for a given SGHX efficiency.

The figure also shows that the SGHX efficiency has very little influence on the system performance for low cooling water temperature. This confirms the statement by Sarkar et al (2004): “...the performance of internal heat exchanger has a minor influence on system optimization at low and moderate gas cooler exit temperatures”. The concept of a suction gas heat exchanger is therefore expected to only give minor improvements in system efficiency when in cooling mode (high cooling water flow).

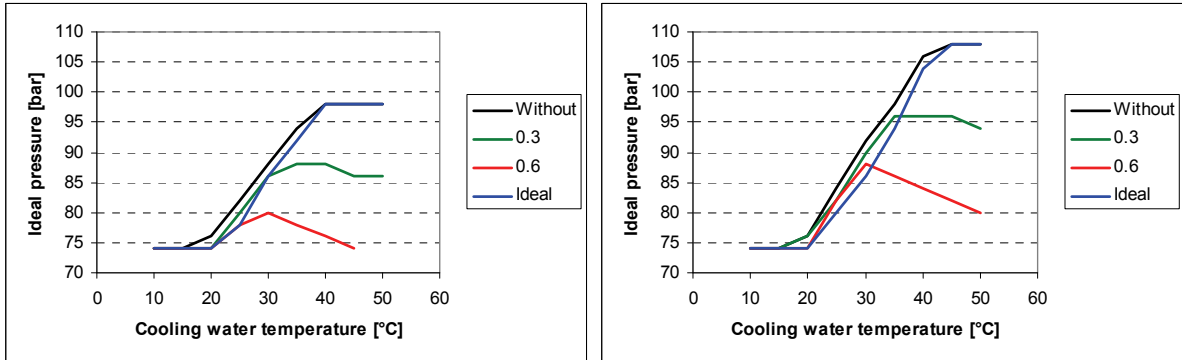


Figure 4-1: Ideal pressure varies with both cooling water temperature and SGHX efficiency for -6°C (left) and -2°C (right).

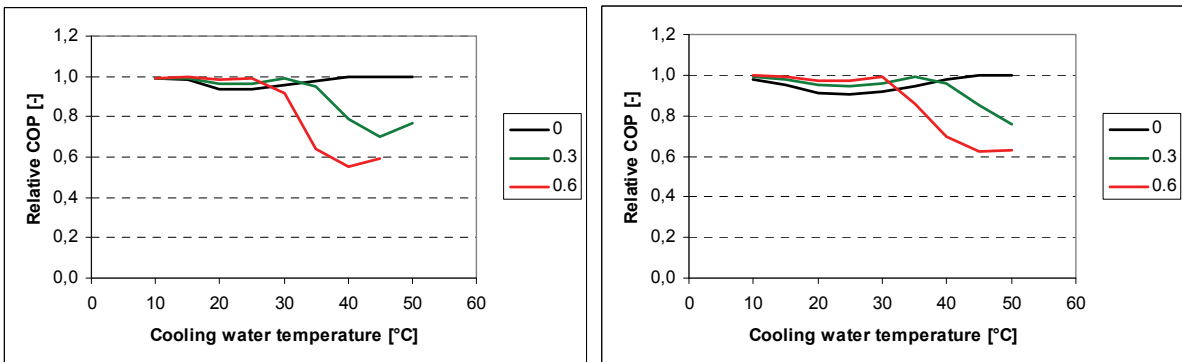


Figure 4-2: Relative COP using different SGHX efficiencies for evaporation temperature -6°C (left) and -2°C (right). The relative COP using the ideal SGHX efficiency is unity (1). A relative COP of 0.8 means the setting gives a COP of only 80% compared to the optimum setting.

For low cooling water temperatures it seems that higher is better when it comes to SGHX efficiency, but only until a certain point (Figure 4-3, left). This point is dependent on the evaporation temperature. However, this shift is not as clear when looking at the choke inlet temperature (right), and has to do with how the efficiency is calculated.

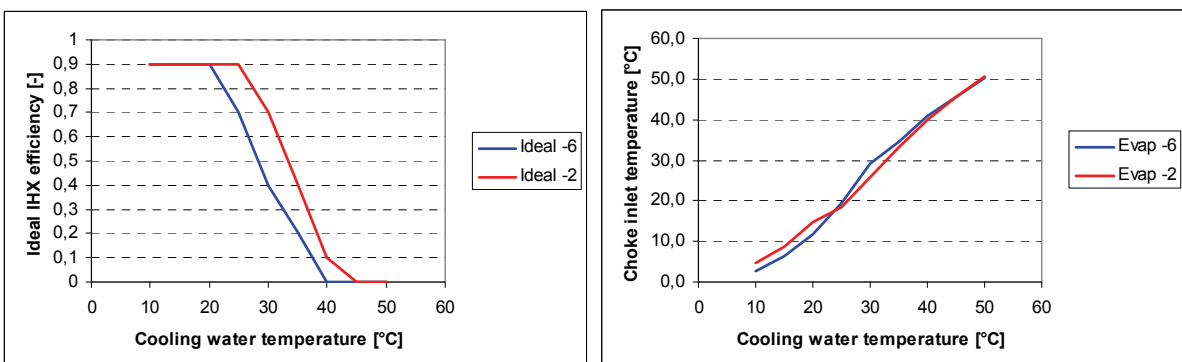


Figure 4-3: Ideal SGHX efficiency (left) and the corresponding choke inlet temperature (right) varies with both the cooling water temperature and evaporation temperature.

4.3 Optimization, system cool down

Compressor outlet pressure was limited to between 74 and 110 bara, and the suction gas heat exchanger efficiency was limited between 0 and 0.6 based on previous experimental results (Appendix 19). The compressor outlet temperature was limited upwards to 130 °C.

Table 4-2: Variable combinations for each operating condition (cooling water temp, cooling water flow, evaporation temperature) used for batch simulations.

Variable	Low	High	Step size	# Steps
Pressure [bara]	74	110	2	19
SGHX efficiency [-]	0	0.6	0.1	7
Total combinations				133

In stead of looking at the SGHX efficiency, the more easily measurable choke inlet temperature was chosen as the control parameter for SGHX bypass. The system cool down (pull down) simulations show how the ideal pressure and choke inlet temperature varies with the evaporation temperature (Table 4-3, Figure 4-4 and Figure 4-5). Both the pressure and choke inlet temperature show an increasing trend as a function to the evaporation temperature. Increasing cooling water temperature also seems to increase the optimum pressure and choke inlet temperature.

Table 4-3: Ideal choke valve inlet temperatures at 5000 kg/h cooling water flow.

Cooling water temp [°C]	Evaporation temperature [°C]								
	-6	-4	-2	0	2	4	6	8	10
10	7,5	8,4	9,3	10,3	12,1	13,2	-	-	-
15	11,3	13,5	14,7	15,9	18,3	19,6	20,9	21,9	-
20	17,8	20,7	20,6	22,0	23,4	24,5	25,8	25,7	26,8
25	21,7	23,2	24,6	24,7	26,0	27,4	28,5	28,6	29,7

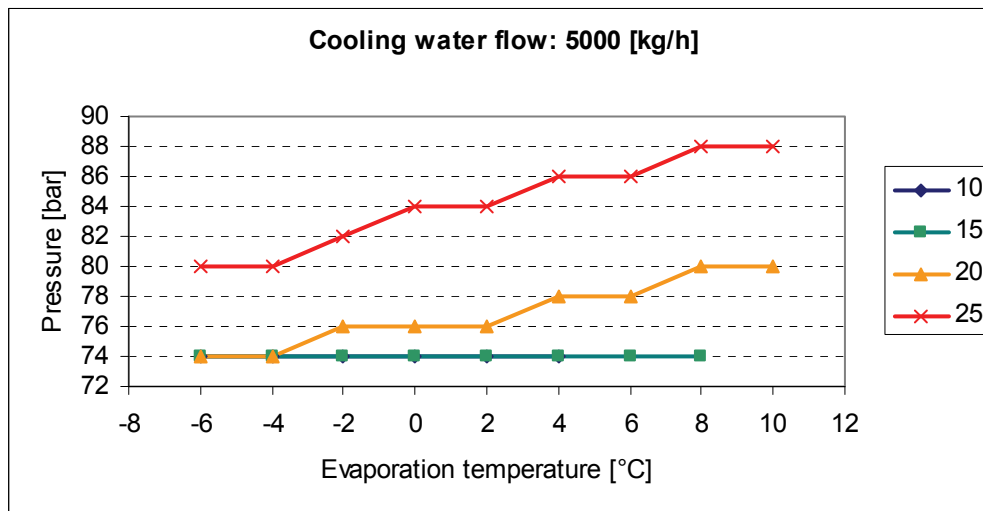


Figure 4-4: Ideal pressure as a function of evaporation temperature and cooling water temperature. The 10 and 15 °C cooling water temperature curves overlap. The step shape is a result of the resolution used for optimization, in this case 2 bar.

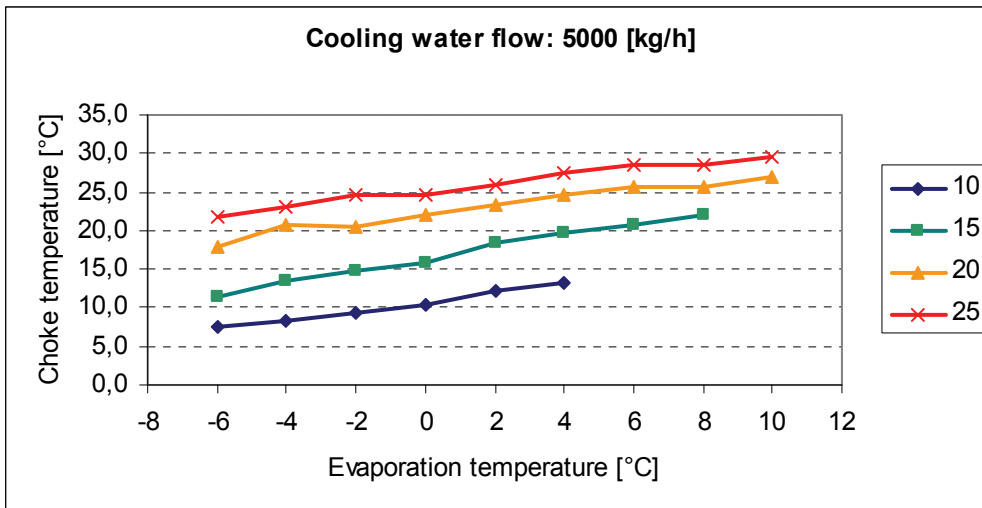


Figure 4-5: Ideal choke valve inlet temperatures as a function of evaporation temperature and cooling water temperature.

The ideal SGHX efficiency shows a declining trend with increasing evaporation temperature (Figure 4-6). It's easy to confuse this with a bypass, but in fact the maximum efficiency for this suction gas heat exchanger is reduced as the evaporation temperature increases, due to the decreased temperature difference. The maximum efficiency can be seen in Figure 4-7, which show that the ideal SGHX efficiency is near the maximum possible when using full cooling water flow.

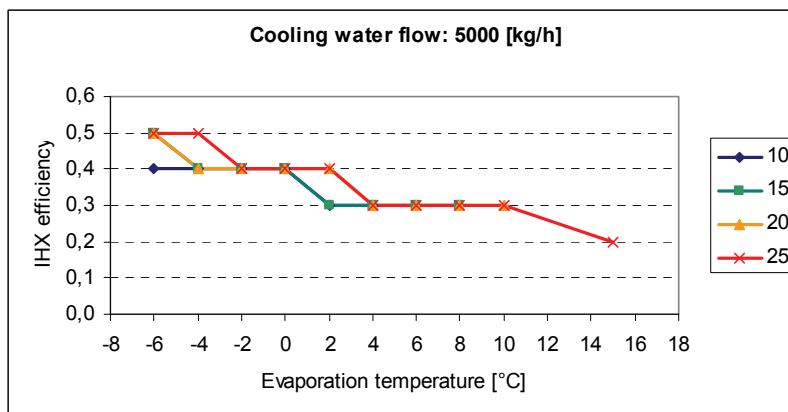


Figure 4-6: The ideal IHX (SGHX) efficiency as a function of evaporation temperature and cooling water temperature.

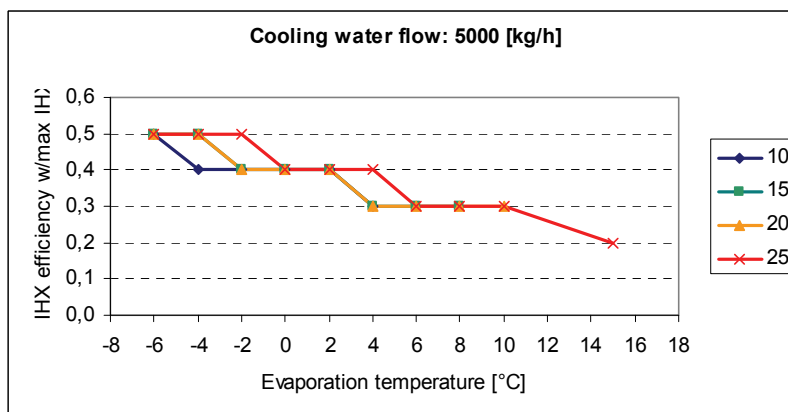


Figure 4-7: The maximum achievable SGHX efficiency at different evaporation temperatures.

4.4 Optimization, cooling mode

For cooling, an evaporation temperature of -6°C was selected based on previous experimental results (Appendix 19). The variable combinations were the same as for the pull down simulations (Table 4-2). Table 4-4 and Table 4-5 show the ideal pressure and choke valve inlet temperatures for 3000 and 5000 kg/h cooling water flow.

Table 4-4: Ideal pressure and choke inlet temperatures for medium cooling water flow rate.

Cooling water temp [$^{\circ}\text{C}$]	Cooling water flow [kg/h]	Evaporation temp [$^{\circ}\text{C}$]	Pressure [bara]	Choke temp [$^{\circ}\text{C}$]	COP [-]
10	3000	-6	74	9,9	2,78
15	3000	-6	74	16,1	2,52
20	3000	-6	78	20,5	2,18
25	3000	-6	84	23,4	1,88

Table 4-5: Ideal pressure and choke inlet temperatures for high cooling water flow rate.

Cooling water temp [$^{\circ}\text{C}$]	Cooling water flow [kg/h]	Evaporation temp [$^{\circ}\text{C}$]	Pressure [bara]	Choke temp [$^{\circ}\text{C}$]	COP [-]
10	5000	-6	74	7,5	2,92
15	5000	-6	74	11,3	2,72
20	5000	-6	74	17,8	2,45
25	5000	-6	80	21,7	2,06

A three dimensional plot of the possible combinations for low cooling water temperature and high flow rate shows the low SGHX sensitivity as close to no gradient in the IHX /SGHX direction (Figure 4-8).

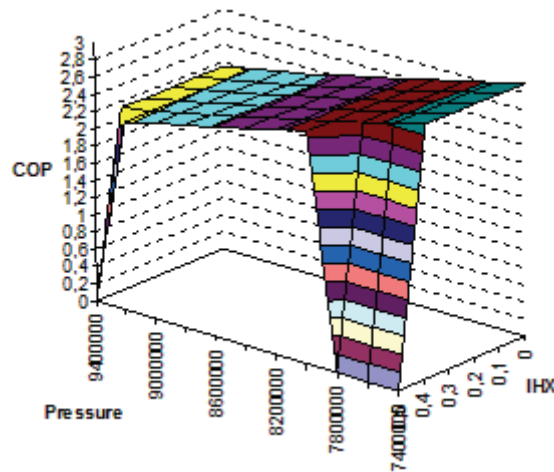


Figure 4-8: The solution space for 10°C and 5000 kg/h cooling water at an evaporation temperature of -6°C . Note the expected absence of inclination for the SGHX (IHX) efficiency (described in section 4.2).

As expected, the ideal pressure increases as the cooling water flow is reduced (Figure 4-9) in order to maintain a low gas cooler outlet temperature. The ideal choke temperature also increases with reduced cooling water flow, due to an increase in the gas cooler outlet temperature (this was explained in section 1.5.3).

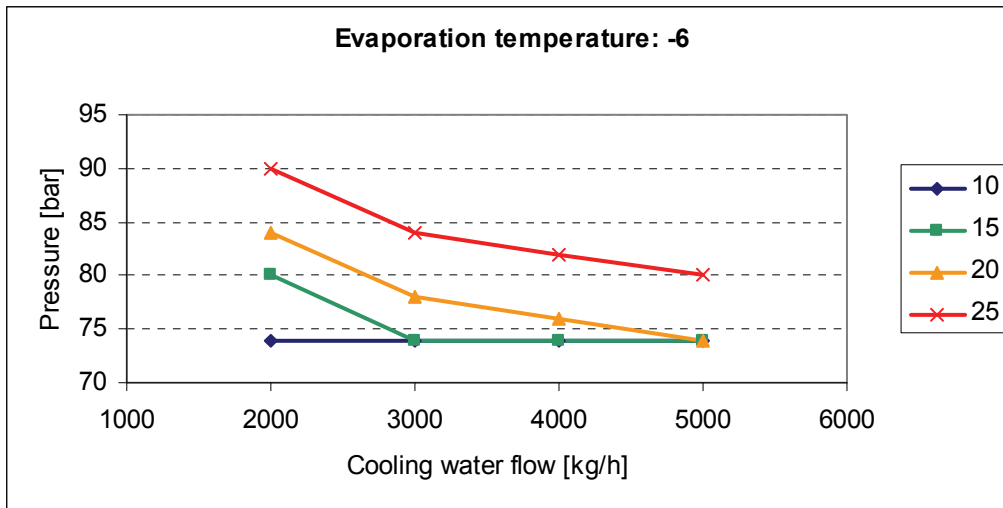


Figure 4-9: Ideal pressure as a function of cooling water flow rate for an evaporation temperature of -6°C.

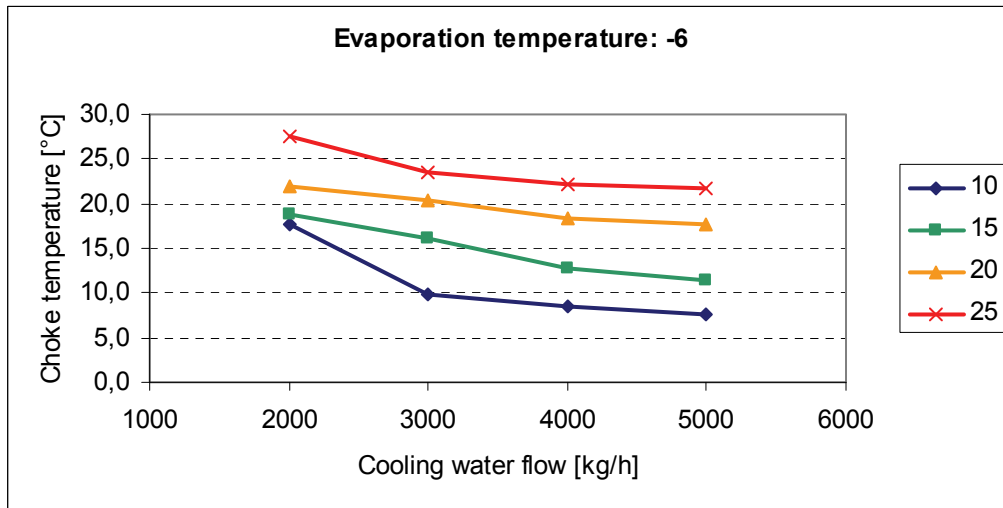


Figure 4-10: Ideal choke valve inlet temperature as a function of cooling water flow for an evaporation temperature of -6°C.

4.5 Optimization, water heating mode

Water heating was previously not possible (2008 experiments) using the installed suction gas heat exchanger because of overheating at the compressor outlet (Figure 2-5). The optimization results show that no internal heat exchange is desired for hot water production (Table 4-6), and that the maximum pressure before overheating is 108 bar at -2 °C (the evaporation temperature was kept constant at -2°C), and this pressure remains constant for all the low water flows. Note that the goal was set to produce the desired hot water temperature at the highest possible COP. Higher COP was possible for the given flow rates, but these resulted in lower hot water temperatures. If one were to use a higher SGHX efficiency, the pressure would have to be reduced significantly in order to prevent overheating at the compressor outlet (Figure 4-1), which would have reduced the system efficiency.

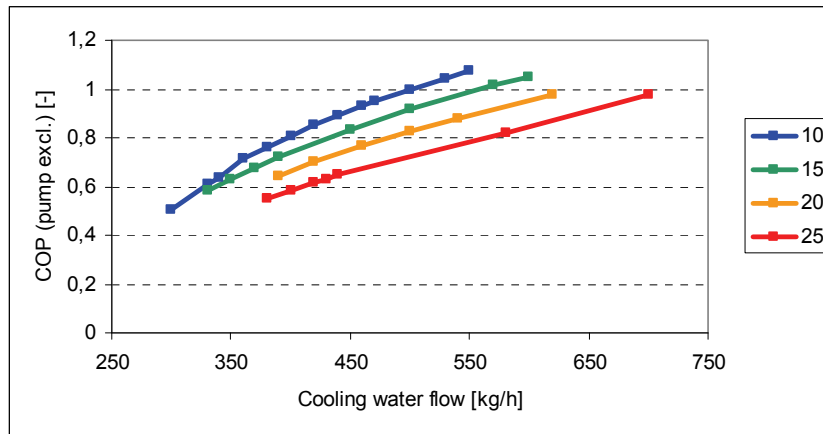


Figure 4-11: COP as a function of cooling water flow.

Table 4-6: The simulated optimum values for water heating mode. COP is based on cooling capacity and compressor work only.

CW temp °C	Outlet temp °C	Water flow kg/h	Pressure bara	Choke °C	IHX eff -	COP -
10	65	530	108	44,2	0,0	1,05
15	65	570	108	44,8	0,0	1,01
20	65	620	108	45,4	0,0	0,98
25	65	700	108	45,4	0,0	0,97
10	70	460	108	46,2	0,0	0,93
15	70	500	108	46,4	0,0	0,92
20	70	540	108	47,0	0,0	0,88
25	70	580	108	48,0	0,0	0,82
10	80	330	108	51,4	0,0	0,61
15	80	370	108	50,3	0,0	0,68
20	80	390	108	50,8	0,0	0,65
25	80	420	108	51,3	0,0	0,62

For the hot water mode it was necessary to find cooling water flow as well as the optimum high side pressure and choke inlet temperature. The corresponding outlet temperature as a function of the cooling water flow can be seen in Figure 4-12.

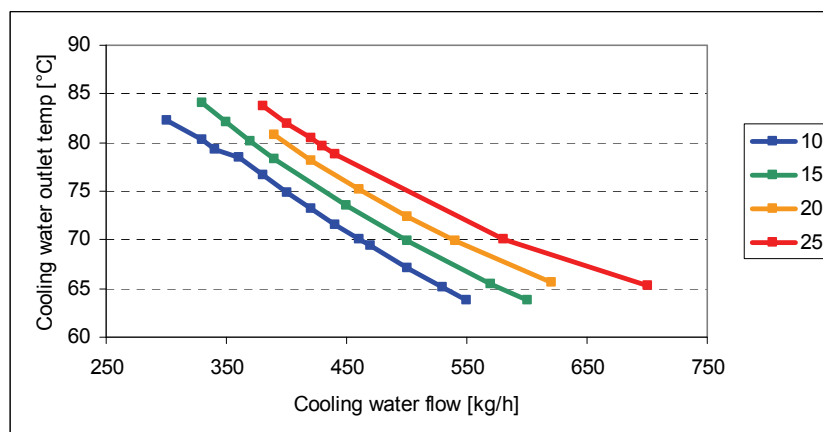


Figure 4-12: Cooling water flow for desired gas cooler outlet temperature. The different colors represent cooling water inlet temperature, in °C.

When plotting the flow rate as a function of the cooling water inlet temperature, one can see that the trend is almost linear.

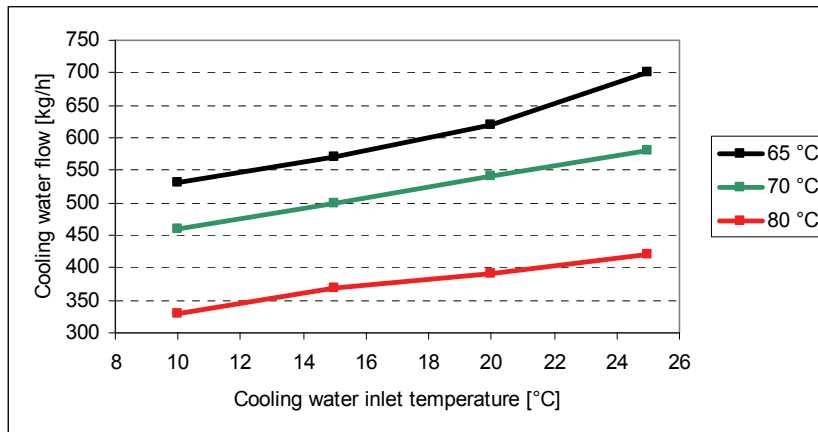


Figure 4-13: The flow rate trend for varying water inlet temperature for each of the goal temperatures.

4.6 Other means of optimization

A function that can be used with any optimization algorithm was also written. The function was tested with the built-in optimization tool Solver in Excel, and seems to work ok if the tolerance settings in Solver are changed and a good starting point is chosen (90 bar and zero SGHX efficiency is a good start). The reason for not using Solver for optimization in the first place is the lack of possibility of running batch simulations, and the function was made just to see if the concept worked. An example setup of Solver can be found in Appendix 22.

5 Experimental results

5.1 Experimental setup

The system has manual control of gas cooler pressure (via the choke valve), cooling water temperature and flow, SGHX bypass, compressor speed and heat input. This made it demanding to keep constant system input. The measurements were logged for 20-30 minutes with one minute intervals in order to get good average values. The measurement locations can be found in Appendix 2.

The experimental performance was calculated based on the circulated mass flow of carbon dioxide in the system. The flow rate was calculated using heat balance over the gas cooler. The refrigeration capacity was calculated as if the evaporation outlet was saturated or superheated, depending on temperature. Thus, COP values may be slightly exaggerated, as liquid out of the evaporator does not contribute to the cooling capacity.

The experiments included cooling at medium and maximum possible cooling water flow, and hot water production with outlet temperatures of 65, 70 and 80°C (Table 5-1).

Table 5-1: Experiment matrix.

Goal	Cooling water temperature			
	10°C	15°C	20°C	25°C
Cooling at medium cooling water flow rate		X	X	X
Cooling at maximum water flow rate	X	X	X	X
Combined cooling and hot water, 65°C outlet	X	X	X	X
Combined cooling and hot water, 70°C outlet	X	X	X	X
Combined cooling and hot water, 80°C outlet	X	X	X	X

5.2 Cooling mode

For the cooling mode experiments the cooling water flow rates were kept high and the gas cooler pressure just above transcritical, as shown in the optimization chapter. The evaporation temperature was kept close to constant, and the choke inlet temperature was kept within $\pm 1\text{K}$ of the values found in the optimization. At medium cooling water flow, tables with a wider cooling water flow rates were created (Appendix 15), and linear interpolation was performed as on the fly as it was difficult to precisely adjust the cooling water flow to a specific value.

The full flow experiments proved to perform very close to the 2008 experiments (Figure 5-1). Only the 25 degree cooling water experiment showed a slight reduction.

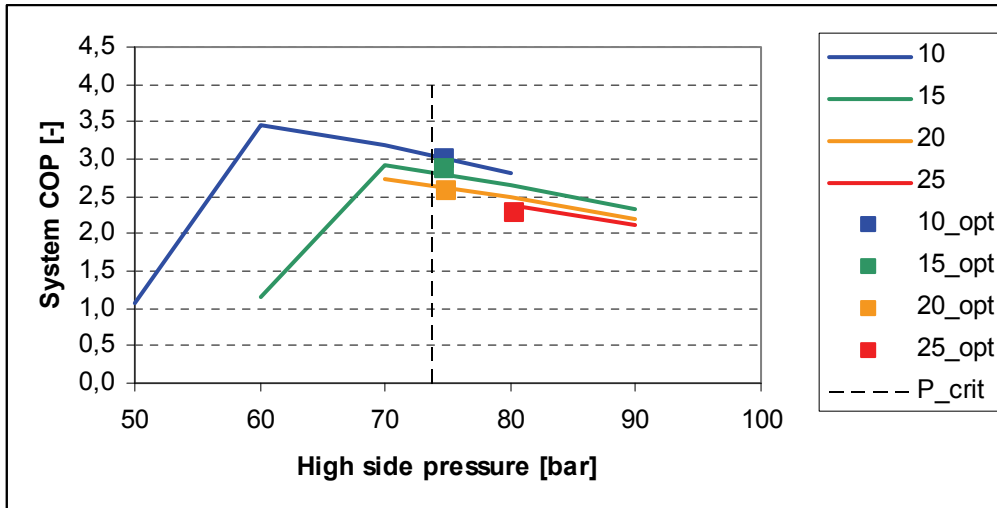


Figure 5-1: The 2008(lines) and 2009 (square markings) cooling results. The dotted vertical line indicates critical pressure. COP values are for compressor work only.

It was difficult to compare medium water flow results, as cooling water flow and temperatures were not exactly as set in the previous experiments. As a workaround the experiments were run using the found optimum settings, and then the simulations were run after hand using the actual data (evaporation temperature, cooling water temperature and cooling water flow) from the experiments as simulation input. In this way the model accuracy could be verified. This was done for all the cooling experiments.

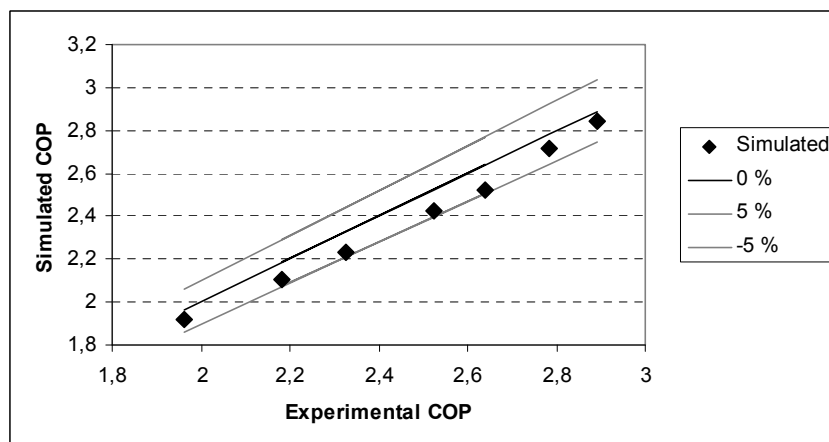


Figure 5-2: Cooling mode COP for both high and medium cooling water flow. Results are within 5%, but are systematically underestimated.

As can be seen in Figure 5-2, the system COP found in the simulations were within an error margin of 5%, but they were systematically underestimated, as are the simulated cooling capacity values (Figure 5-3).

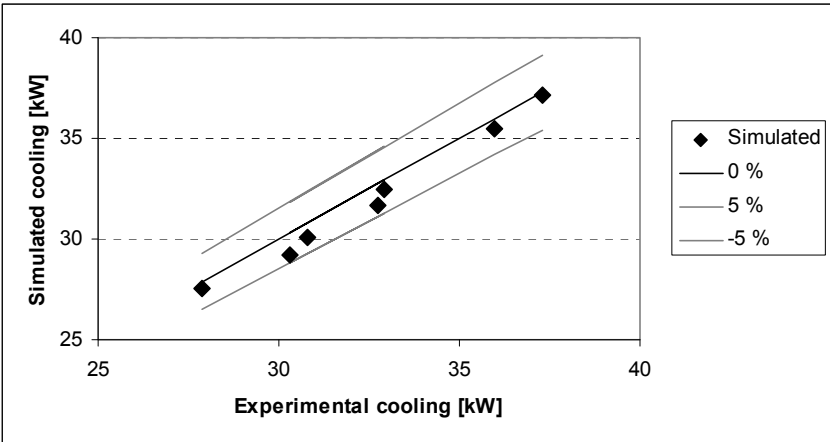


Figure 5-3: Simulated and experimental cooling capacity.

5.3 Water heating mode

There were no earlier experiments using a suction gas heat exchanger, so the experiments were run with settings found through the simulations, and when completed, simulations were run again using the actual data from the experiments and compared (as for the cooling).

COP calculations were quite accurate, but the 20/70 and the 25/80 (inlet/outlet cooling water temperature) experiments deviated more than the rest. This could be linked to problems with the cooling water flow measurements, which behaved rather odd at low cooling water flows, even after recalibrating the flow measurement device.

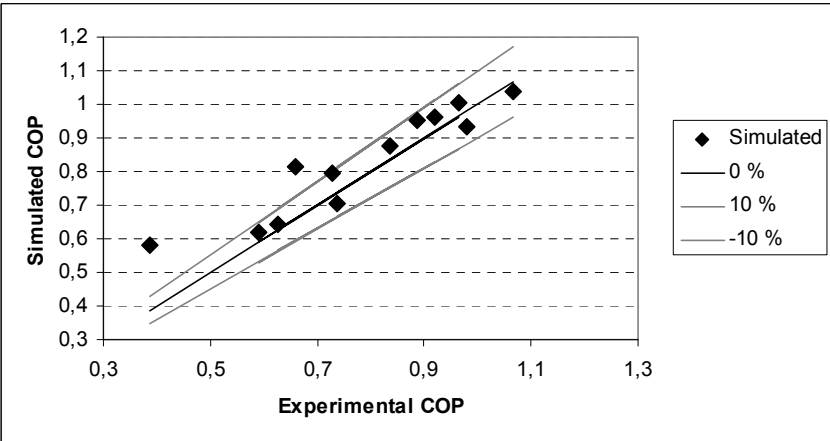


Figure 5-4: Cooling COP for the water heating mode. Deviations are larger, but for the most part within 10%.

The cooling capacity calculations for hot water production were within a 10% error margin, except for the 20/70 heating experiment, which deviated significantly.

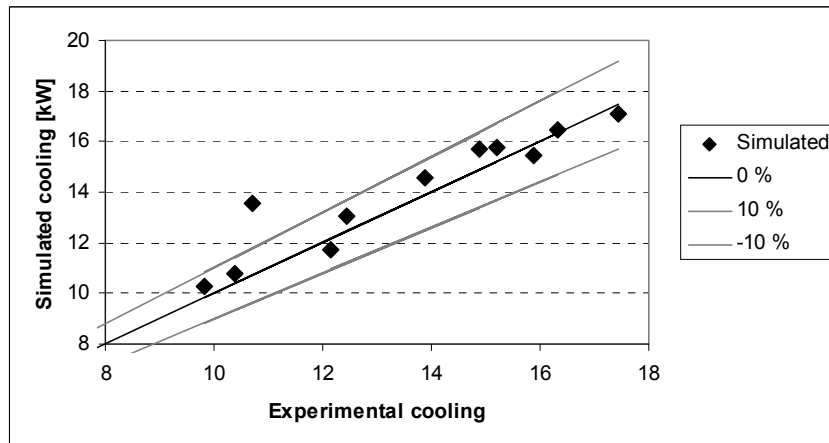


Figure 5-5: Experimental and simulated cooling capacity for water heating.

Combined refrigeration and hot water production contribute to both heating and cooling for a specific input, and one can calculate the combined COP as

$$COP_{combined} = \frac{\dot{Q}_{heat} + \dot{Q}_{cool}}{\dot{W}_{compr}} \quad (5.1)$$

The combined COP calculations are presented in Figure 5-6. The COP values are about the same as for just cooling with high water flows; the reduced cooling capacity takes away most of the benefit of combined operation.

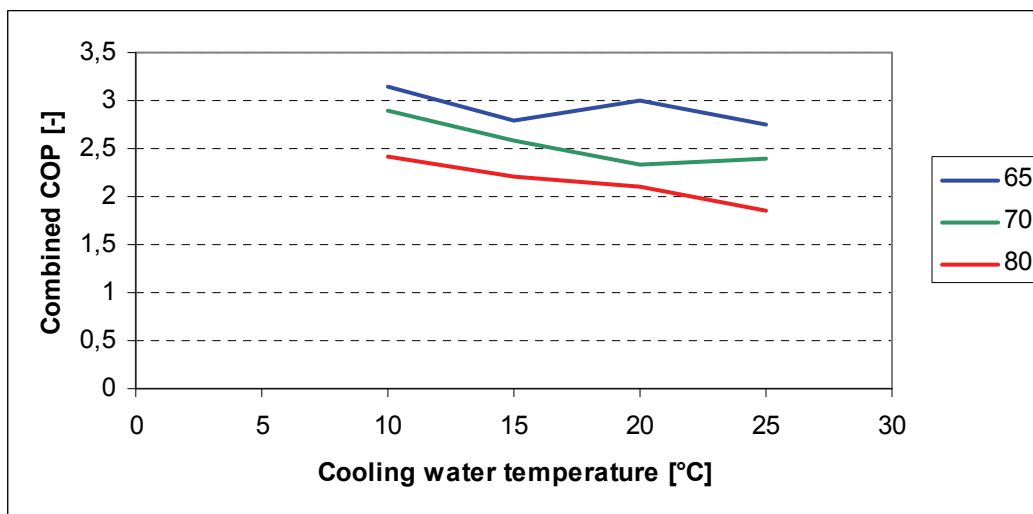


Figure 5-6: Combined COP as a function of cooling water temperature. Each color represents an outlet temperature.

5.4 Model verification

As mentioned earlier in this chapter, the simulations that were run using the actual data from the experiments. These results were used to verify the model components, in order to find model improvement potentials.

5.4.1 Compressor

The volumetric efficiency calculations using the new and improved model proved to be very accurate, within a 5% error margin.

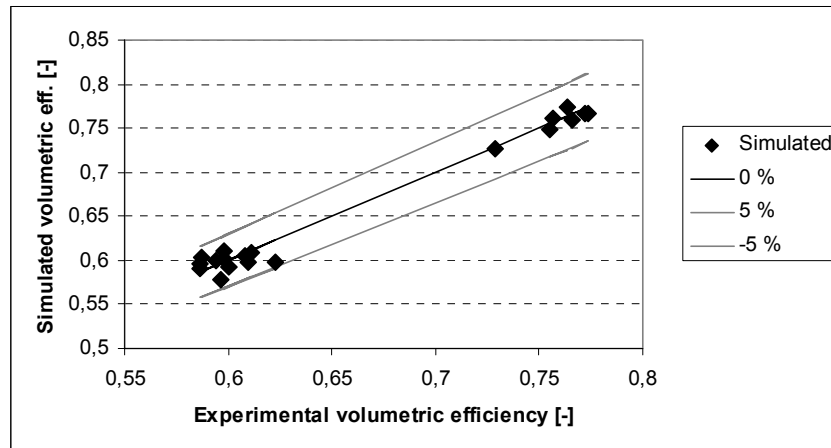


Figure 5-7: Volumetric efficiency calculations compared to the experimental values.

The isentropic efficiency was not quite as accurate, but still well within a 10% error margin. The water heating experiments showed some model overestimation of the isentropic efficiency, and the cooling mode experiments showed slight model underestimation (Figure 5-8).

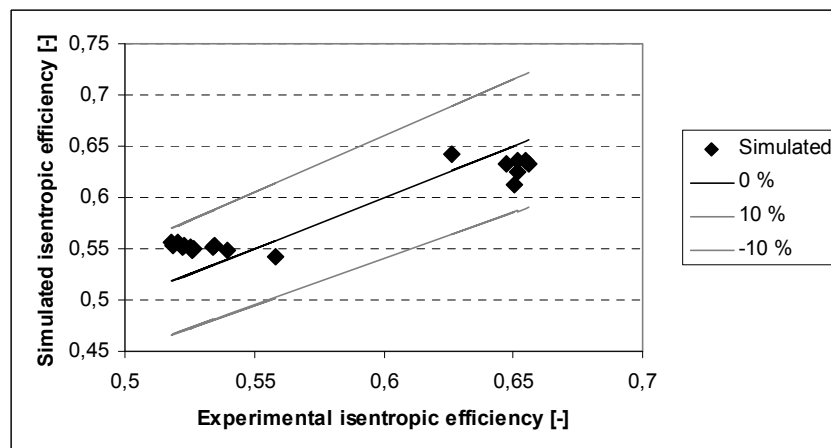


Figure 5-8: The isentropic efficiency was overestimated for hot water production (on the left) and underestimated for the cooling (on the right hand side), but the accuracy is within 8% for all experiments.

The low side pressure drop calculations were overestimated, which led to an underestimation of the suction pressure, but only by a few percent. This is well within the acceptable. The low evaporator temperature pressure drops (cooling mode) deviate more than the higher evaporation temperatures (water heating mode).

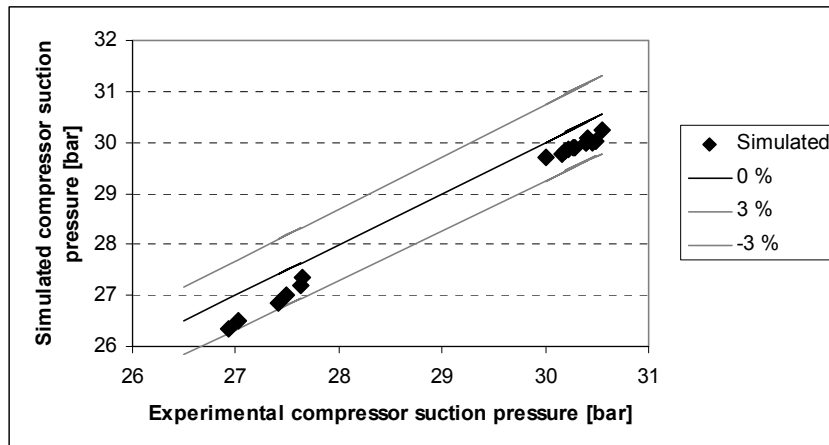


Figure 5-9: Simulated and experimental compressor suction pressures.

5.4.2 Gas cooler

The gas cooler pressure drop was overestimated due to an error in mass transport calculations when modeling. The model was based on the compressor mass flow calculated using an erroneous volumetric efficiency (created before the volumetric efficiency calculation was updated). This is an easy fix which will be discussed further in chapter 7. The overestimation should have no significant impact on the optimization results, as the pressure drops are small in relative terms (an error of ~ 0.2 bar is very small compared to 80 bar high side pressure).

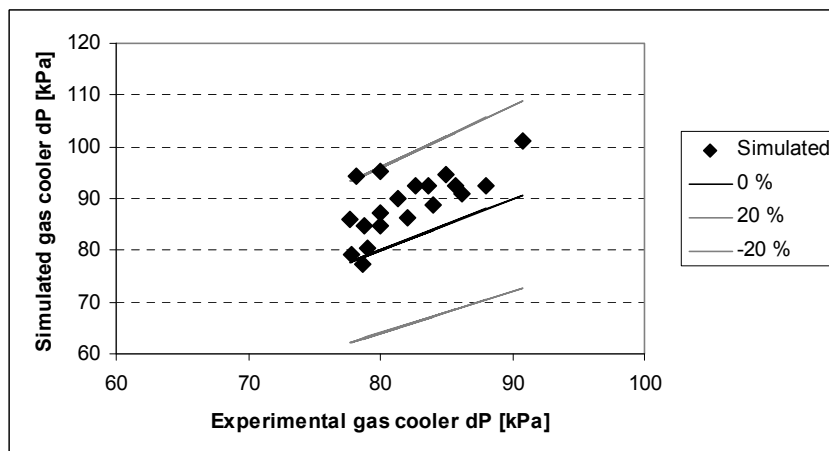


Figure 5-10: Simulated and experimental pressure drop. The percentage error is quite large, but relative to the high pressure it is insignificant.

The gas cooler temperature approach was within 1.5 K for all experiments, except the water heating at 25 °C inlet/80°C outlet temperature.

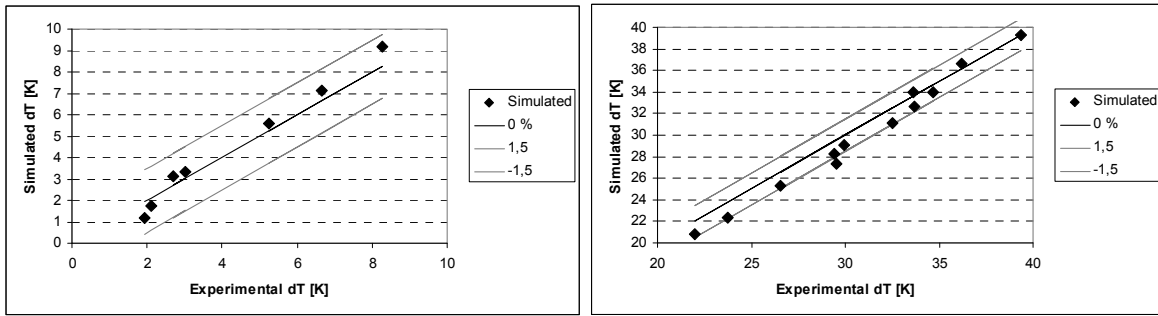


Figure 5-11: Temperature approach cooling on the left, hot water mode on the right. Simulation values are within one exception for the 25/80 hot water mode experiment, within 1.5 K.

5.4.3 Evaporator

The evaporator pressure drop was grossly overestimated for normal cooling. The pressure drop model was based on old experiments without the suction gas heat exchanger. With the heat exchanger, the amount of flash gas was reduced, and it appears to have reduced the pressure drop over the evaporator. This errors here account for more than half of the suction pressure errors.

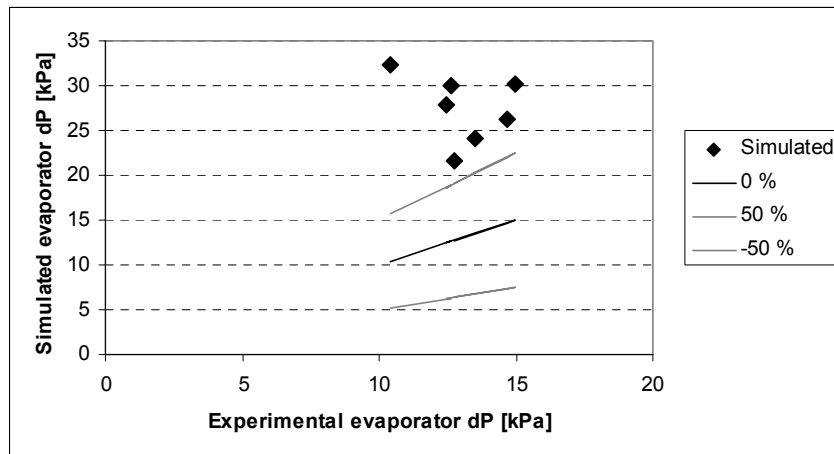


Figure 5-12: The evaporator pressure drop when in cooling mode.

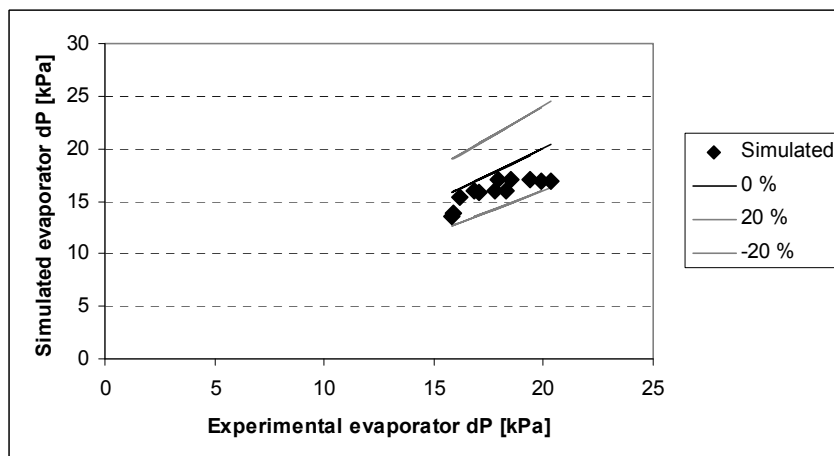


Figure 5-13: Hot water production

6 Discussions

6.1 System performance

A lower gas cooler pressure limit of 74 bar was set in order to ensure transcritical operation, as the model was created for that purpose, but higher efficiencies can be achieved using a lower pressure for high cooling water flow and/or low temperature (as shown in previous experiments, Table 2-5), but this was not tested in this thesis.

The high cooling water flow experiments showed no significant change compared to the 2008 experiments. This was expected due to low sensitivity to the SGXH efficiency, as described in section 4.2. The temperature approach was low due to large temperature difference in the gas cooler, which resulted in very good heat transfer (Figure 6-1).

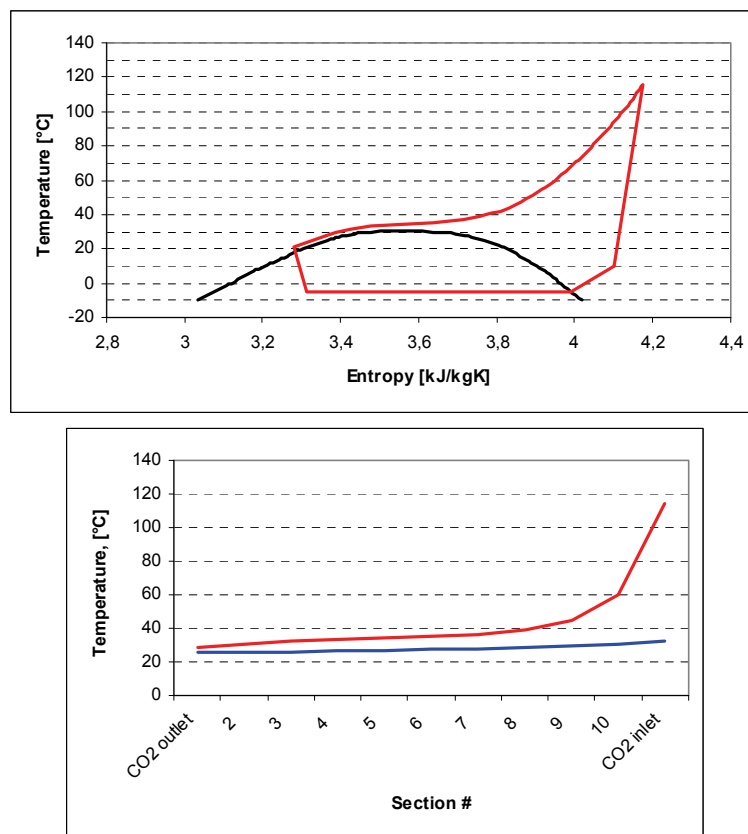


Figure 6-1: Cycle (upper) and gas cooler temperature profile (lower) at full water flow using 25 °C cooling water temperature. The blue line is the cooling water temperature.

The 25 °C cooling water temperature experiment actually showed reduced efficiency, but the 2008 experiment at 80 bar was very close to the optimum choke temperature setting, with slightly higher cooling water flow and evaporation temperature, which is probably the cause of the slight COP reduction.

Combined cooling and water heating on the current system showed very poor performance. The gas cooler temperature approach was very high (Figure 5-11, Figure 6-2), which resulted in low efficiency and low cooling capacity. A gas cooler with higher performance should be

able to improve the performance by reducing the temperature approach. Other improvements are suggested in chapter 8.

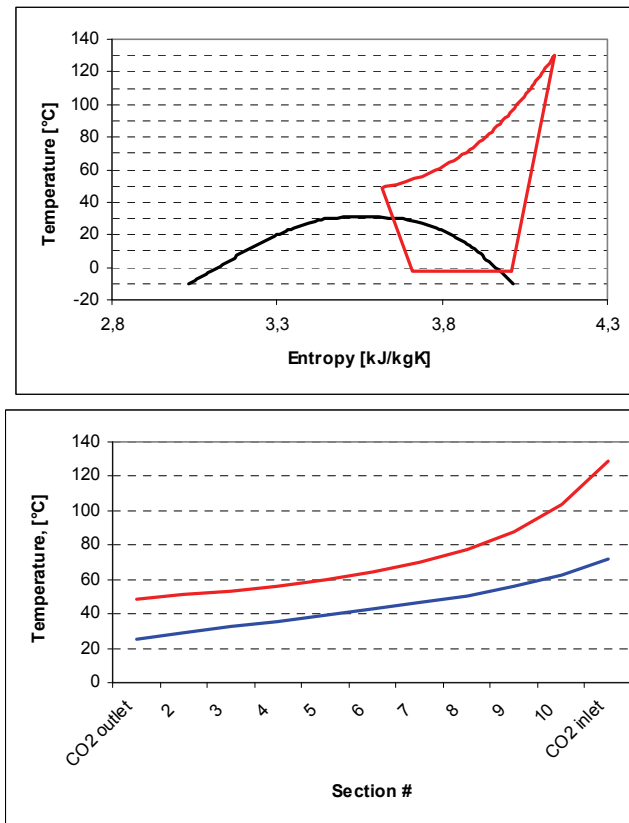


Figure 6-2: Cycle (upper) and gas cooler temperature profile (lower) at heating mode with 70°C outlet temperature using 25 °C cooling water. The temperature difference between the CO₂ and the water was much lower than for the full flow experiment, so less heat was transferred.

By running simulations using the conditions from the experiments, it was possible to check the validity of the model, and it shows good accuracy, within 5% error for the cooling capacity and system efficiency (COP), and within 10% error for most of the water heating experiments. The model shows some improvement potentials, but it was accurate enough for the intended use.

6.2 System control

In a traditional transcritical system the gas cooler temperature approach is used as the control parameter for finding the optimum high side pressure. This works fine with a constant suction gas heat exchanger. When introducing a variable suction gas heat exchanger, the gas cooler outlet temperature can no longer be used for this purpose, as it is affected both by the gas cooler pressure and the efficiency of the suction gas heat exchanger. The high side pressure therefore has to be controlled by other means, for instance cooling medium temperature and flow. The evaporation temperature also has to be taken into account (this was described in section 1.5.3).

For controlling of the suction gas heat exchanger, the choke inlet temperature can be used as a control parameter. As can be seen from the results, the simulations are accurate enough to use the choke inlet temperature as the control parameter. An initial idea is to generate lookup-tables from which a controller can interpolate to find set points. More system control suggestions can be found in section 8.1.

6.3 Model accuracy

The model predicts the system behavior better than expected. Even though the model was very simple, cooling efficiencies (COP) were calculated within 5 % error margin. In the combined cooling and heating experiments (water heating) the simulation error was within 10% (with a few exceptions), and is considered good enough for optimization purposes. The reason for the low errors is likely to be caused by the modeling process, which used previous measurement data. The outliers are probably caused by varying cooling water flow at low flow rates.

The evaporator pressure drop model should have been revised after installing the suction gas heat exchanger. However, the pressure drops are at a very small scale, and the calculation of overall system efficiency seems to be almost unaffected by this. The gas cooler pressure drop is a result of using the erroneous mass flow calculations. The error should have been caught earlier, but the pressure drops are very small compared to the total pressure, so this should have almost no impact on the system performance calculations.

6.4 The concept of variable SGHX bypass

As shown in section 4.2, the benefit of a variable SHGX becomes increasingly more evident when cooling water temperature exceeds 25 °C (or achievable gas cooler outlet temperature above 25°C, since the temperature approach is very small for high cooling water flow rates). For the system in question, because of the low gas cooler outlet temperatures, it is therefore difficult to determine if the concept of a variable SGHX is beneficial.

The simulations show that a RSW system with an efficient gas cooler and low cooling water temperature (up until around 25°C) available does not need a variable SGHX; a high efficiency SGHX will be satisfactory. In this kind of setup, the gas cooler temperature approach can be used for simple gas cooler pressure control.

It's when the cooling water temperature/gas cooler outlet temperature exceeds 25°C that the variable suction gas heat exchanger starts to show real benefit. As can be seen in Figure 4-3 the ideal SGHX efficiency declines with increasing cooling water temperature until zero efficiency (full bypass). Such high cooling temperatures are unlikely for RSW refrigeration using sea water as the cooling medium, but the concept should be useful for refrigeration systems which utilize air as the cooling medium (where the air temperature is high, and the gas cooler temperature approach will be higher). Using air as a cooling medium generally means a higher temperature approach, and will have the same impact on the system as increasing the cooling water temperature. Also, ambient air temperature tends to experience greater variation than sea water.

A word of advice for designing the suction gas heat exchanger is to calculate the UA value for the SGHX at all simulation points, and then select the highest one for manufacturing, as the highest efficiency may not have the highest UA-value (Watts/ΔK). An observation is that too high SGHX efficiency is far worse than not using an SGHX at all (ignoring liquid carryover), as can be seen from Figure 4-2. The best example of this is the 2008 experiments, where hot water production was not even possible due to non-ideal SGHX efficiency. So if it is decided to not use a variable SGHX even though high gas cooler outlet temperature may occur, the efficiency of the SGHX should be kept low enough to allow for sufficiently high gas cooler pressure at the highest cooling medium temperatures.

7 Suggested model improvements

7.1 Calculation tools

The simulation model should be written using another programming language, like C++ or FORTRAN, in order to speed up calculations. The data can be dumped to text files, which can be visualized using MATLAB or other powerful visualization tool. This would simplify simulations and storage of simulation results significantly.

7.2 Gas cooler pressure drop

The current gas cooler pressure drop was overestimated by around 20%. Based on the new measurements and improved mass flow calculations (Appendix 15), a new gas cooler pressure drop model is suggested.

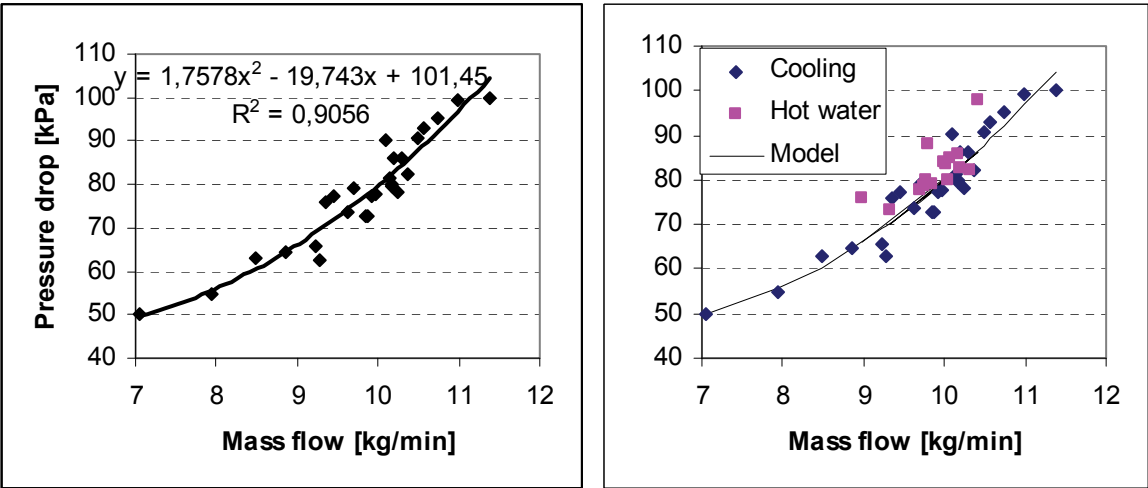


Figure 7-1: Suggested gas cooler pressure drop model based on the circulated mass flow in cooling mode.

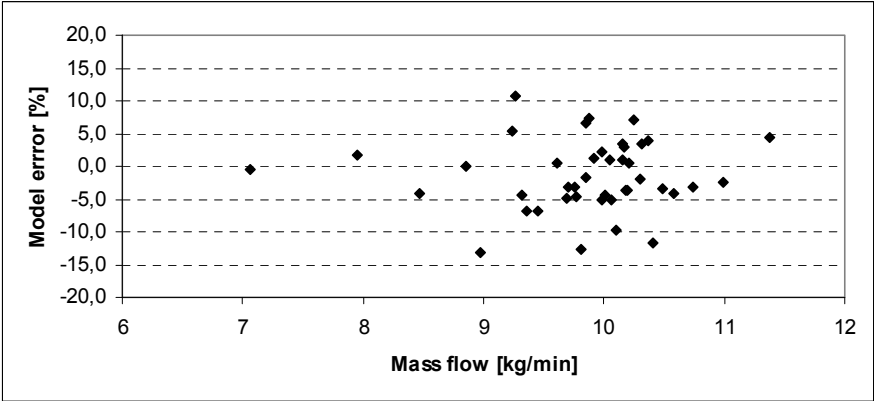


Figure 7-2: Model error is within 15%

7.3 Evaporator pressure drop

As shown in section 5.4.3, the evaporator pressure drop was overestimated. A new model is suggested by assuming that the pressure drop is a function of the Reynolds number, Re. The diameter here is more like a shape factor.

$$dP \propto \text{Re} = \frac{UD}{\nu} \quad (7.1)$$

$$U \propto \frac{m_{\text{gas}}}{D^2} \quad (7.2)$$

If we assume that D is a constant factor dependent on shape, we can assume that

$$dP \propto \frac{m_{\text{gas}}}{\nu} \quad (7.3)$$

Using the experimental data, the model fits pretty well, but has a shift when switching from cooling mode to hot water mode, as shown in Figure 7-3.

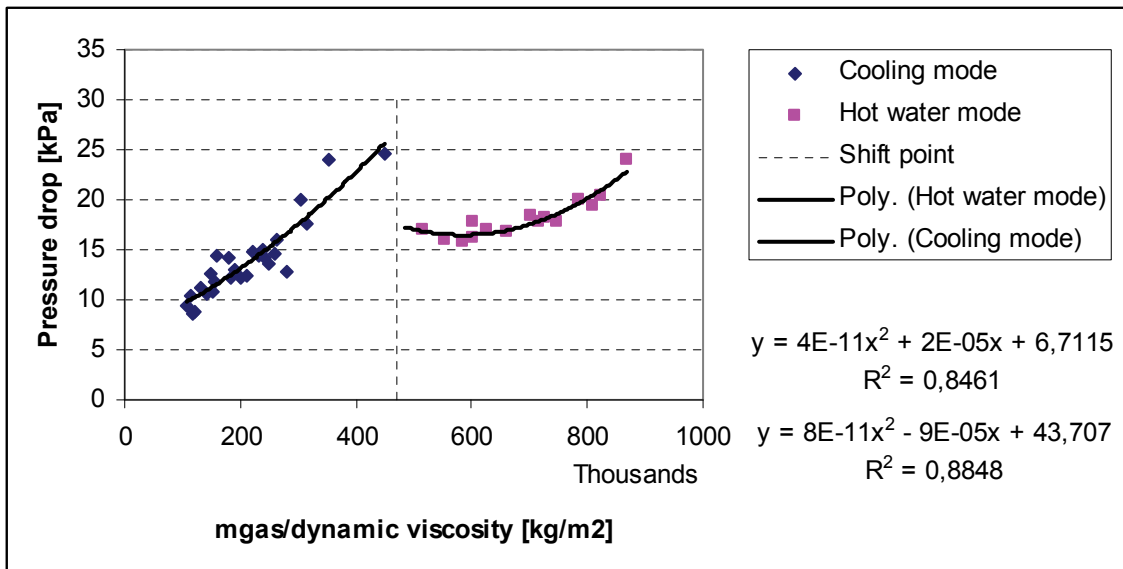


Figure 7-3: Evaporator pressure drop in both cooling and hot water mode

To further increase the accuracy of the model, the heat transfer in un-insulated piping may also be included, but this is assumed to be of very little interest from an optimization point of view, as the impact on system performance is assumed to be extremely small.

7.4 Other possible improvements

- The pressure drop in the suction tube and low side SGHX appears to be too high in the current model. No attempt has been made to make such a model, as it seems to have very little impact on the calculation of the system performance.
- An automated optimization algorithm such as Nelder-Mead could be used to improve the optimization speed and provide more accurate results.
- The model should be extended to also handle sub-critical gas cooler pressures. Low cooling water temperature combined with high cooling water flow rates have an optimum operation which is subcritical (see the 2008 results, Appendix 19).
- The model should calculate SGHX UA-values.

8 Suggested system improvements and future work

8.1 System control

The choke valve has no constant-pressure option. This can be easily modified with the installation of an actuator that can be bolted onto the existing needle valve and connected to a PID controller. The bypass valves should also have an actuator each, in order to be run automatically. The bypass valve control has to coordinate two valves, but this should present no problem. A simplified pseudo-code for controlling the choke inlet temperature can be found in Appendix 3

An initial idea is to create optimized tables (optimum pressure and choke inlet temperature) at different cooling water flow rates and temperatures as well as different evaporation temperatures. These tables can then be used for on-demand interpolation by the system controller.

A way of simplifying future experiments is the installation of a cooling water mixing valve in order to maintain a constant cooling water flow and temperature.

8.2 System design

8.2.1 Multiple gas coolers

The current system has a gas cooler optimized for high cooling water flow, which performs poorly at reduced cooling water flow. A possible solution for combined refrigeration and water heating is using two gas coolers, one for the hot water production (low water flow) and another with higher water flow for bulk heat rejection. In this way, the water heating will not reduce the refrigeration capacity. The optimization model used can easily be altered to incorporate a separate hot water producer, or even several gas coolers for use at different temperature levels.

This approach is just a minor modification to the traditional de-superheater solutions found in vapor-compression systems. A very relevant article by Stene (2005) discusses how three gas coolers can be used at different temperature levels in a transcritical carbon dioxide system for combined space and hot water heating.

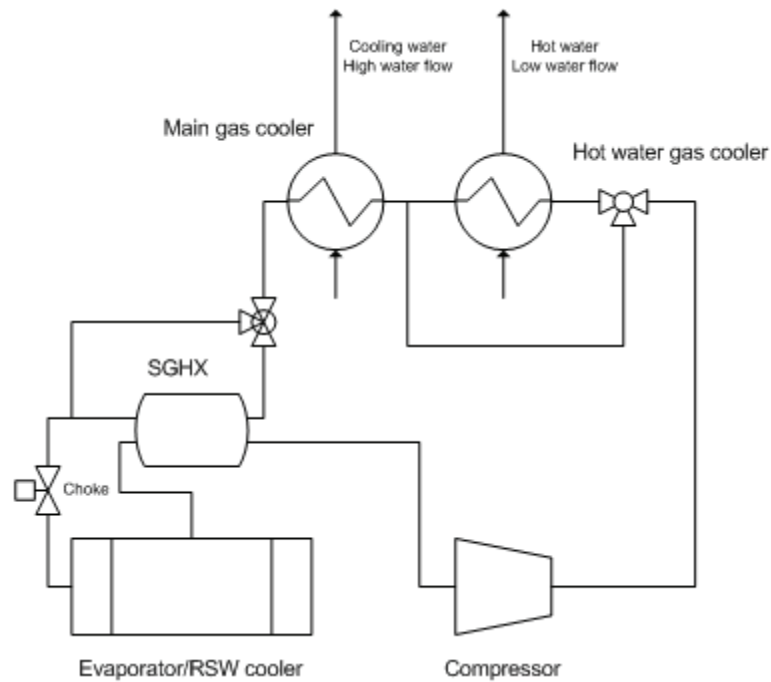


Figure 8-1: Simplified overview of a system with a dedicated gas cooler for water heating.

8.2.2 Ejector

A solution undergoing much research at the moment is the use of an ejector to replace the choke valve. The ejector (Figure 8-2) converts the high side pressure to velocity, thereby reducing the pressure at the secondary inlet to circulate refrigerant through the evaporator. At the ejector outlet the velocity is reduced and some of the pressure recovered, which lets the compressor work at a lower pressure ratio. The ejector uses energy that is normally lost in a choke valve to circulate refrigerant through the evaporator (Chunnanond et al, 2004), and this reduces the work without reducing cooling capacity.

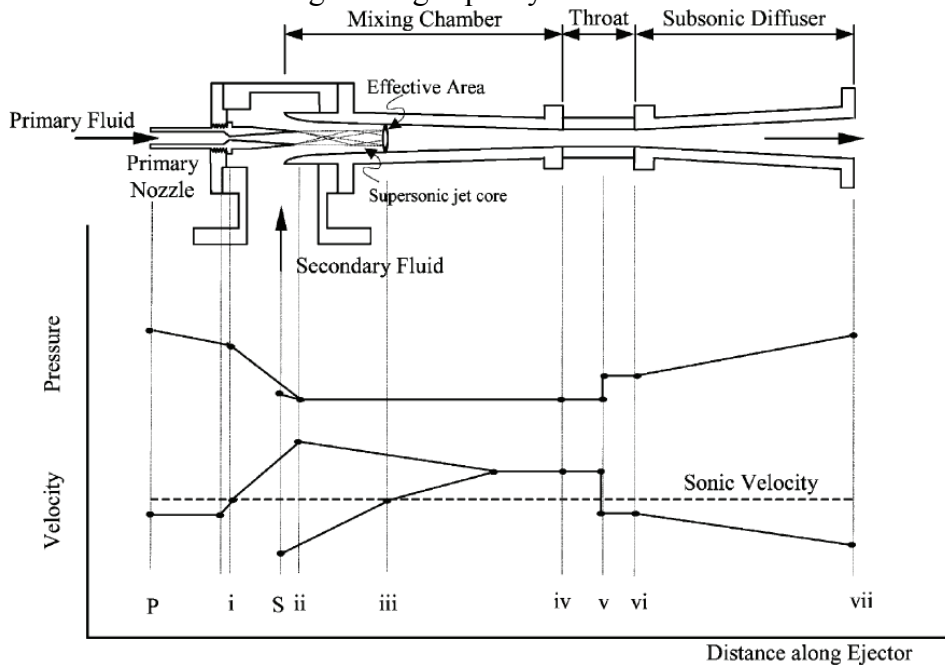


Figure 8-2: Ejector principle. Converting pressure to velocity creates a suction effect at the secondary fluid inlet (from the evaporator). Figure from Chunnanond et al (2004).

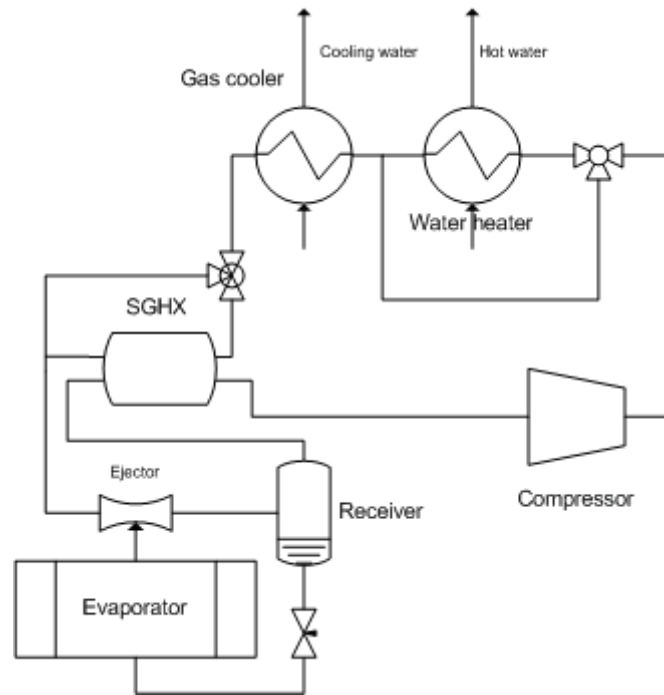


Figure 8-3: Simplified overview of a system with a dedicated gas cooler for water heating and an ejector replacing the choke valve.

9 Conclusions

The simulation results from the developed simulation tool indicate that the RSW system performance can be increased compared to running a system with a traditional non-variable suction gas heat exchanger, but only when the gas cooler outlet temperatures are high (above $\sim 25^{\circ}\text{C}$), which for the system in question would mean high cooling water temperatures or reduced cooling water flow rate. Such operating conditions are not to be expected for a RSW system with low cooling water temperatures available.

The cooling experiments with transcritical gas cooler pressure show little or no improvement in system performance at temperature levels of 25°C and below compared to previous experiments, as the optimum setting turned out to be maximum suction gas heat exchange (no bypass). Previous experiments also show that for low cooling water temperatures (20°C and below), the optimum gas cooler pressure is subcritical. The simulation model showed good accuracy in predicting COP and cooling capacity.

The introduction of a variable suction gas heat exchanger once again made it possible to use the system for water heating. The optimum operation was to bypass the SGHX altogether, and any use for a SGHX should be to evaporate liquid carryover from the evaporator. In other words, if the current system is to be used for water heating, the possibility to fully bypass the SGHX is essential.

The concept of a variable SGHX appears not to be beneficial in a water cooled RSW system, but the simulations indicate that it has potential in areas where air is used as the cooling medium, for instance commercial or mobile refrigeration. For cooling purposes, experiments and simulations show that a non-variable suction gas heat exchanger should be satisfactory for a RSW system when low cooling water temperatures are available. It is strongly recommended that a system to be used for simultaneous cooling and heating should have an improved design compared to the current setup, as this mode of operation shows low cooling capacity and poor energy efficiency.

10 Bibliography

AGK-Kronawitter. *Fish pumps*.

Online: http://www.agkkronawitter.de/AGK_engl/englisch/englischpdf/Group_07.pdf.
[Read date: December 7th, 2008]

Barros-Velazquez, J., Gallardo, J.M., Calo, P., Aubourg, S.P. (2008) Enhanced quality and safety during on-board chilled storage of fish species captured in the Grand Sole North Atlantic fishing bank. *Food Chemistry*, 106 (2), 493-500

Bahuaud, D., Mørkøre, T., Langsrud, Ø., Sinnes, K., Veiseth, E., Ofstad, R., Thomassen, M.S. (2008) Effects of -1.5 °C Super-chilling on quality of Atlantic salmon (*Salmo salar*) pre-rigor Fillets: Cathepsin activity, muscle histology, texture and liquid leakage. *Food chemistry*, 111, 329-339

Cabello, R., Sanchez, D., Llopis, R., Torrella, E. (2008) Experimental evaluation of the energy efficiency of a CO₂ refrigerating plant working in transcritical conditions. *Applied Thermal Engineering*, 28 (13), 1596-160

Calm, J.M. (2008) The next generation of refrigerants – Historical review, considerations, and outlook. *International Journal of Refrigeration*, 31, 1123-1133.

Chen, Y., Gu, J. (2005) The Optimum high pressure for CO₂ transcritical refrigeration systems with internal heat exchangers, *International journal of refrigeration*, 28, 1238-1249.

Chunnanond, K., Aphornratana, S. (2004) Ejectors: applications in refrigeration technology, *Renewable and Sustainable Energy Reviews*, 8, 129-155.

Dagbjartsson, B., Valdimarsson, G., Arason, S. (1982) Icelandic experience in storing fish in chilled seawater. *International Journal of Refrigeration*, 5 (3), 141-145.

DFAGNL (Department of Fisheries and Aquaculture Government of Newfoundland and Labrador). (2002) *Refrigerated Seawater Holding System Tested* [online]. Available at: http://www.fishaq.gov.nl.ca/fdp/ProjectReports/fdp_61.pdf [Read date: October 7th, 2008]

Einstein, A. (1934) On the Method of Theoretical Physics, *Philosophy of Science*, 1 (2), 163-169.

Erikson, U., Hultmann, L., Steen, J.E. (2006) Live chilling of Atlantic salmon (*Salmo salar*) combined with mild carbon dioxide anaesthesia: I. Establishing a method for large-scale processing of farmed fish. *Aquaculture*, 252 (2-4), 183-198.

Forsthoffer. W.E. (2005) Reciprocating compressor control and operation. *Forsthoffer's Rotating Equipment Handbooks*, 2005, 363-370

Ge, Y.T., Tassou, S.A. (2009) Control optimisation of CO₂ cycles for medium temperature retail food refrigeration systems, *International Journal of Refrigeration*, online 2009

- Heen, E. (1982) Developments in chilling and freezing of fish. *International Journal of Refrigeration*, 5 (1), 45-49
- Incropera, F.P., DeWitt, D.P., Bergman, T.L., Lavine, A.S. (2007) *Fundamentals of Heat and Mass Transfer* (6th ed), 620-626. Hoboken, USA: John Wiley & Sons Inc.
- Incropera, F.P., DeWitt, D.P., Bergman, T.L., Lavine, A.S. (2007b) *Fundamentals of Heat and Mass Transfer* (6th ed), 678. Hoboken, USA: John Wiley & Sons Inc.
- Incropera, F.P., DeWitt, D.P., Bergman, T.L., Lavine, A.S. (2007c) *Fundamentals of Heat and Mass Transfer* (6th ed), 116-126. Hoboken, USA: John Wiley & Sons Inc.
- Incropera, F.P., DeWitt, D.P., Bergman, T.L., Lavine, A.S. (2007d) *Fundamentals of Heat and Mass Transfer* (6th ed), 487. Hoboken, USA: John Wiley & Sons Inc.
- Jakobsen, A., Rekstad, H., Skaugen, G., Eikevik, T., Nekså, P. (2007) Prototype liquid chiller using carbon dioxide as refrigerant. Proceeding, *International Congress of Refrigeration*, Beijing, China.
- Jul, M. (1986) Chilling and freezing fishery products: changes in views and usages. *International Journal of Refrigeration*, vol 9, 174-178
- Kim, M.H., Pettersen, J., Bullard, C.W. (2004) Fundamental process and system design issues in CO₂ vapour compression systems. *Progress in Energy and Combustion Science*, 30, 119-174
- Loebl, S., Kraus, W.E., Quack, H. (2005) Pool boiling heat transfer of carbon dioxide on a horizontal tube. *International Journal of Refrigeration*, 28 (8), 1196-1204.
- Lorentzen, G. (1990) Patent application: Trans-critical vapour compression cycle device, *Patent No. WO/07683; 1990*.
- Lorentzen, G. (1994) Revival of carbon dioxide as a refrigerant. *International Journal of Refrigeration*, 17 (5), 292-301
- Magnussen O.M., Haugland, A., Hemmingsen, A.K. Torstveit, Johansen, S., Nordtvedt, T.S. (2008) Advances in superchilling of food - Process characteristics and product quality. *Trends in Food Science & Technology*, 19 (8), 418-424.
- Muñoz-Delgado, J.A. Progress in food science and technology in relation to refrigeration. *International Journal of Refrigeration*, 1 (1), 1978, 33-37
- Musgrove, R., Carragher, J., Mathews, C., Slattery, S. (2007) Value-adding Australian sardines: Factors affecting rates of deterioration in sardine (*Sardinops sagax*) quality during post-harvest handling. *Food Control*, 18 (11), 1372-1382.
- Pearson, A. (2005) Carbon dioxide - new uses for an old refrigerant. *International Journal of Refrigeration*, 28 (8), 1140-1148.

- Piñeiro, C., Barros-Velazquez, J., Aubourg, S.P. (2004) Effects of newer slurry ice systems on the quality of aquatic food products: a comparative review versus flake-ice chilling methods. *Trends in Food Science & Technology*, 15 (12), 575-582.
- Rekstad, H., Skiple, T., Skaugen, G., Neksa, P. (2008) Liquid chiller using Carbon Dioxide in a Transcritical process. Proceeding, *8th IIR Gustav Lorentzen Conference on Natural Working Fluids*, Copenhagen Denmark
- Sarkar, J., Bhattacharyya, S., Ram Gopal, M. (2004) Optimization of a transcritical CO₂ heat pump cycle for simultaneous cooling and heating applications, *International Journal of Refrigeration*, 27 (8), 830-838
- Skjervold, P.O., Fjæra, S.O., Snipen, L. (2002) Predicting live-chilling dynamics of Atlantic salmon (*Salmo salar*), *Aquaculture*, 209 (1-4), 185-195
- Stene, J. (2005) Residential CO₂ heat pump system for combined space heating and hot water production, *International Journal of Refrigeration*, 28 (8), 1259-1265.
- Teknotherm Marine Refrigeration. (2008a) *RSW system*, Available online at <http://www.teknotherm.com/RSW%20system.htm>. Read date: October 31st, 2008.
- Teknotherm Marine Refrigeration. (2008b) *RSW chiller*. Available at <http://www.teknotherm.com/RSW%20chiller.htm>. Read date: December 7th, 2008.
- Thorsteinsson, J.A., Jensson, P., Condra, T., Valdimarsson, P. (2003) Transient simulation of refrigerated and chilled seawater system. Proceeding, *44th Conference on Simulation and Modelling*, Vesteraas Sweden.
- UNEP (United Nations Environment Programme). (2006) *2006 Report of the refrigeration, air conditioning and heat pumps technical options committee*, page 96-103. Available at: http://ozone.unep.org/teap/Reports/RTOC/rtoc_assessment_report06.pdf
- Wang, S.G., Wang, R.Z.(2005) Recent developments of refrigeration technology in fishing vessels. *Renewable Energy*, 30 (4), 589-600.

11 Appendices

Appendix 1 Equations used in calculation of experimental results

Gas cooler temperature approach:

$$\Delta T_{GC} = T_{GC,out} - T_{GC,water\ in} \quad (11.1)$$

Gas cooler heat rejection:

$$\dot{Q}_{GC} = \dot{m}_{coolingwater} \bar{C}_{p,water} (T_{GC,water\ out} - T_{GC,water\ in}) \quad (11.2)$$

Gas cooler mass flow (gas cooler heat balance):

$$\dot{m}_{co_2,GC} = \frac{\dot{Q}_{GC}}{h_{GC,in}(T_{GC,in}, P_{compr,out}) - h_{GC,out}(T_{GC,out}, P_{compr,out} - \Delta P_{GC})} \quad (11.3)$$

Gas cooler mass flow and work based on the compressor model was calculated as described in section 3.2.

Compressor suction superheating:

$$T_{SH,compr} = T_{compr,in} - T_{sat}(P_{compr,in}) \quad (11.4)$$

Compressor work of gas cooler mass flow:

$$\dot{W}_{compr,m_{GC}} = \dot{m}_{CO_2,GC} (h_{compr,out}(T_{compr,out}, P_{compr,out}) - h_{compr,in}(T_{compr,in}, P_{compr,in})) \quad (11.5)$$

Compressor isentropic efficiency:

$$\eta_{is} = \frac{h(s(T_{compr,in}, P_{compr,in}), P_{compr,out}) - h(T_{compr,in}, P_{compr,in})}{h(T_{compr,out}, P_{compr,out}) - h(T_{compr,in}, P_{compr,in})} \quad (11.6)$$

Compressor volumetric efficiency:

$$\lambda_{compr} = \frac{\dot{m}_{co_2,GC} \cdot v(T_{compr,in}, P_{compr,in})}{0,000143139 \frac{RPM}{60}} \quad (11.7)$$

SGHX heat transfer:

$$\dot{Q}_{SGHX} = \dot{m}_{co_2} (h(T_{sghxHP,out}, P_{gc,out}) - h(T_{sghxHP,in}, P_{gc,out})) \quad (11.8)$$

SGHX mass fraction throughput (from heat balance)t:

$$x_{mf} = \frac{h(T_{sghxHP,in}) - h(T_{choke})}{h(T_{sghxHP,in}) - h(T_{sghxHP,out})} \quad (11.9)$$

Overall SGHX efficiency:

$$\varepsilon_{SGHX} = \frac{\dot{Q}_{SGHX}}{\dot{Q}_{max}} \quad (11.10)$$

$$\dot{Q}_{\max} = \dot{m}_{co_2} \cdot \min((h(T_{sghx,HPin}, P_{gc,out}) - h(T_{sghx,LPin}, P_{gc,out})), (h(T_{sghxHPin}, P_{evap,out}) - h(T_{sghx,LPin}, P_{evap,out}))) \quad (11.11)$$

Evaporator LMTD (Incropera et al, 2007b), calculated as countercurrent heat exchanger:

$$\Delta T_{LMTD} = \frac{(T_{brine,out} - T_{evap,in}) - (T_{brine,in} - T_{evap,out})}{\ln \frac{(T_{brine,out} - T_{evap,in})}{(T_{brine,in} - T_{evap,out})}} \quad (11.12)$$

Evaporator K-value:

$$k_{evap} = \frac{\dot{m}_{brine} C_{p,brine} (T_{brine,in} - T_{brine,out})}{A_{surface} \Delta T_{LMTD}} \quad (11.13)$$

where $A_{surface}$ is either the inner or outer water tube surface in the evaporator

System cooling:

$$\dot{Q}_{m_{gc}} = \dot{m}_{co_2,gc} \cdot (h(T_{evap,out}, P_{evap,out}) - h(T_{choke}, P_{gc,out})) \quad (11.14)$$

System COP (pump included):

$$COP = \frac{\dot{Q}_{m_{gc}}}{\dot{W}_{compr,m_{co_2,gc}} + \dot{W}_{pump,brine}} \quad (11.15)$$

System COP (pump not included):

$$COP = \frac{\dot{Q}_{m_{gc}}}{\dot{W}_{compr,m_{co_2,gc}}} \quad (11.16)$$

Hot gas fraction through oil recuperator

$$x_{hotgas} = \frac{h(T_{sghxHP,in}) - h(T_{GC,out})}{h(T_{oilHP,out}) - h(T_{GC,out})} \quad (11.17)$$

Hydraulic diameter for annulus

$$D_h = \frac{4A}{O_{wetted}} = \frac{4 \cdot \frac{1}{4} \pi (D_o - D_i)}{\pi (D_o - D_i)} = D_o - D_i \quad (11.18)$$

Hydraulic diameter round tube

$$D_h = \frac{4A}{O_{wetted}} = D_i \quad (11.19)$$

Appendix 2 Measuring points

Table 11-1: Measuring points, channels and naming

Name used in report	Measuring point name	Description	Channel number
$T_{compr,in}$	TT 1-05	Compressor suction temperature	105
$T_{compr,out}$	TT 1-02	Compressor discharge temperature	102
$T_{GC,in}$	TT 1-03	Gas cooler inlet temperature	103
$T_{GC,out}$	TT 1-04	Gas cooler outlet temperature	104
$T_{sghxHP,in}$	TT 1-06	SGHX high pressure inlet temperature	106
T_{choke}	TT 1-07	Choke inlet temperature	107
$T_{evap,in}$	TT 1-08	Evaporator inlet temperature	108
$T_{evap,out}$	TT 1-09	Evaporator outlet temperature	109
$T_{oilLP,in}$	TT 1-10	Oil recuperator low pressure inlet temperature	110
$T_{oilLP,out}$	TT 1-11	Oil recuperator low pressure outlet temperature	111
$T_{oilHP,out}$	TT 1-12	Oil recuperator high pressure outlet temperature	112
$T_{sghxLP,in}$	TT 4-01	SGHX low pressure inlet temperature	119
$T_{sghxHP,out}$	TT 4-02	SGHX high pressure outlet temperature	120
$T_{brine,out}$	TT 2-01	Brine evaporator outlet temperature	208
$T_{brine,in}$	TT 2-02	Brine evaporator inlet temperature	209
$T_{GC,waterout}$	TT 3-01	Cooling water outlet temperature	117
$T_{GC,waterin}$	TT 3-02	Cooling water inlet temperature	118

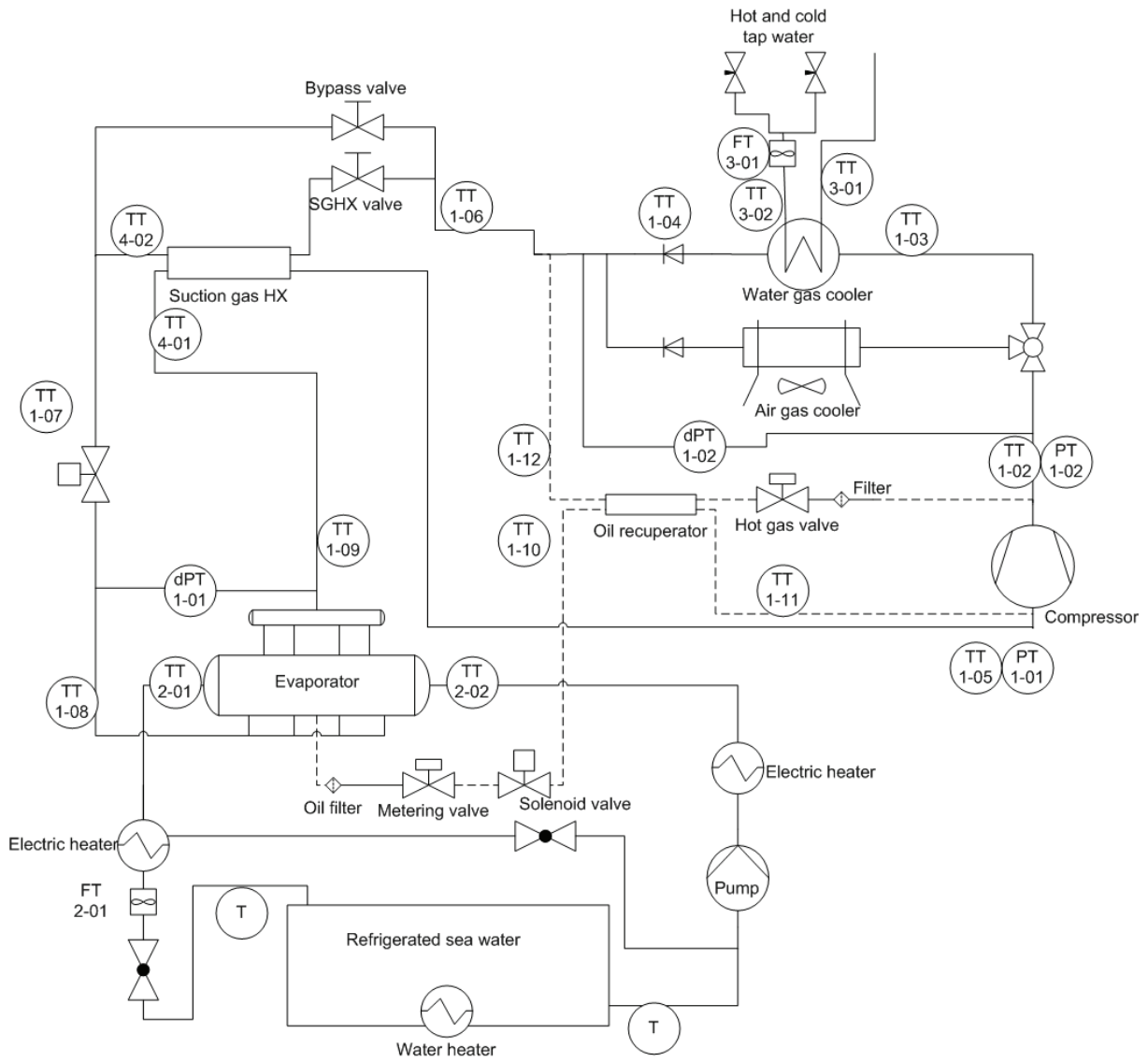


Figure 11-1: The measuring points.

Appendix 3 SGHX control, pseudo-code

Case 1: Decrease the choke inlet temperature/increase flow through SGHX

```
If (SGHX valve not fully open)
    Increase the SGHX valve opening
Else
    Decrease the bypass valve opening
End If
```

Case 2: Increase the choke inlet temperature/decrease flow through SGHX

```
If (bypass valve not fully open)
    Increase the bypass valve opening
Else
    Decrease the SGHX valve opening
End If
```

Appendix 4 Experimental results, cooling

Table 11-2: Experimental cooling results

RSW system								
Refrigerant		R744						
Brine salinity		3,8						
Test condition, cooling water temp_flow		10_5000	15_5000	20_5000	25_5000	15_3000	20_3000	25_3000
Test conditions	Unit	Value	Value	Value	Value	Value	Value	Value
Compressor discharge pressure	bar	74,8	74,8	75,0	80,4	74,0	77,6	83,6
Rotation speed	RPM	1451,0	1451,0	1451,0	1451,0	1451,0	1451,0	1451,0
Brine flow	l/min	543,0	544,0	543,4	543,8	542,1	542,0	541,7
Brine temp at startup	°C	10,0	15,0	20,0	25,0	15,0	20,0	25,0
Cooling water temperature	°C	9,9	14,7	20,5	25,3	14,7	20,0	25,3
Performance		Value	Value	Value	Value	Value	Value	Value
Cooling capacity	kW	37,3	36,0	32,8	30,3	32,9	30,8	27,9
Heating capacity (cooling water side)	kW	50,5	49,2	45,7	43,8	46,3	44,1	41,4
Power consumption (compr + pump)	kW	16,1	16,1	16,1	17,0	15,6	16,4	17,4
COP cooling (pump included)	-	2,3	2,2	2,0	1,8	2,1	1,9	1,6
Evaporator		Value	Value	Value	Value	Value	Value	Value
Inlet temp	°C	-6,3	-5,8	-5,7	-5,0	-5,1	-5,1	-4,9
Outlet temp	°C	-5,9	-5,4	-5,9	-5,1	-5,1	-5,0	-4,9
Outlet superheat	K	0,5	0,5	-0,1	0,0	0,2	0,2	0,2
Pressure drop	kPa	10,4	12,6	12,4	13,5	15,0	14,7	12,7
Cooling capacity, brine side	kW	41,9	39,8	36,6	34,0	37,4	34,7	32,0
Cooling capacity, CO2 (GC mass flow)	kW	37,3	36,0	32,8	30,3	32,9	30,8	27,9
Brine inlet temp	°C	0,5	0,9	0,2	0,5	0,1	-0,1	-0,3
Brine outlet temp	°C	-0,7	-0,1	-0,8	-0,5	-0,9	-1,0	-1,2
Brine flow	l/min	543,0	544,0	543,4	543,8	542,1	542,0	541,7
LMTD	K	6,0	6,0	5,4	5,0	4,7	4,4	4,2
Heat transfer coefficient (CO2 area)	W/m2K	2062,3	1940,0	1983,6	1978,9	2328,6	2296,4	2258,2
Heat transfer coefficient (H2O area)	W/m2K	2304,2	2167,6	2216,3	2211,1	2601,8	2565,8	2523,0
Refrigerant level (% of height)	%	68,9	70,3	70,3	70,3	70,3	70,3	70,3
Gas cooler		Value	Value	Value	Value	Value	Value	Value
Pressure drop	kPa	80,0	78,2	81,3	77,7	90,7	86,2	79,1
CO2 inlet temp	°C	100,0	102,4	105,7	114,5	99,7	106,7	117,6
CO2 outlet temp	°C	11,9	16,8	23,5	28,0	23,0	26,7	30,6
Water inlet temp	°C	9,9	14,7	20,5	25,3	14,7	20,0	25,3
Water outlet temp	°C	19,1	23,4	28,4	32,7	28,9	32,4	37,2
Temperature approach CO2 out	K	1,9	2,1	3,0	2,7	8,3	6,6	5,2
Cooling water flow	kg/h	4730,3	4881,8	4996,2	5088,9	2810,5	3056,5	2998,9
Heating capacity	kW	50,5	49,2	45,7	43,8	46,3	44,1	41,4
CO2 mass flow, m_gc (from heat balance)	kg/min	10,2	10,2	10,1	10,0	10,5	10,2	9,7
Suction gas heat exchanger		Value	Value	Value	Value	Value	Value	Value
Inlet temp high pressure side	°C	12,2	17,1	23,6	27,9	23,1	26,7	30,6
Outlet temp high pressure side	°C	5,9	11,2	14,7	19,2	6,8	12,3	16,8
Inlet temp low pressure side (evap)	°C	-5,9	-5,4	-5,9	-5,1	-5,1	-5,0	-4,9
Inlet temp low pressure side (at SGHX)	°C	-6,7	-6,2	-6,6	-5,9	-6,0	-5,9	-5,7
Mass throughput (fraction of compr flow)	-	0,8	1,0	0,8	0,8	0,3	0,4	0,5
Heat exchanged (HP heat)	W	2005,5	2672,5	3430,3	3880,9	2502,9	3221,7	3718,6
Overall efficiency (pressure drop neglected)	-	0,5	0,5	0,3	0,4	0,3	0,4	0,5
Choke valve inlet	°C	7,5	11,3	17,2	21,4	18,9	21,5	24,8
Brine reservoir		Value	Value	Value	Value	Value	Value	Value
Reservoir inlet	°C	-0,6	0,0	-0,7	-0,4	-0,8	-0,9	-1,1
Reservoir outlet	°C	-0,1	0,4	-0,4	-0,1	-0,5	-0,6	-0,7
Compressor		Value	Value	Value	Value	Value	Value	Value
Suction pressure	bar	26,5	26,9	27,0	27,6	27,4	27,5	27,6
Suction temperature	°C	2,3	5,2	7,5	10,4	3,7	6,7	9,5
Discharge pressure	bar	74,8	74,8	75,0	80,4	74,0	77,6	83,6
Discharge temperature	°C	101,3	103,7	107,0	115,9	100,9	108,0	119,1
Suction superheat	K	12,3	14,7	16,8	18,9	12,5	15,4	18,0
Power consumption (model)	kW	12,8	12,8	12,9	13,7	12,7	13,3	14,2
Power consumption (actual, m_gc)	kW	12,9	12,9	13,0	13,9	12,5	13,2	14,2
Rotation frequency	RPM	1451,0	1451,0	1451,0	1451,0	1451,0	1451,0	1451,0
CO2 mass flow (compressor model)	kg/min	10,1	10,2	10,1	9,9	10,6	10,3	9,7

Appendix 5 Experimental results, water heating

Table 11-3: Experimental water heating results

R744		10_65	10_70	10_80	15_65	15_70	15_80	20_65	20_70	20_80	25_65	25_70	25_80
Brine salinity		Value	Value	Value	Value	Value	Value	Value	Value	Value	Value	Value	Value
Test condition coolingtemp_outlettemp		Value	Value	Value	Value	Value	Value	Value	Value	Value	Value	Value	Value
RSW system													
Refrigerant		107.2	106.6	107.2	106.1	106.0	107.1	108.1	106.0	106.4	106.4	106.1	106.5
Brine salinity	3,8	1451	1451	1451	1451	1451	1451	1451	1451	1451	1451	1451	1451
Test condition coolingtemp_outlettemp		543.7	543.9	543.7	541.5	541.6	540.5	545.3	544.9	545.3	541.9	541.2	541.3
Compressor discharge pressure	bar	10	10	10	15	15	15	20	20	20	25	25	25
Rotation speed	RPM	10.2	9.3	10.3	16.2	14.1	16.7	19.5	19.4	19.5	24.8	25.6	24.1
Brine flow	l/min	17.4	15.9	12.2	15.2	13.9	10.4	16.3	10.7	9.8	14.9	12.5	6.2
Brine temp at startup	°C	34.8	33.3	29.7	32.9	32.0	28.0	33.0	30.1	27.6	32.7	30.7	24.7
Cooling water temperature	°C	19.5	19.4	19.6	19.7	19.8	19.7	20.1	19.4	19.8	19.9	20.2	19.3
Heating capacity (cooling water side)	kW	0.89	0.82	0.62	0.77	0.70	0.53	0.81	0.55	0.50	0.75	0.62	0.32
Power consumption (compr + pump)	kW												
COP-cooling (pump included)	-												
Evaporator													
Inlet temp	°C	-2.1	-2.0	-1.8	-2.2	-1.8	-1.5	-2.2	-1.8	-1.8	-2.0	-2.1	-1.7
Outlet temp	°C	-2.3	-2.0	-2.0	-2.5	-2.0	-1.7	-2.4	-2.1	-2.1	-2.2	-2.3	-1.9
Outlet superheat	K	0.0	0.0	0.0	0.0	0.0	0.0	0.0	0.0	0.0	0.0	0.0	0.0
Pressure drop	kPa	15.9	16.2	18.3	17.1	18.5	19.9	15.8	17.9	19.4	16.9	17.8	12.2
Cooling capacity, brine side	kW	21.3	19.5	15.5	19.8	18.0	14.2	20.0	16.5	13.4	18.7	16.1	6.2
Cooling capacity, CO2 (G.C. mass flow)	kW	17.4	15.9	12.2	15.2	13.9	10.4	16.3	10.7	9.8	14.9	12.5	6.2
Brine inlet temp	°C	1.6	1.3	0.9	0.7	0.9	0.6	1.4	1.0	0.5	0.9	0.4	0.0
Brine outlet temp	°C	1.0	0.8	0.5	0.2	0.5	0.2	0.8	0.6	0.1	0.4	-0.1	-0.3
Brine flow	l/min	543.7	543.9	543.7	541.5	541.6	540.5	545.3	544.9	545.3	541.9	541.2	541.3
LMTD	K	3.5	3.2	2.5	2.8	2.8	2.0	3.4	2.8	2.2	2.8	2.3	1.7
Heat transfer coefficient (CO2 area)	W/m2K	1805.5	1816.7	1794.6	2070.1	2049.8	2069.9	1726.1	1748.5	1780.0	1984.7	2029.7	2138.4
Heat transfer coefficient (H2O area)	W/m2K	2017.3	2029.8	2005.1	2312.9	2290.3	2312.7	1928.6	1953.6	1888.8	2217.5	2267.8	2389.2
Refrigerant level (% of height)	%	66.9	66.9	70.3	70.3	70.3	70.3	66.9	66.9	66.9	70.3	70.3	70.3
Gas cooler													
Pressure drop	kPa	77.8	80.0	84.0	78.8	82.7	84.9	78.7	83.6	85.7	80.0	82.0	88.0
CO2 inlet temp	°C	128.4	128.4	128.4	128.4	128.6	128.7	128.6	128.6	128.8	128.6	129.0	129.0
CO2 outlet temp	°C	43.8	45.5	49.6	46.2	47.8	51.4	46.1	48.9	52.0	46.8	49.3	53.7
Water inlet temp	°C	10.2	9.3	10.2	16.2	14.1	16.7	19.5	19.4	19.5	24.8	25.6	24.1
Water outlet temp	°C	67.0	70.8	79.9	66.3	70.2	79.8	65.1	70.0	79.8	65.1	70.1	80.8
Temperature approach CO2 out	K	33.6	36.2	39.3	30.0	33.7	34.7	26.6	30.0	32.5	22.0	23.7	29.6
Cooling water flow	kg/h	526.3	466.2	366.7	565.9	490.3	382.1	623.9	513.2	393.0	699.3	593.5	374.1
Heating capacity	kW	34.8	33.3	29.7	32.9	32.0	28.0	33.0	30.1	27.6	32.7	30.7	24.7
CO2 mass flow, m. gc (from heat balance)	kg/min	9.7	9.8	10.0	9.9	10.2	10.1	9.8	10.0	10.2	10.1	10.3	9.8
Suction gas heat exchanger													
Inlet temp high pressure side	°C	44.0	45.6	49.5	46.2	47.7	51.2	45.9	48.6	51.6	46.9	49.2	53.3
Outlet temp high pressure side	°C	21.3	25.2	30.3	26.1	23.1	25.1	3.2	15.7	17.4	27.9	27.1	23.0
Inlet temp low pressure side (evap)	°C	-2.3	-2.3	-2.0	-2.5	-2.0	-1.7	-2.4	-2.1	-2.1	-2.2	-2.3	-1.9
Inlet temp low pressure side (at SGHX)	°C	-3.0	-3.1	-2.9	-3.4	-2.9	-2.7	-3.1	-2.9	-3.0	-3.1	-3.2	-2.9
Mass throughput (fraction of compr flow)	-	0.0	0.0	0.0	0.0	0.0	0.0	0.0	0.0	0.0	0.0	0.0	0.0
Heat exchanged (HP heat)	W	221.0	282.3	375.4	338.4	352.2	349.4	498.0	347.4	326.1	353.8	394.8	334.0
Overall efficiency (pressure drop neglected)	-	0.0	0.0	0.0	0.0	0.0	0.0	0.0	0.0	0.0	0.0	0.0	0.0
Choke valve inlet	°C	43.7	45.3	49.2	45.9	47.4	50.9	45.3	48.3	51.2	46.6	48.9	53.0
Brine reservoir													
Reservoir inlet	°C	1.1	0.7	0.3	0.1	0.5	0.0	0.7	0.4	-0.1	0.5	-0.2	-0.5
Reservoir outlet	°C	1.2	0.8	0.5	0.2	0.5	0.2	0.9	0.6	0.0	0.5	-0.1	-0.4
Compressor													
Suction pressure	bar	30.3	30.3	30.5	30.0	30.4	30.5	30.2	30.5	30.4	30.2	30.2	30.4
Suction temperature	°C	-1.6	-2.3	-2.1	-2.2	-2.0	-2.0	-0.9	-2.0	-2.2	-1.6	-2.4	-2.0
Discharge pressure	bar	107.2	106.6	107.2	106.1	106.0	107.1	108.1	106.0	106.4	106.4	106.1	106.5
Discharge temperature	°C	129.9	130.0	129.9	130.9	130.1	130.1	130.2	130.2	130.3	130.1	130.5	128.4
Suction superheat	K	3.6	2.9	2.8	3.3	3.1	2.9	4.4	3.0	2.9	3.7	3.0	3.0
Power consumption (model)	kW	16.5	16.5	16.6	16.3	16.6	16.6	16.4	16.6	16.6	16.5	16.4	16.6
Power consumption (actual, m. gc)	kW	16.4	16.2	16.5	16.5	16.5	16.5	16.4	16.5	16.5	16.5	16.4	16.5
Rotation frequency	RPM	1451	1451	1451	1451	1451	1451	1451	1451	1451	1451	1451	1451
CO2 mass flow (compressor model)	kg/min	9.8	9.9	10.1	9.7	10.2	10.1	9.4	10.2	10.1	9.9	9.9	10.1

Appendix 6 Initial gas cooler model

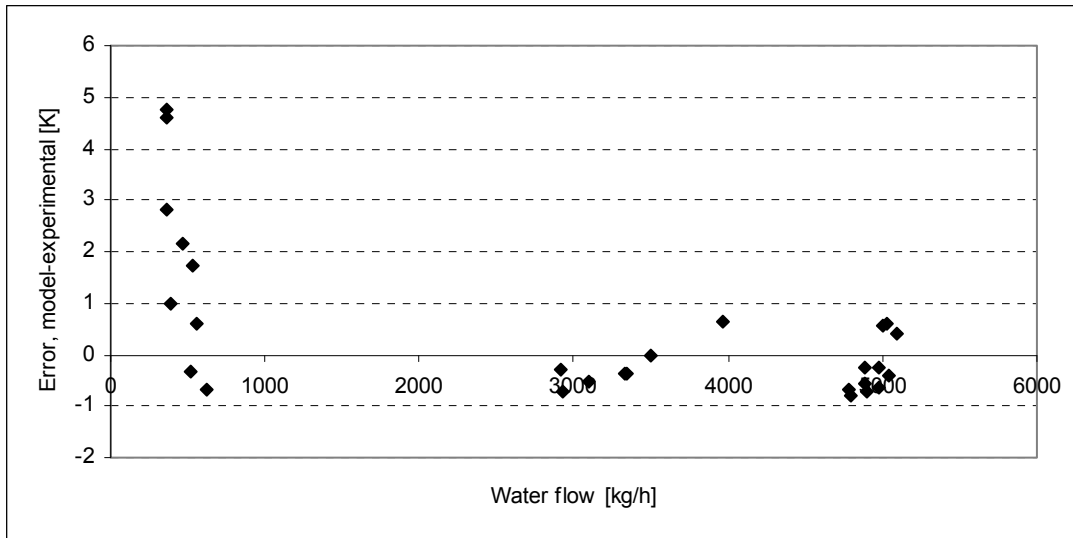


Figure 11-2: Initial gas cooler model error as a function of cooling water flow.

Appendix 7 Gas cooler pressure drop

Table 11-4: Gas cooler pressure drops from the 2007 experiments

Experiments 2007	Compressor mass flow [kg/min]	Inlet temp	Outlet temp	Pressure drop	Inlet pressure
90/15	8,41	112,18	16,39	54,61	89,73
90/20	9,01	113,11	21,70	64,51	89,37
90/25	9,49	111,69	28,33	73,71	89,66
80/10	8,97	98,42	12,31	75,69	79,29
80/15	8,74	97,51	17,67	63,04	79,84
80/20	9,94	94,49	24,74	86,28	79,80
80/25	10,65	89,75	30,28	99,97	79,89
70/10	7,50	81,05	11,62	49,93	70,30
70/15	10,15	79,61	24,42	99,35	68,64
70/20	11,45	74,24	28,90	125,71	69,69
60/10	11,28	61,95	21,90	134,25	59,35
60/15	12,15	58,81	22,21	166,50	59,68
50/10	13,65	43,18	16,51	228,77	52,74

Appendix 8 Suction pipe pressure drop

Table 11-5: Pressure drops based on 2007 experiments without suction gas heat exchanger, and mass flow calculated from the compressor model used at that time.

Exp, 2007	Compr mass flow [kg/min]	Evap outlet pressure [bar]	Compr suction pressure [bar]	Pipe pressure drop [bar]	Average pressure [bar]	Average temp [°C]	Pipe velocity [m/s]	Density [kg/m ³]	Dynamic viscosity [Pa s]	Reynolds number [-]
90_15	8,4	29,0	27,5	1,477	28,247	-3,873	7,484	73,572	1,420E-05	6,980E+05
90_20	9,0	29,1	27,5	1,548	28,276	-4,128	7,988	73,863	1,419E-05	7,483E+05
90_25	9,5	29,5	27,9	1,576	28,664	-4,055	8,259	75,287	1,422E-05	7,872E+05
80_10	9,0	27,5	26,0	1,466	26,772	-5,593	8,484	69,264	1,405E-05	7,527E+05
80_15	8,7	28,8	27,3	1,540	28,023	-4,329	7,836	73,053	1,417E-05	7,271E+05
80_20	9,9	29,4	27,7	1,692	28,551	-4,615	8,645	75,269	1,419E-05	8,255E+05
80_25	10,6	30,6	28,9	1,736	29,720	-3,898	8,792	79,311	1,429E-05	8,787E+05
70_10	7,5	29,5	28,2	1,303	28,874	-3,132	6,511	75,404	1,426E-05	6,195E+05
70_15	10,2	28,5	26,9	1,613	27,729	-5,837	9,106	73,006	1,409E-05	8,490E+05
70_20	11,4	30,8	29,1	1,728	29,948	-4,101	9,323	80,406	1,429E-05	9,441E+05
60_10	11,3	29,2	27,6	1,627	28,386	-6,084	9,753	75,751	1,412E-05	9,416E+05
60_15	12,1	30,9	29,0	1,939	29,920	-4,517	9,866	80,655	1,428E-05	1,003E+06
50_10	13,6	32,0	30,1	1,998	31,049	-3,898	10,536	84,834	1,437E-05	1,119E+06
Pipe inner diameter	0,018meters									
Pipe inner area	2,5447E-04m ²									

Appendix 9 Evaporator pressure drop, data from 2007

Table 11-6: Evaporator pressure drops, 2007 data

Massflow, compressor [kg/min]	Inlet temp [°C]	Outlet temp [°C]	Pressure drop [kPa]	Evap sat gas volume flow [m ³ /s]
8,41	-6,8	-4,4	10,81	1,779E-03
9,01	-6,7	-4,7	14,85	1,901E-03
9,49	-6,2	-4,6	17,54	1,972E-03
8,97	-8,7	-6,1	14,47	2,014E-03
8,74	-7,0	-4,9	12,23	1,863E-03
9,94	-6,3	-5,1	20,07	2,069E-03
10,65	-4,8	-4,3	24,66	2,118E-03
7,50	-6,1	-3,7	8,55	1,553E-03
10,15	-7,4	-6,2	24,01	2,186E-03
11,45	-4,6	-4,4	34,33	2,258E-03
11,28	-6,5	-6,3	35,42	2,367E-03
12,15	-4,5	-4,6	42,90	2,390E-03
13,65	-3,1	-3,8	54,04	2,572E-03

Appendix 10 The original system

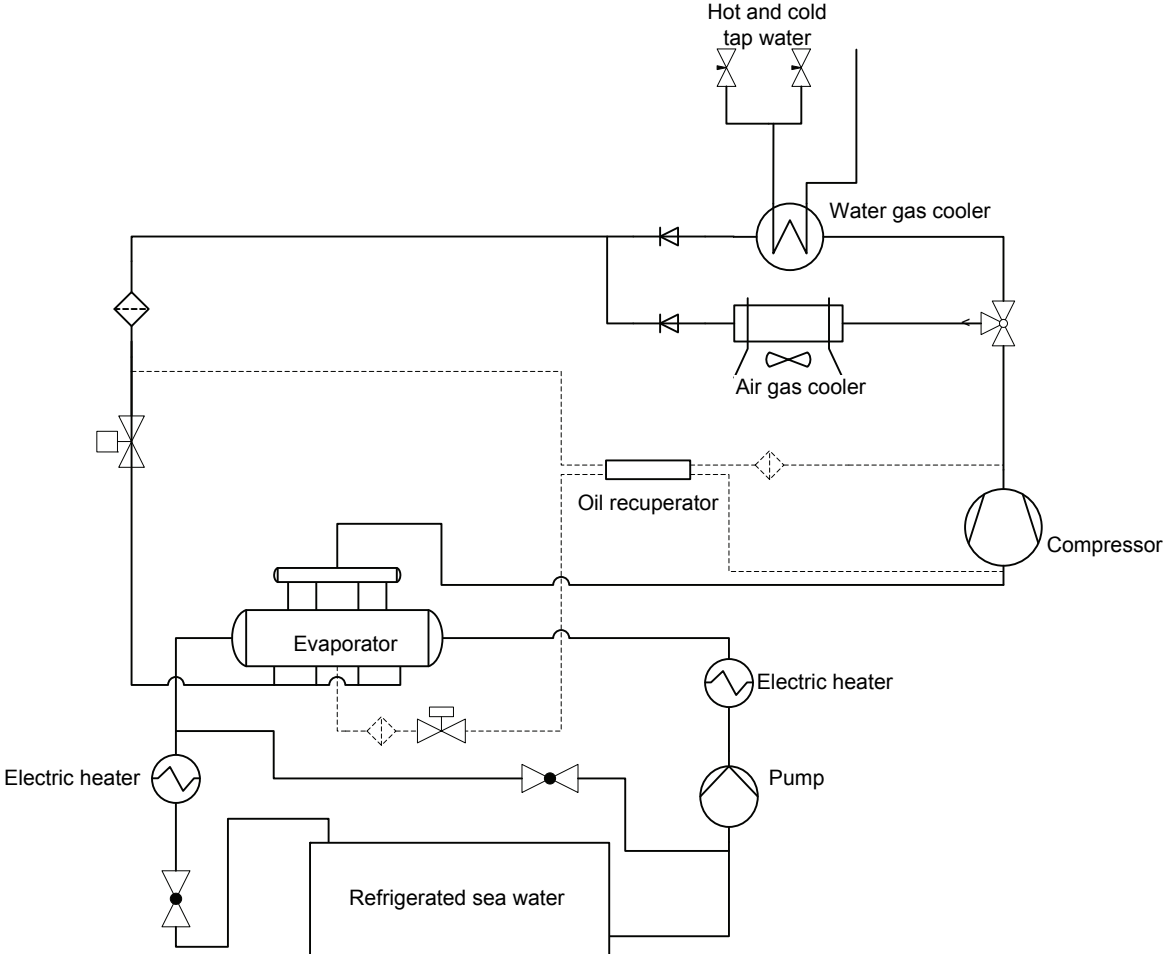
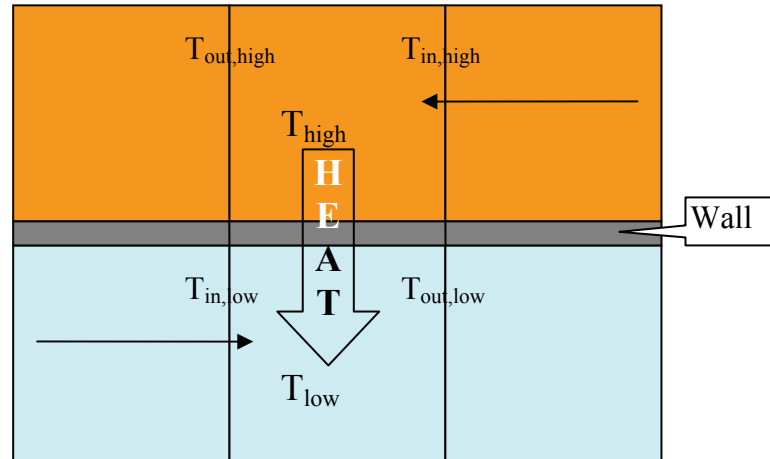


Figure 11-3: The system as it was before any modification.

Appendix 11 Gas cooler solver

The calculations start on the highest index (CO₂ inlet) on the CO₂ side, then calculates to the left. Then the calculation starts on the lowest index (water inlet) on the water side, and proceeding to the right.



```

For loop until convergence
' High side calculation
For i = number_of_sections To 1 Step -1
  Calculate tbh
  Calculate pressure drop from element (i+1,1) to (i,1)
  Calculate pressure at element i,1
  Calculate convection coefficient, hch

  *Based on previous iteration
  Calculate tbc
  Calculate convection coefficient hcc

  Calculate Rtot
  Calculate the heat transfer based on bulk (tbh, tbc)
  Calculate temperature at element i based on enthalpy
Next i

' Low side calculation
For i = 1 To number_of_sections Step 1
  Calculate tbc
  Calculate pressure drop from element (i, 2) to (i+1, 2)
  Calculate pressure at element (i+1, 2)
  Calculate convection coefficient, hcc

  *Based on previous iteration
  Calculate tbh
  Calculate convection coefficient hch

  Calculate Rtot
  Calculate heat transfer (enthalpy) based on bulk temperatures
  Calculate temperature at element (i+1, 2) based on the enthalpy
Next i
End loop

```

Appendix 12 Compressor model data

Table 11-7: Data used for creating models for isentropic and volumetric efficiency for the compressor

	RPM	Compr suction bara	Compr discharge bara	Compr suction °C	Compr discharge °C	Mass gas cooler kg/min	pr	nis	Vol.eff
From Japan (2007)									
90_15	1320	27,51	89,73	-3,34	114,08		3,26202	0,58990	
90_20	1410	27,50	89,37	-3,51	114,86		3,24945	0,57707	
90_25	1451	27,88	89,66	-3,49	113,31		3,21634	0,57804	
80_10	1451	26,04	79,29	-5,06	100,06		3,04510	0,63876	
80_15_b	1320	27,25	79,84	-3,75	99,03		2,92956	0,61916	
80_20	1451	27,70	79,80	-4,11	95,87		2,88035	0,62483	
80_25	1451	28,85	79,89	-3,54	91,00		2,76912	0,63615	
70_10	1020	28,22	70,30	-2,59	82,57		2,49093	0,62921	
70_15	1451	26,92	68,64	-5,49	80,87		2,54973	0,63607	
70_20	1451	29,08	69,69	-3,83	75,39		2,39620	0,64342	
60_10	1451	27,57	59,35	-5,91	63,02		2,15266	0,63793	
60_15	1451	28,95	59,68	-4,45	59,96		2,06128	0,64242	
50_10	1451	30,05	52,74	-4,03	44,40		1,75493	0,65528	
Japan (2007) hot water									
108/65	1428	29,73	107,97	-0,13	129,75		3,63176	0,58832	
95/70	1428	30,60	95,22	-0,58	118,23		3,11218	0,52666	
109/80	1428	30,24	108,52	-0,38	134,00		3,58932	0,53906	
Project work, Sondre Sætrang 2008									
501010	1451	29,05	50,25	-3,63	41,42		1,72939	0,73480	
601010	1451	26,96	60,11	7,92	83,30		2,22940	0,67282	
601515	1451	27,87	60,09	10,37	83,49		2,15583	0,66316	
701010	1451	26,57	70,09	3,70	95,82	10,36430	2,63763	0,66045	0,78607
701515	1451	27,20	69,96	7,73	99,26	10,15916	2,57227	0,65189	0,77003
702020	1451	27,81	70,03	10,66	100,53	10,57599	2,51834	0,65558	0,79533
801010	1451	26,82	79,24	3,11	108,60	9,87926	2,95500	0,64021	0,73712
801515	1451	27,16	79,78	5,95	112,14	9,84481	2,93742	0,63821	0,73788
802020	1451	27,72	80,26	8,32	114,21	9,91026	2,89565	0,63380	0,73607
802525	1451	28,07	80,47	11,24	115,19	10,10586	2,86696	0,65406	0,75405
901515	1451	27,41	89,74	5,75	125,81	9,27060	3,27379	0,61788	0,68560
902020	1451	27,90	89,96	8,25	128,96	9,23582	3,22420	0,60672	0,67981
902525	1451	28,22	90,14	10,74	129,14	9,45062	3,19435	0,62669	0,69791
Testing with variable SGHX									
10/74	1451	26,98	74,44	-2,93	92,81	10,86194	2,75889	0,63475	0,76502
15/74	1451	26,93	74,79	5,24	103,68	10,24748	2,77712	0,65500	0,77251
20/74	1451	27,03	74,99	7,48	107,00	10,14952	2,77439	0,65144	0,77405
25/80	1451	27,63	80,41	10,36	115,92	9,97918	2,90999	0,65193	0,75504
hw1065	1451	30,28	107,19	-1,62	129,93	9,70552	3,53995	0,53947	0,58672
hw1070	1451	30,27	106,64	-2,27	129,97	9,76606	3,52285	0,52641	0,58673
hw1080	1451	30,49	107,16	-2,13	129,89	9,98562	3,51468	0,52508	0,59443
hw2065	1451	30,20	108,11	-0,91	130,21	9,75211	3,58028	0,55800	0,59623
hw2070	1451	30,46	106,02	-1,95	130,18	10,00854	3,48096	0,51799	0,59780
hw2080	1451	30,39	106,40	-2,22	130,32	10,17507	3,50086	0,51864	0,60798

Appendix 13 Gas cooler model testing

Table 11-8. Gas cooler model testing. The length was adjusted to minimize the sum of squared error.

	High side pressure [bar]	Mass flow CO2 [kg/min]	Gas cooler inlet temp [°C]	Gas cooler outlet temp [°C]	Cooling water temp [°C]	Cooling water flow [kg/h]	GC model outlet [°C]	Error	Error ²
2008	80	9,88	107,27	11,63	10,13	4797,25	10,89	-0,74	0,55
	80	9,84	110,69	16,47	14,95	4890,50	15,97	-0,50	0,25
	80	9,91	112,75	21,65	19,83	4971,46	21,49	-0,16	0,03
	80	10,11	113,67	27,26	24,64	5033,71	27,98	0,72	0,51
	90	9,27	124,11	15,97	14,92	4895,27	15,27	-0,70	0,49
	90	9,24	127,21	20,95	19,84	4974,72	20,34	-0,61	0,37
	90	9,45	127,40	26,22	24,95	5043,69	25,87	-0,36	0,13
2007, hot water	108	9,32	128,21	44,00	14,35	562,50	44,29	0,29	0,08
	95	10,41	117,07	47,09	13,16	367,33	46,87	-0,22	0,05
	109	8,98	132,44	48,46	11,21	367,33	48,98	0,52	0,27
2007 transcritical	80	9,35	100,06	12,31	10,30	3340,00	12,04	-0,27	0,07
	80	8,47	99,03	17,67	15,30	2921,40	17,51	-0,17	0,03
	80	10,30	95,87	24,74	20,30	3502,32	24,91	0,17	0,03
	80	11,37	91,00	30,28	24,60	3969,59	31,05	0,77	0,59
	90	7,95	114,08	16,39	14,86	2930,40	15,72	-0,66	0,44
	90	8,86	114,86	21,70	19,69	3092,40	21,26	-0,44	0,20
	90	9,61	113,31	28,33	25,40	3333,60	28,08	-0,25	0,06
2009, testing	74	10,86	91,67	12,35	9,99	4776,58	11,79	-0,56	0,31
	75	10,25	102,39	16,82	14,71	4881,78	16,68	-0,13	0,02
	75	10,15	105,65	23,55	20,52	4996,21	24,25	0,70	0,50
	80	9,98	114,45	28,02	25,32	5088,91	28,57	0,54	0,30
	107	9,71	128,36	43,81	10,17	526,29	44,73	0,93	0,86
	107	9,77	128,44	45,47	9,30	466,15	46,23	0,76	0,58
	107	9,99	128,37	49,59	10,26	366,66	50,08	0,49	0,24
	108	9,75	128,62	46,07	19,51	623,87	45,55	-0,52	0,27
	106	10,01	128,63	48,86	19,43	513,18	47,93	-0,93	0,87
	106	10,18	128,79	51,96	19,45	393,00	51,28	-0,69	0,47

Appendix 14 SGHX model data

Table 11-9: Data used for estimating the SGHX performance

2008 experiments	High side pressure (bar)						
	80	80	80	80	90	90	90
Mass flow (compr)	8,846912	8,829253	8,963501	8,959609	8,521501	8,625329	8,634882
Inlet temp, HP	12,00743	17,17055	21,91359	27,19812	16,25778	21,33266	26,21047
Outlet temp, HP	7,247143	11,40448	15,42108	20,39297	10,53408	14,63523	18,784
Inlet temp, LP	-5,07543	-4,85912	-4,46586	-4,25294	-4,50736	-4,25251	-4,04372
Outlet temp, LP	3,112257	5,947091	8,317838	11,24464	5,753694	8,247143	10,73691
LMTD	10,51595	13,58809	16,54245	19,98563	12,63729	15,80957	18,91294
Qmax	3491,416	4423,628	5313,934	6261,003	4052,847	4976,417	5831,474
Heat transfered	1741,25	2251,865	2812,174	3553,277	2037,836	2584,978	3168,692
U-value (inner)	1464,065	1465,317	1503,107	1572,022	1425,814	1445,721	1481,388
Efficiency	0,498723	0,509054	0,529208	0,567525	0,502816	0,519446	0,543378
U-value average	1479,633	W/m2K					
Inner area	0,113097	m2					

Appendix 15 Medium cooling water flow rate interpolation table

Table 11-10: Medium water flow rate used for linear interpolation.

Water								
CW temp [°C]	flow [kg/h]	Evap [°C]	Pressure [bar]	Choke [°C]	COP [-]	Q0 [kW]	IHX [-]	Gcout [°C]
10	2500	-5	74,0	15,3	2,7	35,0	0,4	19,7
10	2500	-6	74,0	12,7	2,7	34,4	0,5	18,4
10	2800	-5	74,0	13,3	2,8	36,2	0,4	17,5
10	2800	-6	74,0	10,9	2,7	35,4	0,5	16,3
15	2500	-5	76,0	18,9	2,4	32,0	0,5	24,7
15	2500	-6	76,0	17,7	2,4	31,3	0,5	23,6
15	2800	-5	74,0	18,7	2,5	32,4	0,5	24,3
15	2800	-6	74,0	17,5	2,5	31,7	0,5	23,3
20	2500	-5	82,0	21,1	2,1	29,8	0,5	27,2
20	2500	-6	80,0	21,6	2,1	28,5	0,5	27,5
20	3000	-5	78,0	21,6	2,2	30,2	0,5	27,2
20	3000	-6	78,0	20,5	2,2	29,5	0,5	26,4
25	2500	-5	86,0	25,2	1,8	26,7	0,5	31,2
25	2500	-6	84,0	25,7	1,8	25,4	0,5	31,4
25	3000	-5	84,0	24,4	1,9	27,6	0,5	30,3
25	3000	-6	84,0	23,4	1,9	26,7	0,5	29,6

Appendix 16 Model verification data

Table 11-11: Model verification data

	Full water flow rate			Medium water flow rate			Combined heating and cooling													
	10	15	20	25	mr15	mr20	mr25	1065	1070	1080	1565	1570	1580	2065	2070	2080	2565	2570	2580	
COP [-]	Experimental	2.89	2.78	2.52	2.18	2.64	1.96	1.07	0.98	0.74	0.92	0.83	0.63	0.96	0.66	0.59	0.89	0.73	0.39	
	Simulated	2.86	2.71	2.43	2.11	2.62	2.23	1.92	1.04	0.94	0.71	0.96	0.88	0.64	1.00	0.82	0.62	0.95	0.79	0.58
Cooling [kW]	Model error (%)	-1.58	-2.49	-3.77	-3.48	-4.52	-4.06	-2.18	-2.44	-4.58	-4.50	4.60	5.14	2.35	4.20	23.86	5.10	7.56	8.86	49.78
	Experimental	37.29	35.97	32.75	30.32	32.92	30.81	27.87	17.44	15.89	12.16	15.21	13.88	10.38	16.32	10.71	9.83	14.87	12.45	6.25
Mass flow [kg/min]	Simulated	37.11	35.44	31.69	29.20	32.47	30.12	27.51	17.11	15.44	11.71	15.80	14.56	10.75	16.46	13.54	10.29	15.73	13.06	9.66
	Model error (%)	-0.47	-1.47	-3.23	-3.71	-1.38	-2.25	-1.29	-1.93	-2.81	-3.73	3.83	4.91	3.60	0.83	26.48	4.65	5.82	4.84	54.73
Compr suction pressure [bar]	Experimental	10.16	10.25	10.15	9.98	10.48	10.20	9.69	9.71	9.77	9.99	9.85	10.21	10.06	9.75	10.01	10.18	10.06	10.31	9.81
	Simulated	10.06	10.02	9.86	9.72	10.26	9.90	9.50	9.46	9.68	9.82	9.67	9.96	10.03	9.39	9.96	9.96	9.76	9.73	9.96
Compressor isentropic efficiency [-]	Model error (%)	-1.03	-2.21	-2.84	-2.57	-2.15	-3.00	-1.92	-2.52	-0.92	-1.67	-1.81	-2.44	-0.25	-3.73	-0.53	-2.15	-2.94	-5.62	1.56
	Experimental	26.50	26.93	27.03	27.63	27.41	27.50	27.64	30.28	30.27	30.49	30.00	30.39	30.54	30.20	30.46	30.39	30.23	30.16	30.40
Compressor volumetric efficiency [-]	Simulated	25.87	26.33	26.50	27.18	26.86	27.02	27.36	29.88	29.90	30.03	29.71	29.98	30.23	29.82	29.98	29.98	29.87	29.78	30.07
	Model error (%)	-2.35	-2.22	-1.97	-1.64	-2.03	-1.76	-1.03	-1.31	-1.24	-1.50	-0.96	-1.35	-1.03	-1.25	-1.58	-1.37	-1.20	-1.23	-1.10
Gas cooler pressure drop [kPa]	Experimental	0.656	0.655	0.651	0.652	0.626	0.647	0.650	0.539	0.526	0.525	0.526	0.520	0.523	0.558	0.518	0.519	0.534	0.522	0.535
	Simulated	0.632	0.636	0.637	0.625	0.642	0.632	0.613	0.548	0.548	0.552	0.548	0.556	0.553	0.542	0.556	0.554	0.551	0.551	0.563
Gas cooler temperature approach [K]	Model error (%)	-3.58	-2.85	-2.29	-4.19	2.59	-2.30	-5.74	1.54	4.55	5.04	4.22	6.77	5.70	-2.94	7.43	6.74	3.14	5.52	3.53
	Experimental	0.766	0.772	0.774	0.765	0.764	0.757	0.729	0.587	0.587	0.594	0.600	0.611	0.598	0.596	0.598	0.608	0.610	0.622	0.587
Evaporator pressure drop [kPa]	Simulated	0.760	0.766	0.767	0.748	0.775	0.760	0.728	0.591	0.597	0.600	0.592	0.609	0.602	0.577	0.611	0.604	0.598	0.598	0.604
	Model error (%)	-0.72	-0.82	-0.97	-0.98	1.46	0.49	-0.14	0.76	1.75	0.89	-1.28	-0.47	0.66	-3.19	2.16	-0.61	-1.86	-3.90	2.91
Gas cooler pressure drop [kPa]	Experimental	80.0	78.2	81.3	77.7	80.7	86.2	79.1	77.8	80.0	84.0	78.8	82.7	84.9	78.7	83.6	85.7	80.0	82.0	88.0
	Simulated	95.3	94.3	89.8	86.1	101.0	90.8	80.3	79.2	84.9	88.7	84.8	92.5	94.6	77.3	92.5	92.5	87.1	86.3	92.5
Gas cooler temperature approach [K]	Model error (%)	19.01	20.59	10.53	10.76	11.33	5.36	1.53	1.76	6.03	5.65	7.54	11.79	11.34	-1.68	10.60	7.92	8.92	5.22	5.11
	Experimental	1.94	2.11	3.02	2.70	8.27	6.65	5.24	33.64	36.17	39.33	29.96	33.67	34.70	26.55	29.44	32.51	22.00	23.75	29.56
Evaporator pressure drop [kPa]	Simulated	1.18	1.72	3.34	3.15	9.17	7.14	5.57	33.99	36.68	39.30	29.10	32.67	33.99	25.29	28.26	31.12	20.81	22.31	27.38
	Model error (%)	-0.76	-0.39	0.32	0.45	0.90	0.49	0.33	-0.86	-0.02	-0.86	-1.00	-0.71	-1.26	-1.18	-1.39	-1.20	-1.44	-2.18	-2.18
Evaporator pressure drop [kPa]	Experimental	10.4	12.6	12.4	13.5	15.0	14.7	12.7	15.9	16.2	18.3	17.1	18.5	19.9	15.8	17.9	19.4	16.9	17.8	20.4
	Simulated	32.3	30.1	27.9	24.1	30.2	26.3	21.6	13.9	15.4	16.0	15.8	17.1	17.0	13.6	17.1	17.1	16.0	16.0	16.9
Model error (%)	210.1	138.3	124.5	78.6	101.8	79.2	69.6	-12.7	-4.9	-12.4	-7.3	-7.4	-14.7	-14.2	-4.3	-11.6	-4.9	-9.8	-17.1	

Appendix 17 New gas cooler model data

Table 11-12: Data used for the new gas cooler model, sorted by mass flow.

Experiements	Mass flow (gas cooler) [kg/min]	Gas cooler pressure drop [kPa]	Model	Model error (%)
Japan, 2007	7,06	49,93	49,68	-0,5
Japan, 2007	7,95	54,61	55,58	1,8
Japan, 2007	8,47	63,04	60,38	-4,2
Japan, 2007	8,86	64,51	64,47	-0,1
Autumn 2008	9,24	65,58	69,05	5,3
Autumn 2008	9,27	62,75	69,49	10,7
Japan, 2007	9,35	75,69	70,59	-6,7
Autumn 2008	9,45	77,20	71,86	-6,9
Japan, 2007	9,61	73,71	74,12	0,6
Spring 2009	9,69	79,07	75,17	-4,9
Autumn 2008	9,84	72,72	77,45	6,5
Autumn 2008	9,88	72,72	77,96	7,2
Autumn 2008	9,91	77,41	78,43	1,3
Spring 2009	9,98	77,74	79,48	2,2
Autumn 2008	10,11	90,25	81,45	-9,7
Spring 2009	10,15	81,29	82,14	1,0
Autumn 2008	10,16	79,59	82,30	3,4
Spring 2009	10,16	80,04	82,34	2,9
Spring 2009	10,20	86,17	82,97	-3,7
Spring 2009	10,25	78,16	83,72	7,1
Japan, 2007	10,30	86,28	84,64	-1,9
Autumn 2008	10,36	82,38	85,65	4,0
Spring 2009	10,48	90,74	87,68	-3,4
Autumn 2008	10,58	93,05	89,26	-4,1
Autumn 2008	10,74	95,23	92,24	-3,1
Japan, 2007	10,99	99,35	96,83	-2,5
Japan, 2007	11,37	99,97	104,27	4,3

Appendix 18 SGHX pressure drop calculation

Table 11-13. SGHX pressure drop calculations

2008 experiments	60_10	60_15	70_10	70_15	70_20	80_10
Evap pressure [bar]	32,5	29,8	30,9	29,3	30,0	30,5
Evap pressure drop [kPa]	47,4	14,5	22,3	11,2	13,0	16,0
Flow CO ₂ , compr [kg/min]	27,0	27,9	26,6	27,2	27,8	26,8
Evap outlet [°C]	7,9	10,4	3,7	7,7	10,7	3,1
Compr suction temp [°C]	9,6	10,0	9,1	9,2	9,4	8,8

Pressure drop evap outlet-compr suction [bar]	3,0	2,7	2,8	2,6	2,6	2,5
Average pressure (evap outlet, compr suction) [bar]	30,5	28,3	29,3	27,9	28,5	29,1
Average temperature (evap outlet, compr suction) [°C]	-3,3	1,3	2,8	-0,9	1,4	3,1
Reynolds SGHX	3,47E+06	2,56E+06	2,65E+06	2,45E+06	2,45E+06	2,47E+06

Suction pipe model (based on 2007 results)	60_10	60_15	70_10	70_15	70_20	80_10
avg P = suction pressure [bar]	29,1	27,0	27,9	26,6	27,2	27,8
avg t = suction temperature [°C]	-3,6	7,9	10,4	3,7	7,7	10,7
Diameter [m]	0,018	0,018	0,018	0,018	0,018	0,018
Reynolds number [-]	1,07E+06	7,76E+05	7,99E+05	7,45E+05	7,42E+05	7,47E+05
Model pressure drop [bar]	1,962	1,579	1,613	1,532	1,528	1,535

SGHX pressure drop = Actual - 2007 model [Pa]	101320,85	107907,21	115226,79	110251,11	110877,58	96549,65
--	-----------	-----------	-----------	-----------	-----------	----------

2008 experiments	80_15	80_20	80_25	90_15	90_20	90_25
Evap pressure [bar]	29,5	29,9	30,3	30,7	30,0	30,4
Evap pressure drop [kPa]	9,4	10,7	14,1	14,2	8,9	11,9
Flow CO ₂ , compr [kg/min]	27,2	27,7	28,1	27,4	27,9	28,2
Evap outlet [°C]	5,9	8,3	11,2	5,8	8,2	10,7
Compr suction temp [°C]	8,8	9,0	9,0	8,5	8,6	8,6

Pressure drop evap outlet-compr suction [bar]	2,6	2,6	2,4	2,5	2,5	2,3
Average pressure (evap outlet, compr suction) [bar]	28,1	28,5	28,9	29,3	28,7	29,1
Average temperature (evap outlet, compr suction) [°C]	-1,0	0,5	1,9	3,5	0,6	2,0
Reynolds SGHX	2,37E+06	2,35E+06	2,38E+06	2,36E+06	2,27E+06	2,29E+06

Suction pipe model (based on 2007 results)	80_15	80_20	80_25	90_15	90_20	90_25
avg P = suction pressure [bar]	26,8	27,2	27,7	28,1	27,4	27,9
avg t = suction temperature [°C]	3,1	5,9	8,3	11,2	5,8	8,2
Diameter [m]	0,018	0,018	0,018	0,018	0,018	0,018
Reynolds number [-]	7,23E+05	7,15E+05	7,20E+05	7,13E+05	6,90E+05	6,93E+05
Model pressure drop [bar]	1,499	1,486	1,493	1,482	1,446	1,450

SGHX pressure drop = Actual - 2007 model [Pa]	105904,86	110417,57	95423,13	102541,05	106569,66	89983,21
--	-----------	-----------	----------	-----------	-----------	----------

Appendix 19 Cooling, 2008 results

Please take note that the compressor mass flow calculations was calculated using a different model than in the later results (spring 2009). This was corrected in all comparisons made with the new measurements.

Table 11-14: Cooling results, 2008

TEST CONDITIONS	Unit	501010	601010	701010	701515	702020	801010	801515	802020	802525	901515	902020	902525
		Set value	Set value	Set value	Set value	Set value	Set value	Set value	Set value	Set value	Set value	Set value	Set value
Discharge pressure	bar	70	70	70	70	70	70	70	70	70	70	70	70
Compressor rotation speed (manual reading)	RPM	1451	1451	1451	1451	1451	1451	1451	1451	1451	1451	1451	1451
Brine flow (no bypass)	l/min	-	-	-	-	-	-	-	-	-	-	-	-
Vessel brine inlet temperature at cooling down startup	°C	-1	-1	-1	0	-1	-1	-1	0	-1	-1	0	-1
Evaporator brine outlet temperature at steady state	°C	-1	-1	-1	-1	-1	-1	-1	0	-1	-1	0	-1
Evaporator water temperature	°C	10	10	10	15	10	10	15	20	25	15	20	25
PERFORMANCE	Unit	Value	Value	Value	Value	Value	Value	Value	Value	Value	Value	Value	Value
Cooling capacity	kW	17.2	34.7	37.7	34.0	32.5	36.7	34.8	33.3	31.5	33.4	31.6	30.5
Power consumption (compressor+pump)	kW	11.8	13.8	15.1	15.2	15.9	16.3	15.9	16.2	16.3	16.8	17.0	17.1
COP	-	1.5	2.5	2.5	2.3	2.1	2.3	2.2	2.1	1.9	2.0	1.9	1.8
EVAPORATOR	Unit	Value	Value	Value	Value	Value	Value	Value	Value	Value	Value	Value	Value
Evaporation temperature (compressor suction)	°C	-6.7	-9.4	-9.8	-9.1	-8.3	-9.6	-9.1	-8.4	-8.0	-8.8	-8.2	-7.8
Inlet temperature, CO2	°C	-2.6	-5.8	-6.4	-5.6	-5.0	-6.2	-5.7	-5.2	-4.7	-5.5	-5.1	-4.6
Outlet temperature, CO2	°C	-3.0	-5.4	-4.7	-5.0	-4.5	-5.1	-4.9	-4.5	-4.5	-4.5	-4.3	-4.0
Outlet superheat	K	0.1	0.6	0.0	0.7	0.6	1.2	1.1	0.9	0.6	1.1	1.1	0.9
Pressure drop, CO2	kPa	47.4	14.5	22.3	13.0	16.0	9.4	10.7	14.1	14.2	8.9	11.9	12.3
Cooling capacity, CO2 (gascooler mass flow)	kW	5.6	34.7	37.7	34.0	32.5	36.7	34.8	33.3	31.5	33.4	31.6	30.5
Cooling capacity, CO2 (compressor mass flow)	kW	2.3	31.1	-5.3	30.9	28.8	32.9	31.3	30.1	27.9	30.7	28.5	27.9
Cooling capacity, brine	kW	17.2	37.0	39.0	36.1	33.8	37.8	35.6	34.6	32.5	34.0	33.4	31.8
Cooling capacity, electric	kW	12.2	32.8	35.6	32.8	30.0	35.0	32.8	30.0	27.8	31.1	30.0	27.6
Inlet temperature, brine	°C	-0.4	0.2	0.3	0.3	0.3	0.4	0.3	0.5	0.3	0.3	0.3	0.0
Outlet temperature, brine	°C	-0.9	-0.8	-0.7	-0.6	-0.7	-0.7	-0.6	-0.5	-0.9	-0.6	-0.6	-0.9
Flow brine	l/min	541	540	540	571	571	540	572	572	572	571	572	572
Temperature, brine reservoir inlet	°C	-0.9	-0.8	-0.7	-0.6	-0.6	-0.5	-0.6	-0.5	-0.6	-0.6	-0.6	-0.7
Temperature, brine reservoir outlet	°C	-2.1	-0.5	-0.3	-0.4	-0.4	-0.3	-0.3	-0.2	-0.7	-0.3	-0.4	-0.7
LMTD	°C	2.1	5.3	5.7	5.3	4.8	5.2	4.8	4.8	4.0	4.9	4.5	3.9
Overall heat transfer coefficient (CO2 area)	W/m2K	2357	1922	1648	1942	2070	1963	1983	2027	2324	2004	2057	2306
Overall heat transfer coefficient (H2O area)	W/m2K	2634	2148	1843	2170	2313	2193	2216	2264	2596	2239	2298	2576
Cooling down time from 15 to -1°C	min	-	-	-	-	-	-	-	-	-	-	-	-
Refrigerant level	%	70	70	67	64	70	64	64	67	70	64	67	68
COMPRESSOR	Unit	Value	Value	Value	Value	Value	Value	Value	Value	Value	Value	Value	Value
Suction pressure	bara	29.1	27.0	27.8	27.2	27.8	26.8	27.2	27.7	28.1	27.4	27.9	28.2
Discharge pressure	bara	50.2	60.1	70.1	70.0	70.0	79.2	79.8	80.3	80.5	88.7	90.0	80.0
Suction temperature, CO2	°C	-3.6	3.7	7.7	5.9	8.3	3.1	5.8	8.2	11.2	5.8	8.2	10.7
Discharge temperature, CO2	°C	41.4	83.3	93.5	99.3	100.5	108.6	112.1	114.2	115.2	125.8	129.1	129.1
Suction superheat	K	3.1	17.3	18.6	18.8	19.0	12.7	15.1	16.7	19.2	14.6	16.4	18.5
Power consumption	kW	8.6	10.7	10.7	11.9	12.1	12.9	12.9	13.0	13.1	13.6	13.8	13.9
Rotation frequency	RPM	1451	1451	1451	1451	1451	1451	1451	1451	1451	1451	1451	1451
Flow CO2, calculated (RPM, vol. eff. density)	kg/min	13.00	9.63	9.21	9.21	9.37	8.85	8.83	8.86	8.96	8.63	8.63	8.63
GAS COOLER, Water	Unit	Value	Value	Value	Value	Value	Value	Value	Value	Value	Value	Value	Value
Pressure drop	kPa	194.0	95.2	82.4	79.6	93.1	72.7	72.7	77.4	90.2	62.7	65.6	77.2
Inlet temperature, CO2	°C	40.3	82.1	94.6	97.9	99.2	107.3	110.7	112.7	113.7	124.1	127.2	127.4
Outlet temperature, CO2	°C	15.8	19.7	12.6	16.3	25.7	11.6	16.5	21.7	27.3	16.0	20.9	26.2
Inlet temperature, throttle valve	°C	13.9	16.5	8.7	14.9	20.2	7.2	11.4	15.4	20.4	10.5	14.6	18.8
Inlet temperature, water	°C	10.0	10.1	14.8	10.0	19.9	10.1	15.0	19.8	24.6	14.9	19.8	25.0
Outlet temperature, water	°C	14.4	18.5	18.8	23.4	27.7	19.2	23.5	28.0	32.3	23.4	27.9	32.6
Temperature Approach, CO2 outlet	K	5.8	9.5	8.9	3.3	5.7	1.5	2.6	1.8	2.6	1.0	1.1	1.3
Flow water	kg/h	4769	4808	4836	4855	4869	4797	4890	4871	5034	4895	4975	5044
Capacity, water heating	kW	24	48	38	47	45	50	49	47	45	48	48	45
Flow CO2, calculated (heat balance)	kg/min	32.02	10.74	10.36	10.16	10.58	9.88	9.84	9.81	10.11	9.27	9.24	9.45
Outlet condenser subcooling	K	16.3	2.4	3.1	16.1	28.3	28.3	28.3	28.3	10.11	10.11	9.24	9.45
IHX outlet temperature HP-side	°C	15.3	23.8	24.3	31.3	29.3	15.2	26.7	25.2	17.3	16.4	28.9	16.3
L-set liq	-	-6.7	-8.4	-8.2	-9.1	-8.3	-9.6	-9.1	-8.4	-8.0	-8.8	-8.2	-7.8
SUCTION GAS HEAT EXCHANGER	Unit	Value	Value	Value	Value	Value	Value	Value	Value	Value	Value	Value	Value
Inlet temp HP	°C	15.0	21.0	23.6	20.5	26.0	12.0	17.2	21.9	27.2	16.3	21.3	26.2
Outlet temp HP	°C	13.9	16.5	23.1	14.9	20.2	7.2	11.4	15.4	20.4	10.5	14.6	18.8
Inlet temp LP	°C	-3.0	-5.4	-4.7	-5.0	-4.5	-5.1	-4.9	-4.5	-4.3	-4.5	-4.3	-4.0
Outlet temp LP	°C	-3.6	7.9	10.4	7.7	10.7	3.1	5.9	8.3	11.2	5.8	8.2	10.7
Heat exchanged (calculated from HP side)	W	600.5	4570.5	261.9	2667.7	3713.0	1741.2	2251.9	2812.2	3553.3	2037.9	2565.0	3168.7
Hot gas flow rate, from oil recirculator	kg/min	21.16	1.02	-6.03	0.42	0.20	1.05	0.48	0.62	0.07	0.69	0.37	0.01
LMTD	K	17.7	17.1	19.6	16.1	19.7	10.5	13.6	16.5	20.0	12.6	15.8	18.9
Inner area SGHX	m2	0.1130973	0.1130973	0.1130973	0.1130973	0.1130973	0.1130973	0.1130973	0.1130973	0.1130973	0.1130973	0.1130973	0.1130973
Outer area SGHX	m2	0.1507964	0.1507964	0.1507964	0.1507964	0.1507964	0.1507964	0.1507964	0.1507964	0.1507964	0.1507964	0.1507964	0.1507964
U-value inner	W/m2K	299	2363	118	1465	1666	1464	1465	1503	1572	1426	1446	1481
U-value outer	W/m2K	224	1772	88	1099	1250	1098	1099	1127	1179	1069	1084	1111

Appendix 20 Cooling, 2007 results

Table 11-15: Cooling results, 2007 at 90 bara gas cooler pressure

RSW					
Refrigerant used: CO ₂ .		Hovedresultater (version japan)uten_linker.xls			
R744				Ikke helt stabil	
Steady state		90 ss 15	90 ss 20	90 ss 25	
TEST CONDITIONS	Unit	Set value	Set value	Set value	
Discharge pressure	bar	90	90	90	
Compressor rotation speed (manual reading)	RPM	1451	-	-	
Brine flow (no bypass)	l/min	-	-	-	
Vessel brine inlet temperature at cooling down startup	°C	-	-	-	
Vessel brine inlet temperature at steady state	°C	-1	-1	-1	
Cooling water temperature	°C	15	15	15	
PERFORMANCE	Unit	Value	Value	Value	
Cooling capacity, brine side	kW	26,9	27,7	26,6	
Power consumption (compressor+pump)	kW	16,7	17,9	18,6	
Power consumption compressor	kW	13,5	14,8	15,5	
COP	-	1,42	1,36	1,25	
COP without pump		1,99	1,87	1,72	
EVAPORATOR	Unit	Value	Value	Value	
Evaporation temperature (compressor suction)	°C	-8,7	-8,7	-8,2	
Inlet temperature, CO ₂	°C	-6,8	-6,7	-6,2	
Outlet temperature, CO ₂	°C	-4,4	-4,7	-4,6	
Outlet superheat	K	2,4	2,0	1,6	
Pressure drop, CO ₂	kPa	10,8	14,9	17,5	
		15,0	20,0	25,0	
Cooling capacity, CO ₂ (gascooler mass flow)	kW	26,9	27,7	26,6	
Cooling capacity CO ₂ , (compressor mass flow)	kW	28,5	28,1	26,3	
Cooling capacity, brine	kW	23,6	24,3	23,2	
Cooling capacity, electric	kW	27,5	27,2	25,2	
Inlet temperature, brine	°C	0,0	0,0	0,0	
Outlet temperature, brine	°C	-0,6	-0,6	-0,6	
Flow brine	l/min	568	566	566	
Temperature, brine reservoir inlet	°C	-1,1	-1,2	-1,2	
Temperature, brine reservoir outlet	°C	-0,9	-0,9	-0,8	
LMTD	°C	7,9	7,7	7,3	
Overall heat transfer coefficient (CO ₂ area)	W/m ² K	1005	920	1066	
Overall heat transfer coefficient (H ₂ O area)	W/m ² K	1122,5	1028,3	1190,7	
Cooling down time from 10 to -1°C	min		-		
Refrigerant liquid level	%	45	49	50	
COMPRESSOR	Unit	Value	Value	Value	
Suction pressure	bara	27,5	27,5	27,9	
Discharge pressure	bara	89,7	89,4	89,7	
Suction temperature, CO ₂	°C	-3,3	-3,5	-3,5	
Discharge temperature, CO ₂	°C	114,1	114,9	113,3	
Suction superheat	K	5,3	5,2	4,7	
Power consumption	kW	13,5	14,8	15,5	
Power consumption, calculated	kW	12,4	13,2	13,7	
Rotation frequency	RPM	1320	1410	1451	
Flow CO ₂ , calculated (RPM, vol. eff. density)	kg/min	8,41	9,01	9,49	
GAS COOLER, Water	Unit	Value	Value	Value	
Pressure drop	kPa	54,6	64,5	73,7	
Inlet temperature, CO ₂	°C	112,2	113,1	111,7	
Outlet temperature, CO ₂	°C	16,4	21,7	28,3	
Inlet temperature, throttle valve	°C	16,6	22,1	28,5	
Inlet temperature, water	°C	14,9	19,7	25,4	
Outlet temperature, water	°C	26,3	31,2	36,1	
Temperature Approach, CO ₂ outlet	K	1,5	2,0	2,9	
Flow, water	kg/h	2930	3092	3334	
Capacity, water heating	kW	38,9	41,4	41,2	
Flow CO ₂ , calculated (heat balance)	kg/min	7,95	8,86	9,61	
Vænebalance	kW	0,00	-1,5	-1,0	-0,8

Table 11-16: Cooling results, 2007 at 80 bara gas cooler pressure

RSW							
Refrigerant used: CO ₂		Hovedresultat (version japan) uten_linker.xls		Low waterflow			
R744		Incr. CO ₂ water flow		High RPM		Not SS	
Steady state		brine temp falling					
		80 10 10 2007	80 10 10 LWF 2007	80 15 15 b	80 15 15	80 20 20	80 25 25
TEST CONDITIONS							
	Unit	Set value	Set value	Set value	Set value	Set value	Set value
Discharge pressure	bar	80	80	80	80	80	80
Compressor rotation speed (manual reading)	RPM	1450	1450	1451	1451	1451	1451
Brine flow (no bypass)	l/min	-	-	-	-	-	-
Vessel brine inlet temperature at cooling down startup	°C	10	10	-	15	20	25
Vessel brine inlet temperature at steady state	°C	-1	-1	-1	-1	-1	-1
Cooling water temperature	°C	10	10	15	15	20	25
PERFORMANCE							
	Unit	Value	Value	Value	Value	Value	Value
Cooling capacity, gascooler mass flow	kW	30,0	26,2	27,8	29,9	29,8	28,0
Power consumption (compressor+pump)	kW	15,0	14,5	15,2	17,0	17,3	17,4
Power consumption compressor	kW	11,9	11,4	12,1	13,9	14,1	14,2
COP	-	1,9	1,9	1,6	1,9	1,9	1,7
COP excl. Pump	-	2,5	2,3	2,3	2,15	2,1	2,0
EVAPORATOR							
	Unit	Value	Value	Value	Value	Value	Value
Evaporation temperature (compressor suction)	°C	-9,0	-10,0	-9,0	-9,7	-8,4	-7,0
Inlet temperature, CO ₂	°C	-7,2	-7,7	-7,0	-7,4	-6,3	-4,8
Outlet temperature, CO ₂	°C	-4,6	-4,0	-4,9	-5,5	-5,1	-4,3
Outlet superheat	K	2,8	3,8	2,1	1,9	1,2	0,6
Pressure drop, CO ₂	kPa	9,8	8,2	12,2	17,6	20,1	24,7
		10,0	10,0	15,0	15,0	20,0	25,0
Cooling capacity, CO ₂ (gascooler mass flow)	kW	30,0	26,2	27,8	29,9	29,8	28,0
Cooling capacity CO ₂ , (compressor mass flow)	kW	29,0	26,3	28,6	28,6	28,7	26,2
Cooling capacity, brine	kW	29,2	27,0	24,7	32,6	32,2	30,4
Cooling capacity, electric	kW	27,6	20,6	27,7	29,9	27,3	27,5
Inlet temperature, brine	°C	0,1	0,3	-0,2	1,2	0,2	0,4
Outlet temperature, brine	°C	-0,7	-0,6	-0,8	0,4	-0,6	-0,4
Flow brine	l/min	569	568	567,6	529	529	529
Temperature, brine reservoir inlet	°C	-0,7	-0,6	-1,3	0,0	-0,9	-0,7
Temperature, brine reservoir outlet	°C	-0,6	-0,3	-1,0	0,5	-0,6	-0,4
LMTD	°C	8,7	9,9	8,0	10,1	7,8	6,6
Overall heat transfer coefficient (CO ₂ area)	W/m ² K	1016	779	1017	868	1115	1244
Overall heat transfer coefficient (H ₂ O area)	W/m ² K	1135	870	1136	970	1245	1390
Cooling down time from 10 to -1°C	min						
Refrigerant level	%	47	43	46,6	53	57	55
COMPRESSOR							
	Unit	Value	Value	Value	Value	Value	Value
Suction pressure	bara	27,3	26,5	27,3	26,7	27,7	28,9
Discharge pressure	bara	79,8	79,6	79,8	79,8	79,8	28,9
Suction temperature, CO ₂	°C	-6,0	-5,1	-3,7	-4,3	-4,1	79,9
Discharge temperature, CO ₂	°C	99,8	103,0	99,0	98,9	95,9	-3,5
Suction superheat	K	2,9	4,8	5,3	5,3	4,3	3,4
Power consumption	kW	11,9	11,4	12,1	13,9	14,1	14,2
Power consumption, calculated	kW	10,5	9,8	11,6	12,7	12,9	13,1
Rotation frequency	RPM	1190	1135	1320	1451	1451	1451
Flow CO ₂ , calculated (RPM, vol. eff, density)	kg/min	8,07	7,25	8,7	9,33	9,94	10,65
GAS COOLER, Water							
	Unit	Value	Value	Value	Value	Value	Value
Pressure drop	kPa	55,0	48,9	63,0	81,3	86,3	100,0
Inlet temperature, CO ₂	°C	98,5	101,6	97,5	97,5	94,5	89,7
Outlet temperature, CO ₂	°C	11,3	11,2	17,7	21,9	24,7	89,7
Inlet temperature, throttle valve	°C	11,5	11,4	18,2	22,3	25,0	30,3
Inlet temperature, water	°C	10,3	10,0	15,3	14,6	20,3	30,4
Outlet temperature, water	°C	17,6	18,8	26,8	30,6	30,9	24,6
Temperature Approach, CO ₂ outlet	K	1,0	1,2	2,4	7,3	4,4	33,6
Flow water	kg/h	4825	3539	2921	2304	3502	3970
Capacity, water heating	kW	41	36	39	42,8	43,0	41,7
Flow CO ₂ , calculated (heat balance)	kg/min	8,4	7,2	8,5	9,74	10,30	11,37
Heat balance	kW	-0,9	-1,5	-0,8	-0,9	-0,9	-0,5

Table 11-17: Cooling results, 2007 at 70 bara gas cooler pressure

RSW					
Refrigerant used: CO ₂		Hovedresultater (version japan)uten_linker.xls			
R744					
Steady state		70 10 10	70 15 15	70 20 20	
TEST CONDITIONS					
	Unit	Set value	Set value	Set value	
Discharge pressure	bar	70	70	70	
Compressor rotation speed (manual reading)	RPM	1451	1451	1451	
Brine flow (no bypass)	l/min	-	-	-	
Vessel brine inlet temperature at cooling down startup	°C	10	15	20	
Vessel brine inlet temperature at steady state	°C	-1	-1	-1	
Cooling water temperature	°C	10	15	20	
PERFORMANCE					
	Unit	Value	Value	Value	
Cooling capacity, compr or GC	kW	24,7	30,6	21,9	
Power consumption (compressor+pump)	kW	11,5	15,6	15,6	
Power consumption compressor	kW	8,3	12,4	12,4	
COP	-	2,0	1,8	1,3	
COP uten pumpe		3,0	2,5	1,8	
EVAPORATOR					
	Unit	Value	Value	Value	
Evaporation temperature (compressor suction)	°C	-7,8	-9,4	-6,7	
Inlet temperature, CO ₂	°C	-6,1	-7,4	-4,6	
Outlet temperature, CO ₂	°C	-3,7	-6,2	-4,4	
Outlet superheat	K	2,5	1,2	0,2	
Pressure drop, CO ₂	kPa	8,6	24,0	34,3	
		10,0	15,0	20,0	
Cooling capacity, CO ₂ (compressor mass flow)	kW	24,7	30,6	25,6	
Cooling capacity, CO ₂ (Gascooler mass flow)	kW	26,2	28,2	N.A	
Cooling capacity, brine	kW	22,5	27,7	21,0	
Cooling capacity, electric	kW	21,9	27,7	21,9	
Inlet temperature, brine	°C	0,3	-0,5	0,0	
Outlet temperature, brine	°C	-0,3	-1,3	-0,6	
Flow brine	l/min	562	560	562,1	
Temperature, brine reservoir inlet	°C	-0,7	-1,6	-1,1	
Temperature, brine reservoir outlet	°C	-0,4	-1,3	-0,8	
LMTD	°C	7,4	8,1	5,9	
Overall heat transfer coefficient (CO ₂ area)	W/m ² K	893	998	1038,8	
Overall heat transfer coefficient (H ₂ O area)	W/m ² K	997,5	1115,5	1160,7	
Cooling down time from 10 to -1°C	min			-	
Refrigerant level	%	50	53	58,1	
COMPRESSOR					
	Unit	Value	Value	Value	
Suction pressure	bara	28,2	26,9	29,1	
Discharge pressure	bara	70,3	68,6	69,7	
Suction temperature, CO ₂	°C	-2,6	-5,5	-3,8	
Discharge temperature, CO ₂	°C	82,6	80,9	75,4	
Suction superheat	K	5,2	3,9	2,9	
Power consumption	kW	8,3	12,4	12,4	
Power consumption, calculated	kW	8,4	11,6		
Rotation frequency	RPM	1020	1451	1451,0	
Flow CO ₂ , calculated (RPM, vol.eff, density)	kg/min	7,50	10,15	11,4	
GAS COOLER, Water					
	Unit	Value	Value	Value	
Pressure drop	kPa	49,9	99,3	125,7	
Inlet temperature, CO ₂	°C	81,0	79,6	74,2	
Outlet temperature, CO ₂	°C	11,6	24,4	28,9	
Inlet temperature, throttle valve	°C	12,9	24,9	28,3	
Inlet temperature, water	°C	10,0	14,6	20,2	
Outlet temperature, water	°C	18,5	25,1	28,5	
Temperature Approach, CO ₂ outlet	K	1,6	9,9	8,7	
Flow water	kg/h	3305	3499	3747,6	
Capacity, water heating	kW	32,6	43,0	36,1	
Flow CO ₂ , calculated (heat balance)	kg/min	7,06	10,99		
Varmebalance	kW	70bar	-0,4	0,0	-1,9

Table 11-18: Cooling results, 2007 at 60 bar gas cooler pressure

RSW			
Refrigerant used: CO ₂		Hovedresultater (version japon uten linker.xls)	
R744		Incr. GC water flow	
Steady state		60 10 10 2007	60 15 15 2007
TEST CONDITIONS			
	Unit	Set value	Set value
Discharge pressure	bar	60	60
Compressor rotation speed (manual reading)	RPM	1450	1450
Brine flow (no bypass)	l/min	-	-
Vessel brine inlet temperature at cooling down startup	°C	10	15
Vessel brine inlet temperature at steady state	°C	-1	-1
Cooling water temperature	°C	10	10
PERFORMANCE			
	Unit	Value	Value
Cooling capacity (Gas cooler)	kW	34,4	26,1
Power consumption (compressor+pump)	kW	14,4	14,6
Power consumption compressor	kW	11,3	11,4
COP	-	2,3	1,7
COP uten pompe		3,1	2,3
EVAPORATOR			
	Unit	Value	Value
Evaporation temperature (compressor suction)	°C	-9,0	-7,1
Inlet temperature, CO ₂	°C	-6,8	-4,6
Outlet temperature, CO ₂	°C	-5,8	-4,5
Outlet superheat	K	1,3	0,6
Pressure drop, CO ₂	kPa	26,2	41,9
		10,0	10,0
Cooling capacity, CO ₂ (gascooler mass flow)	kW	34,4	-
Cooling capacity CO ₂ , (compressor mass flow)		35,3	26,3
Cooling capacity, brine	kW	33,6	24,5
Cooling capacity, electric	kW	24,4	26,1
Inlet temperature, brine	°C	-0,8	-0,4
Outlet temperature, brine	°C	-1,6	-1,0
Flow brine	l/min	569	567
Temperature, brine reservoir inlet	°C	-2,8	-1,1
Temperature, brine reservoir outlet	°C	-1,7	-1,0
LMTD	°C	7,8	6,4
Overall heat transfer coefficient (CO ₂ area- Qo brine)	W/m ² K	1288	1177
Overall heat transfer coefficient (H ₂ O area - Qo brine)	W/m ² K	1440	1315
Cooling down time from 10 to -1°C	min		
Refrigerant level	%	49	64
COMPRESSOR			
	Unit	Value	Value
Suction pressure	bara	27,2	28,8
Discharge pressure	bara	59,7	60,5
Suction temperature, CO ₂	°C	-7,2	-5,8
Discharge temperature, CO ₂	°C	65,6	61,8
Suction superheat	K	1,8	1,3
Power consumption	kW	11,3	11,3
Power consumption, calculated	kW	10,4	10,6
Rotation frequency	RPM	1451	1451
Flow CO ₂ , calculated (RPM, vol.eff, density)	kg/min	11,15	12,12
GAS COOLER, Water			
	Unit	Value	Value
Pressure drop	kPa	118,3	151,3
Inlet temperature, CO ₂	°C	64,6	60,9
Outlet temperature, CO ₂	°C	21,7	22,8
Inlet temperature, throttle valve	°C	21,4	22,3
Inlet temperature, water	°C	9,9	14,7
Outlet temperature, water	°C	17,9	21,0
Temperature Approach, CO ₂ outlet	K	12	8
Flow water	kg/h	4772	4875
Capacity, water heating	kW	44,56	35,52
Flow CO ₂ , calculated (heat balance)	kg/min	20,11	12,12

Vamebalanse

kW

60bar

-1,1

-1,9

Table 11-19: Cooling results, 2007 at 50 bara gas cooler pressure

RSW		
Refrigerant used: CO ₂ .	Hovedresultater (version Japan) uten linker.xls Incr. GC water flow	
R744		
Steady state		50 10 10 2007
TEST CONDITIONS		
	Unit	Set value
Discharge pressure	bar	50
Compressor rotation speed (manual reading)	RPM	1450
Brine flow (no bypass)	l/min	-
Vessel brine inlet temperature at cooling down startup	°C	10
Vessel brine inlet temperature at steady state	°C	-1
Cooling water temperature	°C	10
PERFORMANCE		
	Unit	Value
Cooling capacity, gas cooler	kW	16,4
Power consumption (compressor+pump)	kW	12,1
Power consumption compressor	kW	8,9
COP	-	1,3
COP uten pumpe	-	1,8
EVAPORATOR		
	Unit	Value
Evaporation temperature (compressor suction)	°C	-5,2
Inlet temperature, CO ₂	°C	-2,8
Outlet temperature, CO ₂	°C	-3,1
Outlet superheat	K	0,3
Pressure drop, CO ₂	kPa	55,4
		10,0
Cooling capacity, CO ₂ (compressor mass flow+ GC capacity)	kW	16,4
Cooling capacity, brine	kW	15,9
Cooling capacity, electric	kW	11,9
Inlet temperature, brine	°C	0,0
Outlet temperature, brine	°C	-0,4
Flow brine	l/min	569
Temperature, brine reservoir inlet	°C	-0,6
Temperature, brine reservoir outlet	°C	-0,4
LMTD	°C	5,0
Overall heat transfer coefficient (CO ₂ area)	W/m ² K	909
Overall heat transfer coefficient (H ₂ O area)	W/m ² K	1015
Cooling down time from 10 to -1°C	min	
Refrigerant level	%	64
COMPRESSOR		
	Unit	Value
Suction pressure	bara	30,3
Discharge pressure	bara	50,5
Suction temperature, CO ₂	°C	-4,9
Discharge temperature, CO ₂	°C	41,4
Suction superheat	K	0,3
Power consumption	kW	9,0
Power consumption, calculated	kW	8,5
Rotation frequency	RPM	1451
Flow CO ₂ , calculated (RPM, vol.eff, density)	kg/min	14,22
GAS COOLER, Water		
	Unit	Value
Pressure drop	kPa	262,3
Inlet temperature, CO ₂	°C	40,2
Outlet temperature, CO ₂	°C	15,0
Inlet temperature, throttle valve	°C	13,8
Inlet temperature, water	°C	10,0
Outlet temperature, water	°C	14,2
Temperature Approach, CO ₂ outlet	K	5
Flow water	kg/h	4750
Capacity, water heating	kW 50bar	23,4

Appendix 21 Suction gas heat exchanger

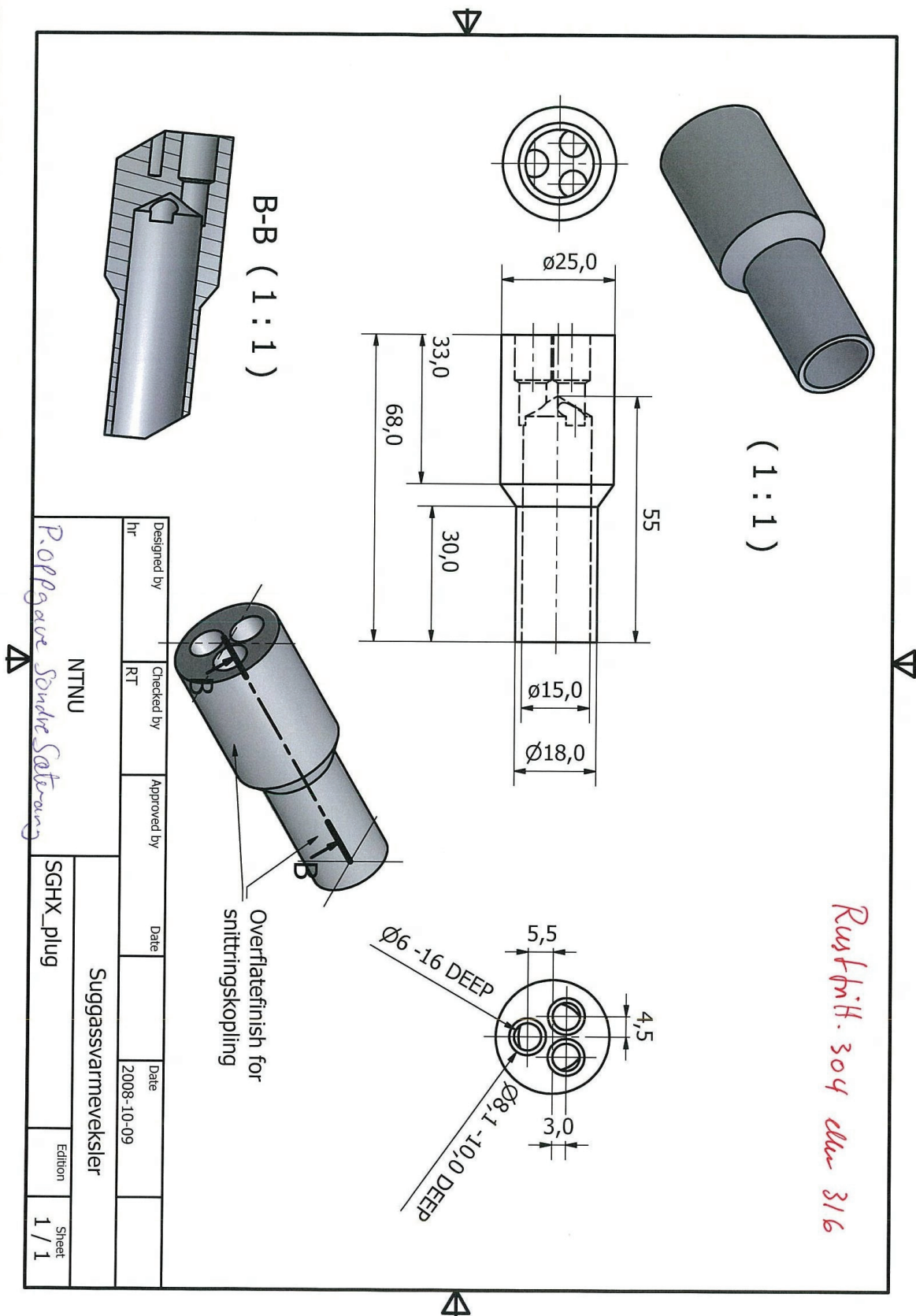


Figure 11-4: CAD drawing of part used to mount the SGHX to the existing piping.

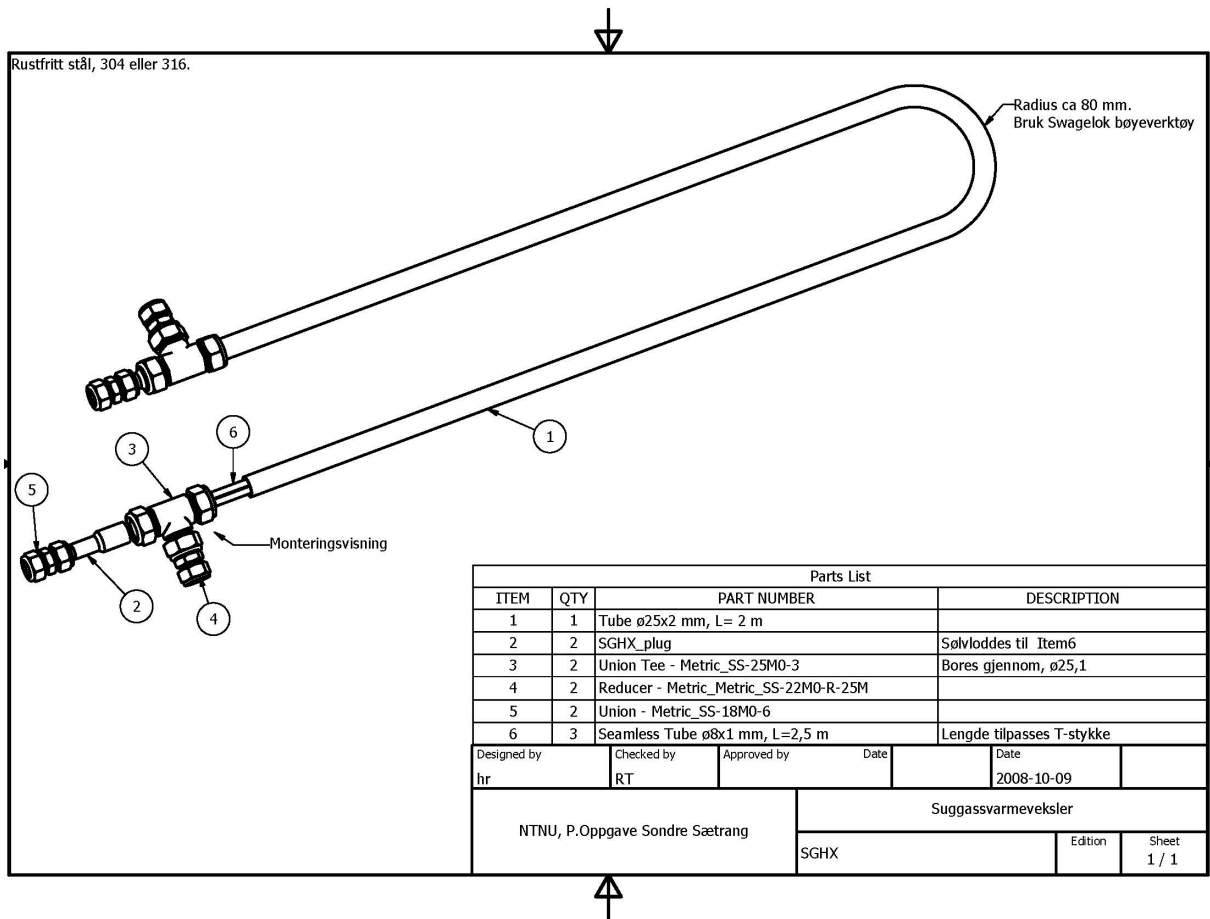


Figure 11-5: Details of the suction gas heat exchanger.

Appendix 22 Excel Solver set up

	A	B	C	D	E	F
1						
2		Function forsolver(property As String, cwtemp As Double, watermassflow				
3		' This function can be used for optimization using an optimization techniqu				
4		' It returns the system cop, the cooling capacity, choke temperature or co				
5		' Property options: cop, q0, choke or watertemp				
6		'				
7		' Usage: forsolver(property,cwtemp,watermassflow[kg/h],evaptemp,ihxeffic				
8		'				
9		' Usage example:				
10		' Want to check the cop for 10 deg C cooling water temp at 2500 kg/h coc				
11		' and IHX efficiency of 0.5 with a 78 bar high side pressure				
12		' forsolver("cop",10,2500,-6,0.5,78)				
13		'				
14		' Author: Sondre Sætrang (sondres84@gmail.com)				
15						
16		Cooling mode, highest COP				
17		Property	COP			
18		Cwtemp	11			
19		Water mass flow	2500			
20		Evaporation temperature	-5,5			
21						
22		Solver variables	Solver_Var	Lowlimit	Highlimit	
23		IHX efficiency	0,4	0	0,6	
24		High side pressure	78	74	110	
25						
26						
27		Goal function	2.5612849			
28		Solver Parameters				
29		Set Target Cell:	\$C\$27			Solve
30		Equal To:	<input checked="" type="radio"/> Max <input type="radio"/> Min <input type="radio"/> Value of:	0		Close
31		By Changing Cells:	\$C\$23:\$C\$24			Guess
32		Subject to the Constraints:				Options
33			\$C\$23 <= \$E\$23			Add
34			\$C\$23 >= \$D\$23			Change
35			\$C\$24 <= \$E\$24			Delete
36			\$C\$24 >= \$D\$24			Reset All
37						Help
38						
39						
40						
41						
42						

Solver Options	
Max Time:	120 seconds OK
Iterations:	100 Cancel
Precision:	0,000001 Load Model...
Tolerance:	1 % Save Model...
Convergence:	0,0001 Help
<input type="checkbox"/> Assume Linear Model	<input checked="" type="checkbox"/> Use Automatic Scaling
<input checked="" type="checkbox"/> Assume Non-Negative	<input type="checkbox"/> Show Iteration Results
Estimates	Derivatives
<input type="radio"/> Tangent	<input checked="" type="radio"/> Forward
<input checked="" type="radio"/> Quadratic	<input type="radio"/> Central
	Search
	<input checked="" type="radio"/> Newton
	<input type="radio"/> Conjugate

Figure 11-6: Excel Solver setup

Evaluation of a variable suction gas heat exchanger in a liquid chiller system using carbon dioxide as the refrigerant

T. Eikevik, H. Rekstad, S. Sætrang

Norwegian University of Science and Technology, Dept. Energy and Process Engineering
N-7491 Trondheim, Norway

Abstract

In a refrigerated seawater (RSW) system using carbon dioxide (CO₂) as the refrigerant, a variable bypass valve was installed in front of a suction gas heat exchanger (SGHX). A simulation tool was developed and utilized to optimize the systems transcritical performance (COP) with respect to the gas cooler pressure and choke valve inlet temperature for cooling and combined cooling and water heating. The simulations indicate that the RSW system performance can be increased compared to running a system with a traditional non-variable suction gas heat exchanger, but only when the cooling water temperatures are high (above ~25°C).

Experimental testing of the cooling performance with transcritical gas cooler pressure show little or no improvement at cooling water temperature levels below 25°C compared to previous experiments. The optimum setting turned out to be maximum suction gas heat exchange (no bypass). Previous experiments also show that for low cooling water temperatures (20°C and below), the optimum gas cooler pressure is subcritical.

The introduction of a variable suction gas heat exchanger made it possible to also use the system for water heating. The optimum and only possible SGHX setting was to bypass the SGHX altogether, as heat exchange would cause overheating at the compressor outlet. In other words, if the current system is to be used for water heating, the possibility to fully bypass the SGHX was essential.

The concept of a variable SGHX appears not to be beneficial in a water cooled RSW system, but the simulations indicate that it has potential in areas where air is used as the cooling medium, for instance commercial or mobile refrigeration. For cooling purposes, experiments and simulations show that a non-variable suction gas heat exchanger can reach near-optimum conditions in the RSW system when low cooling water temperatures are available. It is strongly recommended that a system to be used for simultaneous cooling and heating should have an improved design compared to the current setup, as this mode of operation shows low cooling capacity and poor energy efficiency.

1 Introduction

Table 1-1: Nomenclature

Symbol	Description	Unit
D	Diameter	m
D_h	Hydraulic diameter	m
h	Enthalpy, specific	$\frac{kJ}{kg}$
P	Pressure	Pa (absolute)
R	Thermal resistance	$\frac{K}{W}$
s	Entropy, specific	$\frac{kJ}{kgK}$
T	Temperature	$^{\circ}C$
U	Velocity	$\frac{m}{s}$
v	Specific volume	$\frac{m^3}{kg}$
ϵ_{SCHX}	Suction gas heat exchanger efficiency	-
η_{is}	Isentropic efficiency	-
λ	Volumetric efficiency	-
μ	Dynamic viscosity	$Pa \cdot s$
ν	Kinematic viscosity	$\frac{m^2}{s}$
ρ	Density	$\frac{kg}{m^3}$

Leakage of refrigerants with high greenhouse warming potential (GWP) poses a threat to our environment, and one of the possible replacements is carbon dioxide (CO_2), which does not have any negative impact when leaked. There are challenges however, and these challenges will be addressed further in this master thesis.

In a refrigeration system using CO_2 the gas cooler pressure has to be controlled for transcritical operation. In traditional systems of this kind, a non-variable suction gas heat exchanger is specifically tailored to a specific operating condition. The optimum gas cooler pressure varies with the evaporation temperature and the cooling medium flow and temperature (Sarkar et al, 2004).

For systems undergoing large variations in operating conditions, it is impossible to design a suction gas heat exchanger (SGHX) that ensures optimum system efficiency for all conditions. In order to compensate for this, one can introduce a suction gas heat exchanger bypass, so that the SGHX efficiency (countercurrent heat exchanger efficiency) can be varied according to the current operating condition. The optimum gas cooler pressure then also has

to consider the SGHX efficiency in addition to the evaporation temperature, cooling medium flow and temperature (Sarkar et al, 2004)

The main objective of this project was to investigate if there is any benefit of controlling both gas cooler pressure and suction gas heat exchanger efficiency in a RSW system, and create a tool for optimizing system efficiency using gas cooler pressure and choke inlet temperature as the controlled parameters.

2 The system

The system in question was originally built without a suction gas heat exchanger. The system was designed for transcritical operation with a high cooling water flow. Under-dimensioned evaporator outlet tubes caused liquid carryover (droplets in the compressor suction gas), which required the system to be run with reduced capacity. A suction gas heat exchanger was then installed, but at some conditions the compressor outlet temperature overheated. The last modification was the installation of a bypass solution, so that the suction gas heat exchanger efficiency can be modified depending on the operating condition.

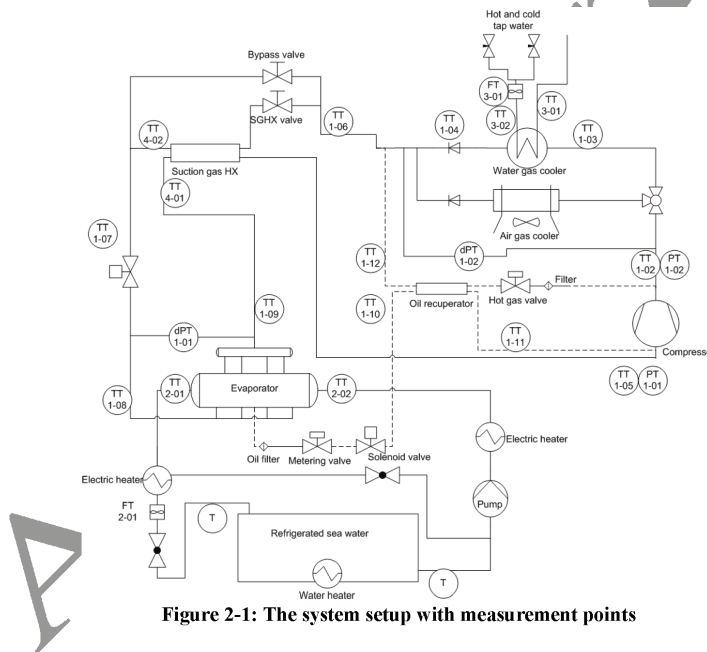


Figure 2-1: The system setup with measurement points

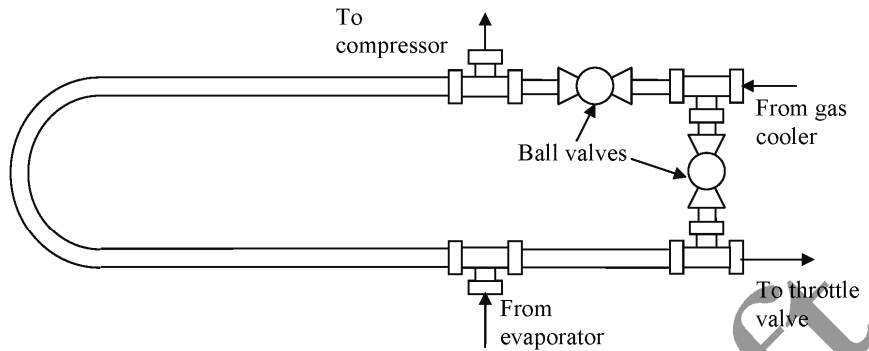


Figure 2-2: The modified suction gas heat exchanger. By opening the vertical ball valve and closing the horizontal ball valve one can bypass the suction gas heat exchanger.

The instrumentation consisted of

- 19 temperature measurements (thermocouples on tube walls, wrapped with alu-tape and insulation)
- 2 pressure transducers for absolute pressure measurements at the compressor inlet and outlet.
- 2 pressure difference measurements, across gas cooler and evaporator.
- 2 flow meters for measuring cooling water and brine (RSW) flow.
- The electric heaters had known power consumption, and the total heat input was logged manually.

A more detailed instrumentation description can be found in Jakobsen et al (2007). All measurements were logged using a computer logging software.

Table 2-1: The result of installing the suction gas heat exchanger.

Conditions	Cooling capacity (kW)			COP (-)		
	Old	New	Change (%)	Old	New	Change (%)
50 bar, 10°C	16,4	17,2	4,8	1,8	2,0	8,8
60 bar, 10°C	34,4	34,7	0,8	3,1	3,3	6,6
70 bar, 10°C	24,7	37,7	52,7	3,0	3,2	7,9
80 bar, 10°C	26,2	36,7	40,0	2,3	2,9	25,4
	2007	2008		2007	2008	
60 bar, 15°C	26,1	23,9	-8,4	2,3	2,2	-2,8
70 bar, 15°C	30,6	34,0	11,4	2,5	2,9	15,8
80 bar, 15°C	27,8	34,8	25,4	2,3	2,7	17,9
90 bar, 15°C	26,9	33,4	23,9	2,0	2,4	22,6
70 bar, 20°C	21,9	32,5	48,3	1,8	2,7	52,7
80 bar, 20°C	29,8	33,3	11,7	2,1	2,6	20,8
90 bar, 20°C	27,7	31,6	14,3	1,9	2,3	22,0
80 bar, 25°C	28,0	31,5	12,4	2,0	2,4	21,5
90 bar, 25°C	26,6	30,5	14,8	1,7	2,2	27,3

3 The system model

The system model was based on experimental data which was already available, both with (experiments from 2008) and without the suction gas heat exchanger installed (experiments from 2007). The model was kept fairly simple, but as will be shown, the results are adequate

The component models are based on libraries made by SINTEF for calculating thermodynamic properties. The libraries had an Excel front-end, which made it logical to use Excel and macros to create a simple system model. For most cases, traditional model parameters were used, with the exception of pressure drops in the gas cooler and evaporator. All thermodynamic data are calculated using these libraries.

rnlib (a refrigerant library) was used for calculating water properties and finding dynamic viscosity for carbon dioxide. *co2lib* (a library for calculation of thermodynamic properties based on Span-Wagners equation of state for carbon dioxide) was used to find all carbon dioxide related properties except dynamic viscosity, and finally *htelib*, a library for calculation of convection coefficients, was used for heat transfer calculations for both carbon dioxide and water in the gas cooler model.

3.1 Compressor model

The compressor has a swept volume of 143.14ccm per revolution, giving a swept volume (\dot{V}_{swept}) of 12.46 m³/hour at full speed (1451 RPM). Some initial tests after installation indicated that the assumed isentropic and volumetric efficiencies previously used for calculation were not suitable, and it was decided to make new models based on previous measurements. The model uses the pressure ratio (p_r) as a variable to calculate volumetric (λ) and isentropic (η_{is}) efficiency. Both models are based on the work performed on the gas, calculated using the inlet and outlet properties, as well as the circulated mass of CO₂ based on the gas cooler heat balance.

The isentropic efficiency was calculated from previous experiments as

$$\eta_{\text{is}} = \frac{h_{\text{compr out, isentropic}} - h_{\text{compr in}}}{h_{\text{compr out, measured}} - h_{\text{compr in}}} \quad (3.1)$$

and the volumetric efficiency as

$$\lambda = \frac{\dot{m}_{\text{co2, gc}} \dot{V}_{\text{compr in}}}{\dot{V}_{\text{swept}}} \quad (3.2)$$

The final compressor model uses the following equations:

$$\dot{V}_{\text{swept}} = 0.000143139 \cdot \frac{\text{RPM}}{60} \left[\frac{\text{m}^3}{\text{s}} \right] \quad (3.3)$$

$$\dot{V}_{\text{suction}} = \dot{V}_{\text{swept}} \cdot \lambda \quad (3.4)$$

$$h_{\text{discharge}} = h_{\text{suction}} + \frac{(h_{\text{isentropic}} - h_{\text{suction}})}{\eta_{\text{is}}} \quad (3.5)$$

$$\eta_{\text{is}} = -0.0442775 p_r^2 + 0.1636479 p_r + 0.5233507 \quad (3.6)$$

$$\lambda = -0.1427691 p_r^2 + 0.6725351 p_r + 0.0003813 \quad (3.7)$$

$$p_r = \frac{p_{\text{discharge}}}{p_{\text{suction}}} \quad (3.8)$$

$$\dot{m}_{\text{circulated}} = \dot{V}_{\text{suction}} \cdot \rho_{\text{suction}} \quad (3.9)$$

$$\dot{W}_{\text{compressor}} = \dot{m}_{\text{circulated}} (h_{\text{discharge}} - h_{\text{suction}}) \quad (3.10)$$

3.2 Gas cooler model

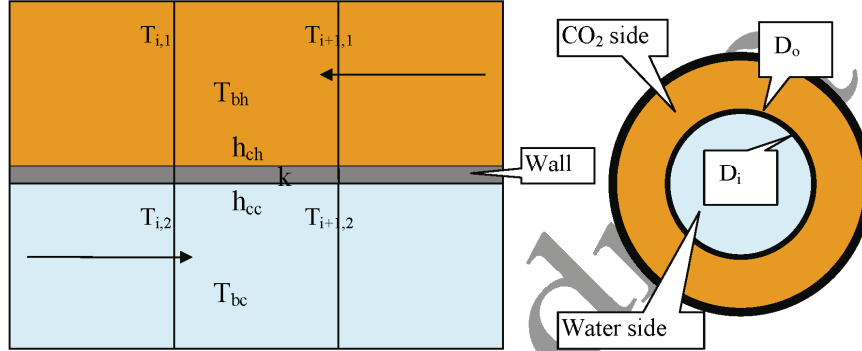


Figure 3-1: The finite elements, directions, symbols and indexing used in the gas cooler simulation.

$$\dot{Q}_{\text{convective}} = \frac{T_{\text{high}} - T_{\text{low}}}{R_{\text{tot}}} \quad (3.11)$$

$$R_{\text{tot}} = \frac{1}{A_{\text{inner}} \cdot h_{\text{inner}}} + \frac{L/n_{\text{sections}}}{2\pi k} \ln(D_o/D_i) + \frac{1}{A_{\text{outer}} \cdot h_{\text{outer}}} \quad (3.12)$$

$$\dot{Q}_{\text{flow}} = \dot{m}_{\text{co2}} (h_{\text{co2,gc in}} - h_{\text{co2,gc out}}) \quad (3.13)$$

$$\text{Error} = \dot{Q}_{\text{convective}} - \dot{Q}_{\text{flow}} \quad (3.14)$$

T_{high} and T_{low} are the bulk temperatures in the section on the high and low-pressure side of the gas cooler, calculated as the section average of the inlet and outlet temperature. h is the convective heat transfer coefficient, k is the thermal conductivity of the wall. D_i is the inner diameter of the small inside tubes (CO₂ tubes), D_o is the outer diameter. A_{inner} is the section area based on the inner circumference and section length, and A_{outer} is the section area based on the inner tube's outer circumference. The wall heat resistance equation (3.12) was based on equations from Incropera et al (2007c).

The first attempts to create a gas cooler model showed poor accuracy for low cooling water flow rates. The heat transfer for low water flow rates were underestimated. An explanation can be that in real life, the tube bends in the gas cooler induces more turbulence than a straight tube, and consequently the model underestimated the heat transfer for low cooling water flows, giving too high gas cooler outlet temperatures. In order to compensate for this, it was decided to introduce a factor that narrows the effective tube cross sectional area, thereby increasing the convection coefficient. The factor decreases linearly until 600 l/h:

$$F_{reduction} = \max(1 + 0.001 \cdot (600 - massflow); 1.0), \quad (3.15)$$

where *massflow* is the cooling water flow in kg/hour

At 10°C cooling water, 600 l/h corresponds to a Reynolds number (Re) of approximately 3000 in the gas cooler. The transition from laminar to turbulent flow is usually set to 2300, but fully turbulent conditions are not reached until Re is around 10000 (Incropera et al, 2007d), so a shift below Re of 3000 is understandable, and can be the cause of the need for such a modification. The Reynolds number was calculated using the equation

$$Re = \frac{UD_h}{\nu}, \quad (3.16)$$

where U is the bulk water velocity, D_h is the hydraulic diameter for an annulus and ν is the kinetic viscosity.

$$dP_{GC} = (1.8469 \text{ m}^2 - 9.1012 \text{ m}) \cdot 10^3 \text{ [Pa]} \quad (3.17)$$

3.3 SGHX model

In the 2008 experiments, the suction gas heat exchanger (SHGX) showed a quite stable U-value in the transcritical area, with values ranging from 1425.8-1572.0 W/m²K, with an average of 1479.63 W/m²K, based on the inner area. The average value was used to estimate the maximum performance of the SGHX. If the heat transfer exceeded this value, the result was discarded (see equation (3.21)).

Heat transfer from the high pressure side in the SGHX was calculated as follows:

$$\dot{Q}_{max} = \dot{m} \cdot \min((h_{in} - h_{out})_{hot}, (h_{out} - h_{in})_{cold}) \quad (3.18)$$

$$\dot{Q}_{transferred} = \dot{Q}_{max} \cdot \epsilon_{SGHX} \quad (3.19)$$

$$h_{out} = h_{in} - \dot{Q}_{transfer} / \dot{m} \quad (3.20)$$

In order to check for a viable solution (obtainable in the actual system), a validity check for suction gas heat exchanger was introduced:

$$\dot{Q}_{transfer} \leq \Delta T_{LMTD} \cdot A_{HX} \cdot h_{experimental} \quad (3.21)$$

where $h_{experimental}$ is the average heat transfer coefficient and the logarithmic mean temperature difference (Incropera et al, 2007b):

$$\Delta T_{LMTD} = \frac{(T_{SGHX,HPin} - T_{SGHX,LPout}) - (T_{SGHX,HPout} - T_{SGHX,LPin})}{\ln \frac{(T_{SGHX,HPin} - T_{SGHX,LPout})}{(T_{SGHX,HPout} - T_{SGHX,LPin})}} \quad (3.22)$$

3.4 Evaporator model

$$dP_{evap} = (2 \cdot 10^7 \cdot V_{satflow}^2 - 26466 \cdot V_{satflow}) \cdot 10^3 \text{ [Pa]} \quad (3.23)$$

$$V_{satflow} = \dot{m} \cdot v_{satgas}(t_{evap}) \quad (3.24)$$

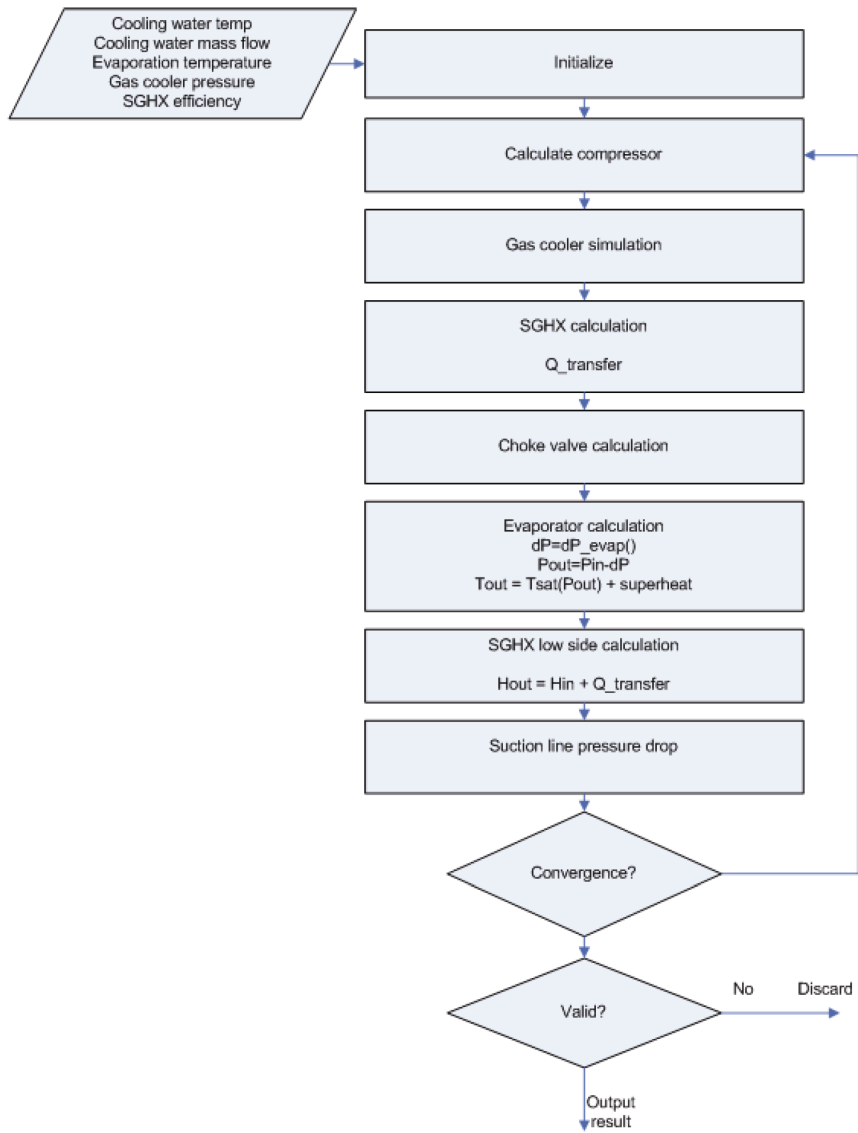


Figure 3-2: The iterative approach for solving the system.

4 Optimization results

The optimization process is focused on transcritical operation, as this has particular use for high pressure control. The goal of this master thesis is not to find the perfect optimization algorithm; the purpose here is to see if the concept of a variable SGHX can be beneficial. The simulations were run with a number of combinations of pressure and SGHX efficiency, and then automatically choosing the setting combination which provided the highest COP. As the SGHX efficiency is not directly measurable in a real system, the throttling valve inlet temperature was selected as the controlled parameter in addition to the gas cooler pressure.

4.1 Goal function

The system simulations calculate all properties of the system. The goal function outputs the COP (neglecting brine pump work), and by running combinations of gas cooler pressure and SGHX efficiency the highest COP for each cooling water flow, cooling water temp and evaporation temperature (later referred to as operating conditions) was selected.

The system COP was calculated using the cooling capacity and compressor work,

$$COP = \frac{h(T_{evap,out}, P_{evap,out}) - h(T_{choke}, P_{gc,out})}{h(T_{compr,out}, P_{compr,out}) - h(T_{compr,in}, P_{compr,in})} \quad (4.1)$$

If the system did not converge or the converged result violated any of the restrictions set (exceeding the maximum compressor outlet temperature (130°C) or the heat transfer was higher than obtainable in the SGHX), the COP was set to zero.

For water heating (combined cooling and heating) it was necessary to use a trial and error approach on the cooling water flow in order to reach the desired outlet temperature, since the highest COP for a given cooling water flow not necessarily meant that the correct water temperature had been reached.

4.2 Proof of concept

In order to show the use of the variable SGHX concept, a series of simulations was run with a theoretical suction gas heat exchanger with a maximum efficiency of 0.9; in other words, the SGHX heat transfer restriction was temporarily removed from the system simulation model. The simulations were run at full cooling water flow (5000 kg/h) with inlet temperatures ranging from 10 to 50 °C. Simulations were also run with constant SGHX efficiencies of 0.3 and 0.6 in order to plot the differences. The compressor outlet temperature was limited to 130 °C.

Table 4-1: Combinations used for proof of concept

Variable	Low	High	Step size	# Steps
Pressure [bar]	74	110	2	19
SGHX efficiency [-]	0	0.9	0.1	10
Total combinations				190

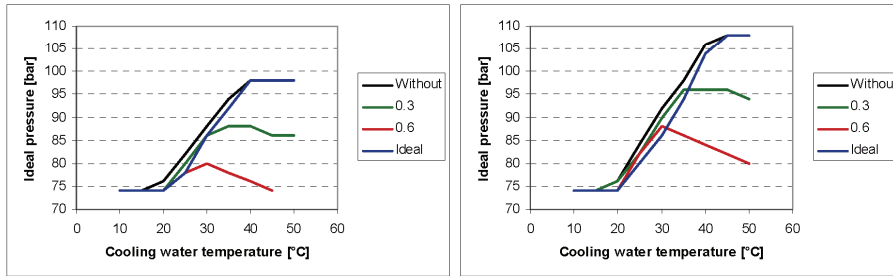


Figure 4-1: The ideal high side pressure (absolute, bara) at evaporation temperature -6°C (left) and -2°C (right)

As seen in Figure 4-2, the COP can deviate far from the optimum with different cooling water temperatures for a given SGHX efficiency. The figure also shows that the SGHX efficiency has very little influence on the system performance for low cooling water temperature. This confirms the statement by Sarkar et al (2004): “...the performance of internal heat exchanger has a minor influence on system optimization at low and moderate gas cooler exit temperatures”. The concept of a suction gas heat exchanger is therefore expected to only give minor improvements in system efficiency when in cooling mode (high cooling water flow).

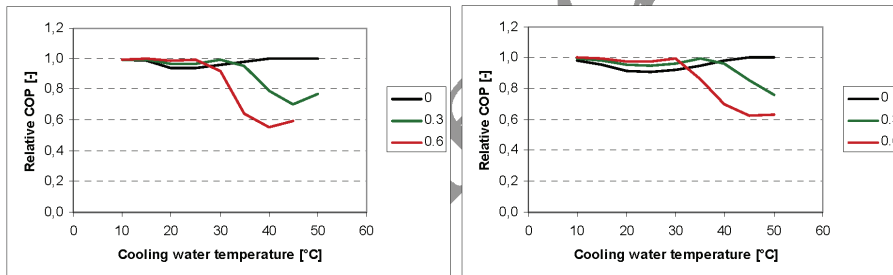


Figure 4-2: Relative COP using different SGHX efficiencies for evaporation temperature -6°C (left) and -2°C (right). The relative COP using the ideal SGHX efficiency is unity (1). A relative COP of 0.8 means the setting gives a COP of only 80% compared to the optimum setting.

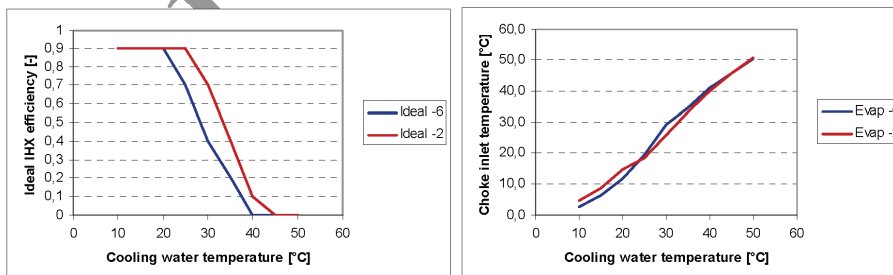


Figure 4-3: The ideal IHX (SGHX) efficiency (left) and the corresponding choke valve inlet temperature (right) as a function of cooling water temperature for different evaporation temperatures.

4.3 Cooling results

For cooling, an evaporation temperature of -6°C was selected based on previous experimental results. The variable combinations were can be found in Table 4-2. Figure 4-4 shows the ideal pressure and choke valve inlet temperatures for 5000 kg/h cooling water flow at varying evaporation temperature for different cooling water temperatures.

Table 4-2: Variable combinations for each operating condition (cooling water temp, cooling water flow, evaporation temperature) used for batch simulations.

Variable	Low	High	Step size	# Steps
Pressure [bara]	74	110	2	19
SGHX efficiency [-]	0	0.6	0.1	7
Total combinations				133

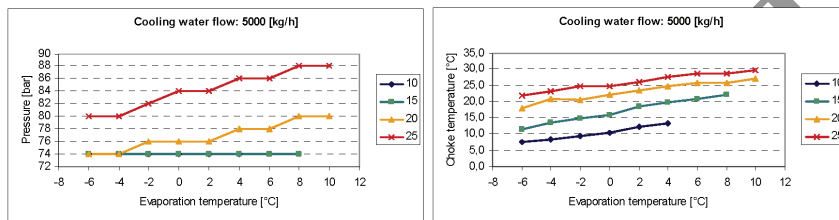


Figure 4-4: The optimum pressure (left) and optimum choke inlet temperature (right) as a function of the evaporation temperature, at different cooling water temperatures.

4.4 Heating results

Water heating was previously not possible (2008 experiments) using the installed suction gas heat exchanger because of overheating at the compressor outlet. The optimization results show that no internal heat exchange is desired for hot water production, and that the maximum pressure before overheating is 108 bar at -2°C (the evaporation temperature was kept constant at -2°C), and this pressure remains constant for all the low water flows. Note that the goal was set to produce the desired hot water temperature at the highest possible COP. Higher COP was possible for the given flow rates, but these resulted in lower hot water temperatures. If one were to use a higher SGHX efficiency, the pressure would have to be reduced significantly in order to prevent overheating at the compressor outlet (Figure 4-1), which would have reduced the system efficiency.

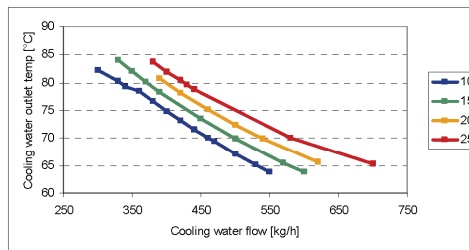


Figure 4-5: The outlet temperatures for different cooling water flows and cooling water temperatures.

5 Experimental results

The system has manual control of gas cooler pressure (via the choke valve), cooling water temperature and flow, SGHX bypass, compressor speed and heat input. This made it demanding to keep constant system input. The measurements were logged for 20-30 minutes with one minute intervals in order to get good average values.

The experimental performance was calculated based on the circulated mass flow of carbon dioxide in the system. The flow rate was calculated using heat balance over the gas cooler. The refrigeration capacity was calculated as if the evaporation outlet was saturated or superheated, depending on temperature. Thus, COP values may be slightly exaggerated, as liquid out of the evaporator does not contribute to the cooling capacity.

Table 5-1: Experiment matrix.

Goal	Cooling water temperature			
	10°C	15°C	20°C	25°C
Cooling at medium cooling water flow rate		X	X	X
Cooling at maximum water flow rate	X	X	X	X
Combined cooling and hot water, 65°C outlet	X	X	X	X
Combined cooling and hot water, 70°C outlet	X	X	X	X
Combined cooling and hot water, 80°C outlet	X	X	X	X

5.1 Cooling

For the cooling mode experiments the cooling water flow rates were kept high and the gas cooler pressure just above transcritical, as shown in the optimization chapter. The evaporation temperature was kept close to constant, and the choke inlet temperature was kept within $\pm 1\text{K}$ of the values found in the optimization. At medium cooling water flow, tables with a wider cooling water flow rates were created and linear interpolation was performed as on the fly as it was difficult to precisely adjust the cooling water flow to a specific value.

It was difficult to compare medium water flow results, as cooling water flow and temperatures were not exactly as set in the previous experiments. As a workaround the experiments were run using the found optimum settings, and then the simulations were run after hand using the actual data (evaporation temperature, cooling water temperature and cooling water flow) from the experiments as simulation input. In this way the model accuracy could be verified. This was done for all the cooling experiments. Simulated performance of COP and cooling capacity are within a 5% error margin when compared to the actual experimental values (Figure 5-1).

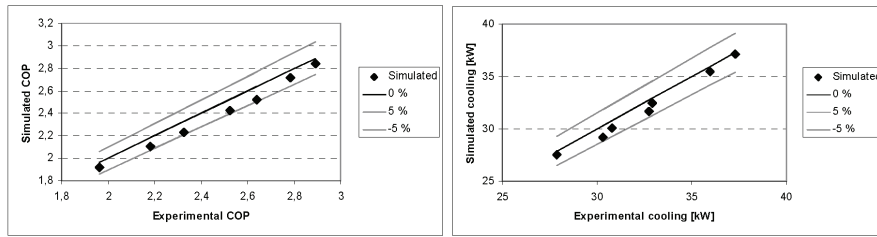


Figure 5-1: Model accuracy, cooling. COP (left), cooling capacity (right)

5.2 Heating

There were no earlier experiments using a suction gas heat exchanger, so the experiments were run with settings found through the simulations, and when completed, simulations were run again using the actual data from the experiments and compared (as for the cooling).

COP calculations were quite accurate, but the 20/70 and the 25/80 experiments deviated more than the rest. This could be linked to problems with the cooling water flow measurements, which behaved rather odd at low cooling water flows, even after recalibrating the flow measurement device.

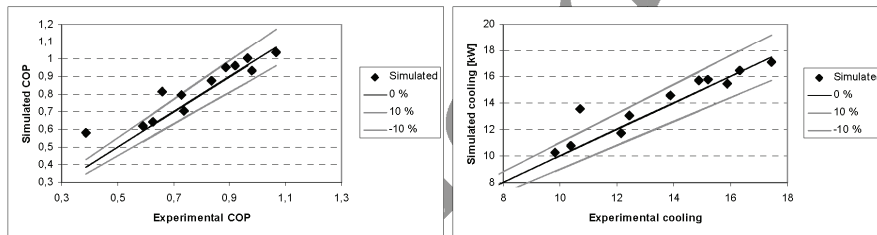


Figure 5-2: Model accuracy, heating. COP (left), cooling capacity (right)

6 Discussions

6.1 System performance

A lower gas cooler pressure limit of 74 bar was set in order to ensure transcritical operation, as the model was created for that purpose, but higher efficiencies can be achieved using a lower pressure for high cooling water flow and/or low temperature (as shown in previous experiments, Table 2-1), but this was not tested in this thesis.

The high cooling water flow experiments showed no significant change compared to the 2008 experiments. This was expected due to low sensitivity to the SGXH efficiency). The temperature approach was low due to large temperature difference in the gas cooler, which resulted in very good heat transfer (Figure 6-1).

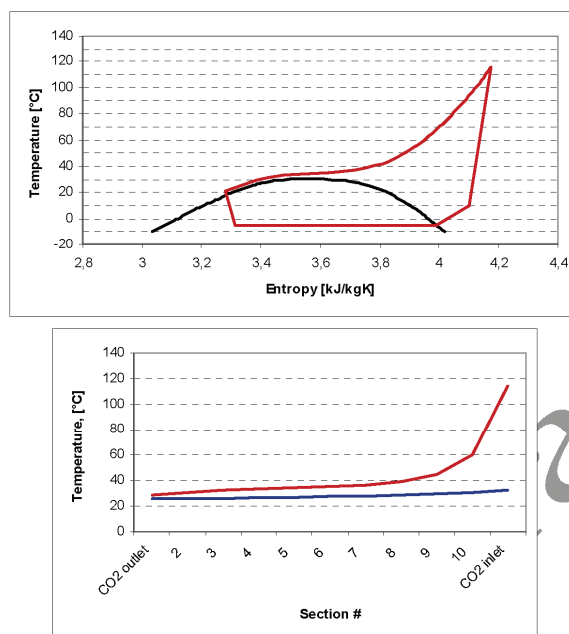


Figure 6-1: Cycle (upper) and gas cooler temperature profile (lower) at full water flow using 25 °C cooling water temperature. The blue line is the cooling water temperature.

The 25 °C cooling water temperature experiment actually showed reduced efficiency, but the 2008 experiment at 80 bar was very close to the optimum choke temperature setting, with slightly higher cooling water flow and evaporation temperature, which is probably the cause of the slight COP reduction.

Combined cooling and water heating on the current system showed very poor performance. The gas cooler temperature approach was very high (Figure 6-2), which resulted in low efficiency and low cooling capacity. A gas cooler with higher performance should be able to improve the performance by reducing the temperature approach.

By running simulations using the conditions from the experiments, it was possible to check the validity of the model, and it shows good accuracy, within 5% error for the cooling capacity and system efficiency (COP), and within 10% error for most of the water heating experiments. The model shows some improvement potentials, but it was accurate enough for the intended use.

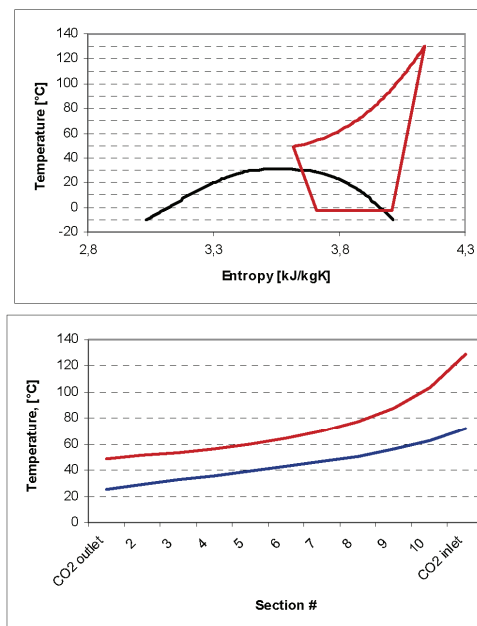


Figure 6-2: Cycle (upper) and gas cooler temperature profile (lower) at heating mode with 70°C outlet temperature using 25 °C cooling water. The temperature difference between the CO₂ and the water was much lower than for the full flow experiment, so less heat was transferred.

6.2 System control

In a traditional transcritical system the gas cooler temperature approach is used as the control parameter for finding the optimum high side pressure. This works fine with a constant suction gas heat exchanger. When introducing a variable suction gas heat exchanger, the gas cooler outlet temperature can no longer be used for this purpose, as it is affected both by the gas cooler pressure and the efficiency of the suction gas heat exchanger. The high side pressure therefore has to be controlled by other means, for instance cooling medium temperature and flow. The evaporation temperature also has to be taken into account (Sarkar et al, 2004).

For controlling of the suction gas heat exchanger, the choke inlet temperature can be used as a control parameter. As can be seen from the results, the simulations are accurate enough to use the choke inlet temperature as the control parameter. An initial idea is to generate lookup-tables from which a controller can interpolate to find set points.

6.3 Model accuracy

The model predicts the system behavior better than expected. Even though the model was very simple, cooling efficiencies (COP) were calculated within 5 % error margin. In the combined cooling and heating experiments (water heating) the simulation error was within 10% (with a few exceptions), and is considered good enough for optimization purposes. The reason for the low errors is likely to be caused by the modeling process, which used previous measurement data. The outliers are probably caused by varying cooling water flow at low flow rates.

The evaporator pressure drop model should have been revised after installing the suction gas heat exchanger. However, the pressure drops are at a very small scale, and the calculation of overall system efficiency seems to be almost unaffected by this. The gas cooler pressure drop is a result of using the erroneous mass flow calculations. The error should have been caught earlier, but the pressure drops are very small compared to the total pressure, so this should have almost no impact on the system performance calculations.

6.4 The concept of variable SGHX bypass

As shown in section 4.2, the benefit of a variable SGHX becomes increasingly more evident when cooling water temperature exceeds 25 °C (or achievable gas cooler outlet temperature above 25°C, since the temperature approach is very small for high cooling water flow rates). For the system in question, because of the low gas cooler outlet temperatures, it is therefore difficult to determine if the concept of a variable SGHX is beneficial.

The simulations show that a RSW system with an efficient gas cooler and low cooling water temperature (up until around 25°C) available does not need a variable SGHX; a high efficiency SGHX will be satisfactory. In this kind of setup, the gas cooler temperature approach can be used for simple gas cooler pressure control.

It's when the cooling water temperature/gas cooler outlet temperature exceeds 25°C that the variable suction gas heat exchanger starts to show real benefit. As can be seen in Figure 4-3 the ideal SGHX efficiency declines with increasing cooling water temperature until zero efficiency (full bypass). Such high cooling temperatures are unlikely for RSW refrigeration using sea water as the cooling medium, but the concept should be useful for refrigeration systems which utilize air as the cooling medium (where the air temperature is high, and the gas cooler temperature approach will be higher). Using air as a cooling medium generally means a higher temperature approach, and will have the same impact on the system as increasing the cooling water temperature. Also, ambient air temperature tends to experience greater variation than sea water.

A word of advice for designing the suction gas heat exchanger is to calculate the UA value for the SGHX at all simulation points, and then select the highest one for manufacturing, as the highest efficiency may not have the highest UA-value (Watts/ΔK). An observation is that too high SGHX efficiency is far worse than not using an SGHX at all (ignoring liquid carryover), as can be seen from Figure 4-2. The best example of this is the 2008 experiments, where hot water production was not even possible due to non-ideal SGHX efficiency. So if it is decided to not use a variable SGHX even though high gas cooler outlet temperature may occur, the efficiency of the SGHX should be kept low enough to allow for sufficiently high gas cooler pressure at the highest cooling medium temperatures.

7 Conclusions

The simulation results from the developed simulation tool indicate that the RSW system performance can be increased compared to running a system with a traditional non-variable suction gas heat exchanger, but only when the gas cooler outlet temperatures are high (above ~25°C), which for the system in question would mean high cooling water temperatures or reduced cooling water flow rate. Such operating conditions are not to be expected for a RSW system with low cooling water temperatures available.

The cooling experiments with transcritical gas cooler pressure show little or no improvement in system performance at temperature levels of 25 °C and below compared to previous

experiments, as the optimum setting turned out to be maximum suction gas heat exchange (no bypass). Previous experiments also show that for low cooling water temperatures (20°C and below), the optimum gas cooler pressure is subcritical. The simulation model showed good accuracy in predicting COP and cooling capacity.

The introduction of a variable suction gas heat exchanger once again made it possible to use the system for water heating. The optimum operation was to bypass the SGHX altogether, and any use for a SGHX should be to evaporate liquid carryover from the evaporator. In other words, if the current system is to be used for water heating, the possibility to fully bypass the SGHX is essential.

The concept of a variable SGHX appears not to be beneficial in a water cooled RSW system, but the simulations indicate that it has potential in areas where air is used as the cooling medium, for instance commercial or mobile refrigeration. For cooling purposes, experiments and simulations show that a non-variable suction gas heat exchanger should be satisfactory for a RSW system when low cooling water temperatures are available. It is strongly recommended that a system to be used for simultaneous cooling and heating should have an improved design compared to the current setup, as this mode of operation shows low cooling capacity and poor energy efficiency.

8 Bibliography

- Jakobsen, A., Rekstad, H., Skaugen, G., Eikevik, T., Nekså, P. (2007) Prototype liquid chiller using carbon dioxide as refrigerant. Proceeding, *International Congress of Refrigeration*, Beijing, China.
- Incropera, F.P., DeWitt, D.P., Bergman, T.L., Lavine, A.S. (2007) *Fundamentals of Heat and Mass Transfer* (6th ed), 620-626. Hoboken, USA: John Wiley & Sons Inc.
- Incropera, F.P., DeWitt, D.P., Bergman, T.L., Lavine, A.S. (2007b) *Fundamentals of Heat and Mass Transfer* (6th ed), 678. Hoboken, USA: John Wiley & Sons Inc.
- Incropera, F.P., DeWitt, D.P., Bergman, T.L., Lavine, A.S. (2007c) *Fundamentals of Heat and Mass Transfer* (6th ed), 116-126. Hoboken, USA: John Wiley & Sons Inc.
- Incropera, F.P., DeWitt, D.P., Bergman, T.L., Lavine, A.S. (2007d) *Fundamentals of Heat and Mass Transfer* (6th ed), 487. Hoboken, USA: John Wiley & Sons Inc.
- Sarkar, J., Bhattacharyya, S., Ram Gopal, M. (2004) Optimization of a transcritical CO₂ heat pump cycle for simultaneous cooling and heating applications, *International Journal of Refrigeration*, 27 (8), 830-838